

**Numerical Investigation of Heat and Mass
Transfer by Mixed Convection Flow from a Vertical
Porous Plate with Induced Magnetic Field,
Constant Heat and Mass Fluxes**



A Thesis

Submitted for the partial Fulfillment of the Degree of

**MASTER OF PHYLOSOPHY
in
Mathematics**

by

Mohammad Rafiqul Islam

Roll No. 0151503, Session : 2001-2002

to

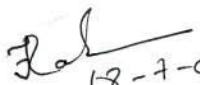
**DEPARTMENT OF MATHEMATICS
KHULNA UNIVERSITY OF ENGINEERING & TECHNOLOGY
KHULNA – 9203, BANGLADESH**

JUNE, 2007


We, the Examination Committee, recommend that the thesis prepared by Mohammad Rafiqul Islam, Roll No. 0151503, Registration No. 24, Session: 2001-2002, titled "*Numerical investigation of heat and mass transfer by mixed convection flow from a vertical porous plate with induced magnetic field, constant heat and mass fluxes.*" be accepted as fulfilling the part of the requirement for the degree of Master of Philosophy in Mathematics from the Department of Mathematics, Khulna University of Engineering & Technology, Khulna.

Examination Committee


1. Professor Dr. Fouzia Rahman
Head & Supervisor
Department of Mathematics
Khulna University of Engineering & Technology, Khulna-9203


.....18-7-07
Chairman

2. Dr. Md. Mahmud Alam
Joint Supervisor
Associate Professor
Mathematics Discipline
Khulna University, Khulna-9208


.....18-7-2007
Member

3. Dr. Mohammad Arif Hossain
Professor
Department of Mathematics
Khulna University of Engineering & Technology, Khulna-9203


.....18/7/07
Member

4. Dr. Md. Abul Kalam Azad
Associate Professor
Department of Mathematics
Khulna University of Engineering & Technology, Khulna-9203

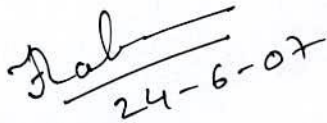

.....
Member 28/7/07

5. Professor Dr. M. Shamsul Alam Sarkar
Examiner(External)
Department of ^{Applied} Mathematics
Rajshahi University
Rajshahi


.....18.07.07
Member(External)

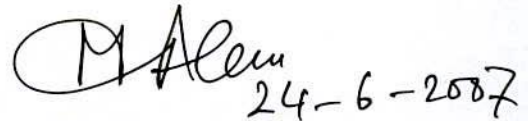
Declaration

We hereby declare that the thesis submitted for the partial fulfillment for the Master of Philosophy degree is done by the student himself and is not submitted elsewhere for any other degree or diploma.


24-6-07

Supervisor

Dr. Fouzia Rahman
Professor
Department of Mathematics
Khulna University of Engineering & Technology
Khulna-920300


24-6-2007

Joint Supervisor

Dr. Md. Mahmud Alam
Associate Professor
Mathematics Discipline
Khulna University
Khulna- 9208

Abstract

Combined heat and mass transfer by mixed convection flow from a vertical porous plate with induced magnetic field, constant heat and mass fluxes has been studied. Nachtsheim Swigert iteration technique is used as the main tool for the numerical approach. The above mentioned problem is studied with two different aspects of the flow. These studies are mainly based on the similarity approach. In the first case one-dimensional unsteady heat and mass transfer by mixed convection flow past an infinite vertical porous plate with induced magnetic field, constant heat and mass fluxes problem have been considered and its similarity solution have been obtained. Similarity equations of the corresponding momentum, magnetic induction, energy and concentration equations are derived by introducing a time dependent length scale which infact plays the role of a similarity parameter. The suction velocity is taken to be inversely proportional to that parameter. The dimensionless similarity equations for momentum, magnetic induction, energy and concentration equations are solved numerically by Nachtsheim Swigert iteration technique. The above problem has further been considered in two-dimension in the steady state problem taking into account the transverse magnetic field along with the induced magnetic field and constant heat and mass fluxes. The similarity equations of the above mentioned problem are obtained by employing the usual similarity technique. These are also solved numerically by Nachtsheim Swigert iteration technique. With the help of graphs and tables the effects of the various important parameters entering into each of the problems, on the velocity, induced magnetic field, current density, temperature, concentration, skin friction and current density at the plate are separately discussed.

Introduction

Many transport processes can be found in various ways in both nature and technology, in which the heat and mass transfer by mixed convection flow occur due to the buoyancy force caused by thermal diffusion (temperature difference), mass diffusion (concentration difference). The heat and mass transfer by mixed convection flow has great significance in stellar, planetary, magnetosphere studied and also in the field of aeronautics, chemical engineering and electronics. In many engineering application heat and mass transfer process in fluid condensing or boiling at a solid surface play a decisive role. Boiling and condensing are characteristic for many separation processes in chemical engineering. As examples of this type of process, the evaporation, condensation, distillation, rectification absorption of a fluid should all be mentioned (Baehr and Stephan,1998).

Magneto fluid dynamics (MFD) is the study of flow of electrically conducting fluid in electric and magnetic field. It unifies in a common framework the electromagnetic and fluid dynamic theories to yield descriptions of the concurrent effects of magnetic field on the flow and the flow on the magnetic field. Magneto fluid dynamics deals with an electrically conducting fluid whereas its subtopics; Magnetohydrodynamics (MHD) and Magneto Gas dynamics (MGD) are specifically concerned with electrically conducting liquids and ionized compressible gases.

The problem of laminar natural convection flow in channels with wall temperature and heat transfer of fluid has been studied by Ostrach (1952). The natural convection flow along a vertical isothermal plate is a classical problem of fluid mechanics that has been solved with the similarity method by Ostrach(1953). Combined natural and forced convection laminar flow with and without heat source has been studied extensively by Ostrach(1953,1954,1955).

Kawase and Ulbrecht(1984) and Martynenko et al.(1984) investigated the free convection flow past an infinite vertical plate with constant suction. It was assumed that the plate temperature oscillates in such way that its amplitude is small. Weiss et al.(1994), further extended the problem of natural convection on a vertical flat plate. Free convection heat transfer on a vertical semi-infinite plate was studied by Berezovsky et al.(1977). Mollendrof and Grebhart(1974) studied the natural convection resulting from the combined buoyancy effect of the thermal and mass diffusion. Lin and Wu (1995,1997) have analyzed the problem of simultaneous heat and mass transfer with the entire range of buoyancy ratio for most practical chemical species in dilute and aqueous solutions.

MHD is currently undergoing a period of great enlargement and differentiation of subject matter. The MHD heat and mass transfer flow of a viscous incompressible fluid past an infinite vertical porous plate under oscillatory suction velocity normal to the plate was investigated by Singh et al. (2003). The problem of combined heat and mass transfer of an electrically conducting fluid in MHD natural convection adjacent to a vertical surface was analyzed by Chen (2004). All the above works are related to the stationary vertical surface; however, the flow past a continuously moving surface has many applications in manufacturing processes. Such processes are hot rolling, the metal and plastic extrusion, continuous casting, glass fiber production and paper production (Altan et al., 1979).

Soundalgekar and Ramana Murty (1980) studied the heat transfer flow past a continuous moving plate with variable temperature. Sami and Al-Sanea (2004) studied the steady laminar flow and heat transfer characteristics of a continuously moving vertical sheet of extruded material. Very recently an analytical study of the combined heat and mass transfer by laminar mixed convection flow of an incompressible electrically conducting viscous fluid past an electrically non-conducting continuously moving infinite vertical porous plate under the action of a uniform transverse magnetic field is done by Chaudhary and Sharma (2006).

In *Chapter 1*, some available information's on MHD heat and mass transfer flows, along with various effects are presented and from both analytical and numerical point of view they have been discussed. The standard form of the basic governing equations and their forms in the considered situations are introduced in *Chapter 2*. In *Chapter 3*, the calculation technique is discussed. In *Chapter 4*, a specific one dimensional unsteady heat and mass transfer by mixed convection flow past an infinite vertical porous plate taking into account of induced magnetic field with constant heat and mass fluxes problem is considered. Two dimensional steady state problem of heat and mass transfer by mixed convection flow past a semi-infinite vertical porous plate taking into account of induced magnetic field with constant heat and mass fluxes is considered in *Chapter 5*.

Table of Contents

	Page
Declaration	i
Abstract	ii
Introduction	iii-iv
Table of contents	v-vi
Acknowledgement	vii
List of Figures	viii-xii
List of Tables	xiii
Chapter 1	1-10
Some Available Information on MHD	
1.1. Magnetohydrodynamics	
1.2. Some Useful Dimensionless Parameters	
1.3. MHD Boundary Layer and Related Transfer Phenomena	
1.4. MHD and heat Transfer	
1.5. Mixed Convection	
1.6. Heat and Mass transfer	
1.7. Thermal Diffusion	
Chapter 2	11-25
The Basic Governing Equations	
Chapter 3	26-29
The Calculation Technique	
Chapter 4	30-64
<i>Unsteady heat and mass transfer by mixed convection flow from a vertical porous plate with induced magnetic field, constant heat and mass fluxes.</i>	
4.1. Introduction	
4.2. The Governing Equations	
4.3. Mathematical Formulation	
4.4. Skin friction Co-efficient, and Current Density at the Plate	
4.5. Numerical Solution	
4.6. Results and Discussion	

Chapter 5

65-94

Steady heat and mass transfer by mixed convection flow from a vertical porous plate with induced magnetic field, constant heat and mass fluxes

- 5.1. Introduction
- 5.2. The Governing Equations
- 5.3. Mathematical Formulation
- 5.4. Skin friction Co-efficient, and Current Density at the Plate
- 5.5. Numerical Solution
- 5.6. Results and Discussion

References

95-96



Acknowledgement

The author would like to express his deepest gratitude and appreciation to Dr. Fouzia Rahman, Supervisor, Professor and Head, Department of Mathematics, Kulna University of Engineering and technology (KUET), Khulna under whose guidance the work was accomplished. The author would like to thank Professor Dr. Fouzia Rahman for her earnest feelings and help in matters concerning author's research affairs as well as personal affairs.

I express my deepest sense of gratitude to my reverend joint supervisor Dr. Md. Mahmud Alam, Associate Professor, Mathematics Discipline, Khulna University, Khulna for his willingness to accept me as a research student. He helped me immensely with his supervision, invaluable instructions, encouragement and constructive discussion throughout this research work.

I take the opportunity to express my great indebtedness to Dr. Mohammad Arif Hossain, Professor, Department of mathematics, KUET for his help in matter concerning thesis review.

I thank all other teachers of Mathematics Department, KUET for their necessary advice and cordial cooperation during the period of study. I thank all the research students of this Department for their help in many respects.

I would also like to thank Md. Nurunnabi Molla, Principal, Sheikh Mujibur Rahman Degree College, Tungipara, Gopalganj for providing me with an opportunity to undertake this work in the Department of Mathematics, KUET, Khulna. I also like to express my gratitude to my colleagues of Sheikh Mujibur Rahman Degree College.

Finally, I would express a special thank to my beloved wife Sonia Islam (Anne) for her constant encouragement and generous help. My profound debts to mother is also unlimited.

List of figures

Unsteady case

page 42-62

- Fig.4.1. Physical Configuration and Coordinate System.
- Fig. 4.2. Velocity profiles (f) for different values of v_o , taking $G_r=5.0$, $G_m=2.0$, $M=1.0$, $P_m=1.0$, $P_r=0.71$, $S_o=2.0$, $S_c=0.6$ and $E_c=0.5$ as fixed.
- Fig. 4.3. Velocity profiles (f) for different values of M , taking $v_o=1.0$, $G_r=5.0$, $G_m=2.0$, $P_m=1.0$, $P_r=0.71$, $S_o=2.0$, $S_c=0.6$ and $E_c=0.5$ as fixed.
- Fig. 4.4. Velocity profiles (f) for different values of P_m , taking $v_o=1.0$, $G_r=5.0$, $G_m=2.0$, $M=1.0$, $P_r=0.71$, $S_o=2.0$, $S_c=0.6$ and $E_c=0.5$ as fixed.
- Fig. 4.5. Velocity profiles (f) for different values of S_o , taking $v_o=1.0$, $G_r=5.0$, $G_m=2.0$, $M=1.0$, $P_m=1.0$, $P_r=0.71$, $S_c=0.6$ and $E_c=0.5$ as fixed.
- Fig. 4.6. Velocity profiles (f) for different values of E_c , taking $v_o=1.0$, $G_r=5.0$, $G_m=2.0$, $M=1.0$, $P_m=1.0$, $P_r=0.71$, $S_o=2.0$, and $S_c=0.6$ as fixed.
- Fig. 4.7. Velocity profiles (f) for different values of G_r , taking $v_o=1.0$, $G_m=2.0$, $M=1.0$, $P_m=1.0$, $P_r=0.71$, $S_o=2.0$, $S_c=0.6$ and $E_c=0.5$ as fixed.
- Fig. 4.8. Velocity profiles (f) for different values of P_r , taking $v_o=1.0$, $G_r=5.0$, $G_m=2.0$, $M=1.0$, $P_m=1.0$, $S_o=2.0$, $S_c=0.6$ and $E_c=0.5$ as fixed.
- Fig. 4.9. Velocity profiles (f) for different values of S_c , taking $v_o=1.0$, $G_r=5.0$, $G_m=2.0$, $M=1.0$, $P_m=1.0$, $P_r=0.71$, $S_o=2.0$, and $E_c=0.5$ as fixed.
- Fig. 4.10. Induced magnetic field (H) for different values of v_o , taking $G_r=5.0$, $G_m=2.0$, $M=1.0$, $P_m=1.0$, $P_r=0.71$, $S_o=2.0$, $S_c=0.6$ and $E_c=0.5$ as fixed.
- Fig. 4.11. Induced magnetic field (H) for different values of M , taking $v_o=1.0$, $G_r=5.0$, $G_m=2.0$, $P_m=1.0$, $P_r=0.71$, $S_o=2.0$, $S_c=0.6$ and $E_c=0.5$ as fixed.
- Fig. 4.12. Induced magnetic field (H) for different values of P_m , taking $v_o=1.0$, $G_r=5.0$, $G_m=2.0$, $M=1.0$, $P_r=0.71$, $S_o=2.0$, $S_c=0.6$ and $E_c=0.5$ as fixed.
- Fig. 4.13. Induced magnetic field (H) for different values of S_o , taking $v_o=1.0$, $G_r=5.0$, $G_m=2.0$, $M=1.0$, $P_m=1.0$, $P_r=0.71$, $S_c=0.6$ and $E_c=0.5$ as fixed.

- Fig. 14. Induced magnetic field (H) for different values of E_c , taking $\nu_o=1.0$, $G_r=5.0$, $G_m=2.0$, $M=1.0$, $P_m=1.0$, $P_r=0.71$, $S_o=2.0$, and $S_c=0.6$ as fixed.
- Fig. 4.15. Induced magnetic field (H) for different values of G_r , taking $\nu_o=1.0$, $G_r=5.0$, $M=1.0$, $P_m=1.0$, $P_r=0.71$, $S_o=2.0$, $S_c=0.6$ and $E_c=0.5$ as fixed.
- Fig. 4.16. Induced magnetic field (H) for different values of P_r , taking $\nu_o=1.0$, $G_r=5.0$, $G_m=2.0$, $M=1.0$, $P_m=1.0$, $S_o=2.0$, $S_c=0.6$ and $E_c=0.5$ as fixed.
- Fig. 4.17. Induced magnetic field (H) for different values of S_c , taking $\nu_o=1.0$, $G_r=5.0$, $G_m=2.0$, $M=1.0$, $P_m=1.0$, $P_r=0.71$, $S_o=2.0$, and $E_c=0.5$ as fixed.
- Fig. 4.18. Current density profiles (J) for different values of ν_o , taking $G_r=5.0$, $G_m=2.0$, $M=1.0$, $P_m=1.0$, $P_r=0.71$, $S_o=2.0$, $S_c=0.6$ and $E_c=0.5$ as fixed.
- Fig. 4.19. Current density profiles (J) for different values of M , taking $\nu_o=1.0$, $G_r=5.0$, $G_m=2.0$, $P_m=1.0$, $P_r=0.71$, $S_o=2.0$, $S_c=0.6$ and $E_c=0.5$ as fixed.
- Fig. 4.20. Current density profiles (J) for different values of P_m , taking $\nu_o=1.0$, $G_r=5.0$, $G_m=2.0$, $M=1.0$, $P_r=0.71$, $S_o=2.0$, $S_c=0.6$ and $E_c=0.5$ as fixed.
- Fig. 4.21. Current density profiles (J) for different values of S_o , taking $\nu_o=1.0$, $G_r=5.0$, $G_m=2.0$, $M=1.0$, $P_m=1.0$, $P_r=0.71$, $S_c=0.6$ and $E_c=0.5$ as fixed.
- Fig. 4.22. Current density profiles (J) for different values of E_c , taking $\nu_o=1.0$, $G_r=5.0$, $G_m=2.0$, $M=1.0$, $P_m=1.0$, $P_r=0.71$, $S_o=2.0$, and $S_c=0.6$ as fixed.
- Fig. 4.23. Current density profiles (J) for different values of G_r , taking $\nu_o=1.0$, $G_m=2.0$, $M=1.0$, $P_m=1.0$, $P_r=0.71$, $S_o=2.0$, $S_c=0.6$ and $E_c=0.5$ as fixed.
- Fig. 4.24. Current density profiles (J) for different values of P_r , taking $\nu_o=1.0$, $G_r=5.0$, $G_m=2.0$, $M=1.0$, $P_m=1.0$, $S_o=2.0$, $S_c=0.6$ and $E_c=0.5$ as fixed.
- Fig. 4.25. Current density profiles (J) for different values of S_c , taking $\nu_o=1.0$, $G_r=5.0$, $G_m=2.0$, $M=1.0$, $P_m=1.0$, $P_r=0.71$, $S_o=2.0$, and $E_c=0.5$ as fixed.
- Fig. 4.26. Temperature profiles (θ) for different values of ν_o , taking $G_r=5.0$, $G_m=2.0$, $M=1.0$, $P_m=1.0$, $P_r=0.71$, $S_o=2.0$, $S_c=0.6$ and $E_c=0.5$ as fixed.
- Fig. 4.27. Temperature profiles (θ) for different values of M , taking $\nu_o=1.0$, $G_r=5.0$, $G_m=2.0$, $P_m=1.0$, $P_r=0.71$, $S_o=2.0$, $S_c=0.6$ and $E_c=0.5$ as fixed.
- Fig. 4.28. Temperature profiles (θ) for different values of P_m , taking $\nu_o=1.0$, $G_r=5.0$, $G_m=2.0$, $M=1.0$, $P_r=0.71$, $S_o=2.0$, $S_c=0.6$ and $E_c=0.5$ as fixed.
- Fig. 4.29. Temperature profiles (θ) for different values of S_o , taking $\nu_o=1.0$, $G_r=5.0$, $G_m=2.0$, $M=1.0$, $P_m=1.0$, $P_r=0.71$, $S_c=0.6$ and $E_c=0.5$ as fixed.

- Fig. 4.30. Temperature profiles (θ) for different values of E_c , taking $\nu_o=1.0$, $G_r=5.0$, $G_m=2.0$, $M=1.0$, $P_m=1.0$, $P_r=0.71$, $S_o=2.0$, and $S_c=0.6$ as fixed.
- Fig. 4.31. Temperature profiles (θ) for different values of G_r , taking $\nu_o=1.0$, $G_m=2.0$, $M=1.0$, $P_m=1.0$, $P_r=0.71$, $S_o=2.0$, $S_c=0.6$ and $E_c=0.5$ as fixed.
- Fig. 4.32. Temperature profiles (θ) for different values of P_r , taking $\nu_o=1.0$, $G_r=5.0$, $G_m=2.0$, $M=1.0$, $P_m=1.0$, $S_o=2.0$, $S_c=0.6$ and $E_c=0.5$ as fixed.
- Fig. 4.33. Temperature profiles (θ) for different values of S_c , taking $\nu_o=1.0$, $G_r=5.0$, $G_m=2.0$, $M=1.0$, $P_m=1.0$, $P_r=0.71$, $S_o=2.0$, and $E_c=0.5$ as fixed.
- Fig. 4.34. Concentration profiles (ϕ) for different values of ν_o , taking $G_r=5.0$, $G_m=2.0$, $M=1.0$, $P_m=1.0$, $P_r=0.71$, $S_o=2.0$, $S_c=0.6$ and $E_c=0.5$ as fixed.
- Fig. 4.35. Concentration profiles (ϕ) for different values of M , taking $\nu_o=1.0$, $G_r=5.0$, $G_m=2.0$, $P_m=1.0$, $P_r=0.71$, $S_o=2.0$, $S_c=0.6$ and $E_c=0.5$ as fixed.
- Fig. 4.36. Concentration profiles (ϕ) for different values of P_m , taking $\nu_o=1.0$, $G_r=5.0$, $G_m=2.0$, $M=1.0$, $P_r=0.71$, $S_o=2.0$, $S_c=0.6$ and $E_c=0.5$ as fixed.
- Fig. 4.37. Concentration profiles (ϕ) for different values of S_o , taking $\nu_o=1.0$, $G_r=5.0$, $G_m=2.0$, $M=1.0$, $P_m=1.0$, $P_r=0.71$, $S_c=0.6$ and $E_c=0.5$ as fixed.
- Fig. 4.38. Concentration profiles (ϕ) for different values of E_c , taking $\nu_o=1.0$, $G_r=5.0$, $G_m=2.0$, $M=1.0$, $P_m=1.0$, $P_r=0.71$, $S_o=2.0$, and $S_c=0.6$ as fixed.
- Fig. 4.39. Concentration profiles (ϕ) for different values of G_r , taking $\nu_o=1.0$, $G_m=2.0$, $M=1.0$, $P_m=1.0$, $P_r=0.71$, $S_o=2.0$, $S_c=0.6$ and $E_c=0.5$ as fixed.
- Fig. 4.40. Concentration profiles (ϕ) for different values of P_r , taking $\nu_o=1.0$, $G_r=5.0$, $G_m=2.0$, $M=1.0$, $P_m=1.0$, $S_o=2.0$, $S_c=0.6$ and $E_c=0.5$ as fixed.
- Fig. 4.41. Concentration profiles (ϕ) for different values of S_c , taking $\nu_o=1.0$, $G_r=5.0$, $G_m=2.0$, $M=1.0$, $P_m=1.0$, $P_r=0.71$, $S_o=2.0$, and $E_c=0.5$ as fixed.

Steady case

page 74-92

- Fig. 5.1. Physical model and coordinate system.
- Fig. 5.2. Velocity profiles (f') for different values of f_w , taking $G_r=5.0$, $G_m=2.0$, $M=1.0$, $P_m=1.0$, $S_o=2.0$, $S_c=0.6$ and $E_c=0.2$ as fixed.
- Fig. 5.3. Velocity profiles (f') for different values of M , taking $f_w=2.0$, $G_r=5.0$, $G_m=2.0$, $P_m=1.0$, $S_o=2.0$, $S_c=0.6$ and $E_c=0.2$ as fixed.
- Fig. 5.4. Velocity profiles (f') for different values of P_m , taking $f_w=2.0$, $G_r=5.0$, $G_m=2.0$, $M=1.0$, $S_o=2.0$, $S_c=0.6$ and $E_c=0.2$ as fixed.

- Fig.5.5. Velocity profiles (f') for different values of S_o taking $f_w=2.0$, $G_r=5.0$, $G_m=2.0$, $M=1.0$, $P_m=1.0$, $S_c=0.6$ and $E_c=0.2$ as fixed.
- Fig.5.6. Velocity profiles (f') for different values of E_c , taking $f_w=2.0$, $G_r=5.0$, $G_m=2.0$, $M=1.0$, $P_m=1.0$, $S_o=2.0$ and $S_c=0.6$ as fixed.
- Fig.5.7. Velocity profiles (f') for different values of G_r , taking $f_w=2.0$, $G_m=2.0$, $M=1.0$, $P_m=1.0$, $S_o=2.0$, $S_c=0.6$ and $E_c=0.2$ as fixed.
- Fig.5.8. Velocity profiles (f') for different values of S_c taking $f_w=2.0$, $G_r=5.0$, $G_m=2.0$, $M=1.0$, $P_m=1.0$, $S_o=2.0$ and $E_c=0.2$ as fixed.
- Fig.5.9. Induced magnetic field (H) for different values of f_w , taking $G_r=5.0$, $G_m=2.0$, $M=1.0$, $P_m=1.0$, $S_o=2.0$, $S_c=0.6$ and $E_c=0.2$ as fixed.
- Fig.5.10. Induced magnetic field (H) for different values of M , taking $f_w=2.0$, $G_r=5.0$, $G_m=2.0$, $P_m=1.0$, $S_o=2.0$, $S_c=0.6$ and $E_c=0.2$ as fixed.
- Fig.5.11. Induced magnetic field (H) for different values of P_m , taking $f_w=2.0$, $G_r=5.0$, $G_m=2.0$, $M=1.0$, $S_o=2.0$, $S_c=0.6$ and $E_c=0.2$ as fixed.
- Fig.5.12. Induced magnetic field (H) for different values of S_o taking $f_w=2.0$, $G_r=5.0$, $G_m=2.0$, $M=1.0$, $P_m=1.0$, $S_c=0.6$ and $E_c=0.2$ as fixed.
- Fig.5.13. Induced magnetic field (H) for different values of E_c , taking $f_w=2.0$, $G_r=5.0$, $G_m=2.0$, $M=1.0$, $P_m=1.0$, $S_o=2.0$ and $S_c=0.6$ as fixed.
- Fig.5.14. Induced magnetic field (H) for different values of G_r , taking $f_w=2.0$, $G_m=2.0$, $M=1.0$, $P_m=1.0$, $S_o=2.0$, $S_c=0.6$ and $E_c=0.2$ as fixed.
- Fig.5.15. Induced magnetic field (H) for different values of S_c taking $f_w=2.0$, $G_r=5.0$, $G_m=2.0$, $M=1.0$, $P_m=1.0$, $S_o=2.0$ and $E_c=0.2$ as fixed.
- Fig.5.16. Current density profiles (J) for different values of f_w , taking $G_r=5.0$, $G_m=2.0$, $M=1.0$, $P_m=1.0$, $S_o=2.0$, $S_c=0.6$ and $E_c=0.2$ as fixed.
- Fig.5.17. Current density profiles (J) for different values of M , taking $f_w=2.0$, $G_r=5.0$, $G_m=2.0$, $P_m=1.0$, $S_o=2.0$, $S_c=0.6$ and $E_c=0.2$ as fixed.
- Fig.5.18. Current density profiles (J) for different values of P_m , taking $f_w=2.0$, $G_r=5.0$, $G_m=2.0$, $M=1.0$, $S_o=2.0$, $S_c=0.6$ and $E_c=0.2$ as fixed.
- Fig.5.19. Current density profiles (J) for different values of S_o taking $f_w=2.0$, $G_r=5.0$, $G_m=2.0$, $M=1.0$, $P_m=1.0$, $S_c=0.6$ and $E_c=0.2$ as fixed.
- Fig.5.20. Current density profiles (J) for different values of E_c , taking $f_w=2.0$, $G_r=5.0$, $G_m=2.0$, $M=1.0$, $P_m=1.0$, $S_o=2.0$ and $S_c=0.6$ as fixed.

- Fig.5.21. Current density profiles (J) for different values of G_r , taking $f_w=2.0$, $G_m=2.0$, $M=1.0$, $P_m=1.0$, $S_o=2.0$, $S_c=0.6$ and $E_c=0.2$ as fixed.
- Fig.5.22. Current density profiles (J) for different values of S_c taking $f_w=2.0$, $G_r=5.0$, $G_m=2.0$, $M=1.0$, $P_m=1.0$, $S_o=2.0$ and $E_c=0.2$ as fixed.
- Fig.5.23. Temperature profiles (θ) for different values of f_w , taking $G_r=5.0$, $G_m=2.0$, $M=1.0$, $P_m=1.0$, $S_o=2.0$, $S_c=0.6$ and $E_c=0.2$ as fixed.
- Fig.5.24. Temperature profiles (θ) for different values of M , taking, $f_w=2.0$, $G_r=5.0$, $G_m=2.0$, $P_m=1.0$, $S_o=2.0$, $S_c=0.6$ and $E_c=0.2$ as fixed.
- Fig.5.25. Temperature profiles (θ) for different values of P_m , taking $f_w=2.0$, $G_r=5.0$, $G_m=2.0$, $M=1.0$, $S_o=2.0$, $S_c=0.6$ and $E_c=0.2$ as fixed.
- Fig.5.26. Temperature profiles (θ) for different values of S_o taking $f_w=2.0$, $G_r=5.0$, $G_m=2.0$, $M=1.0$, $P_m=1.0$, $S_c=0.6$ and $E_c=0.2$ as fixed.
- Fig.5.27. Temperature profiles (θ) for different values of E_c , taking $f_w=2.0$, $G_r=5.0$, $G_m=2.0$, $M=1.0$, $P_m=1.0$, $S_o=2.0$ and $S_c=0.6$ as fixed.
- Fig.5.28. Temperature profiles (θ) for different values of G_r , taking $f_w=2.0$, $G_m=2.0$, $M=1.0$, $P_m=1.0$, $S_o=2.0$, $S_c=0.6$ and $E_c=0.2$ as fixed.
- Fig.5.29. Temperature profiles (θ) for different values of S_c , taking $f_w=2.0$, $G_r=5.0$, $G_m=2.0$, $M=1.0$, $P_m=1.0$, $S_o=2.0$ and $E_c=0.2$ as fixed.
- Fig.5.30. Concentration profiles (ϕ) for different values of f_w , taking $G_r=5.0$, $G_m=2.0$, $M=1.0$, $P_m=1.0$, $S_o=2.0$, $S_c=0.6$ and $E_c=0.2$ as fixed.
- Fig.5.31. Concentration profiles (ϕ) for different values of M , taking $f_w=2.0$, $G_r=5.0$, $G_m=2.0$, $P_m=1.0$, $S_o=2.0$, $S_c=0.6$ and $E_c=0.2$ as fixed.
- Fig.5.32. Concentration profiles (ϕ) for different values of P_m , taking $f_w=2.0$, $G_r=5.0$, $G_m=2.0$, $M=1.0$, $S_o=2.0$, $S_c=0.6$ and $E_c=0.2$ as fixed.
- Fig.5.33. Concentration profiles (ϕ) for different values of S_o taking $f_w=2.0$, $G_r=5.0$, $G_m=2.0$, $M=1.0$, $P_m=1.0$, $S_c=0.6$ and $E_c=0.2$ as fixed.
- Fig.5.34. Concentration profiles (ϕ) for different values of E_c , taking $f_w=2.0$, $G_r=5.0$, $G_m=2.0$, $M=1.0$, $P_m=1.0$, $S_o=2.0$ and $S_c=0.6$ as fixed.
- Fig.5.35. Concentration profiles (ϕ) for different values of G_r , taking $f_w=2.0$, $G_m=2.0$, $M=1.0$, $P_m=1.0$, $S_o=2.0$, $S_c=0.6$ and $E_c=0.2$ as fixed.
- Fig.5.36. Concentration profiles (ϕ) for different values of S_c taking $f_w=2.0$, $G_r=5.0$, $G_m=2.0$, $M=1.0$, $P_m=1.0$, $S_o=2.0$ and $E_c=0.2$ as fixed.

List of Tables

Unsteady case

page 63-64

- Table 4.1. Numerical values proportional to τ and J_w for $G_r=5.0$, $G_m=2.0$, $M=1.0$, $P_m=1.0$, $P_r=0.71$, $S_o=2.0$, $S_c=0.6$ and $E_c=0.5$.
- Table 4.2. Numerical values proportional to τ and J_w for $v_o=1.0$, $G_r=5.0$, $G_m=2.0$, $P_m=1.0$, $P_r=0.71$, $S_o=2.0$, $S_c=0.6$ and $E_c=0.5$.
- Table 4.3. Numerical values proportional to τ and J_w for $v_o=1.0$, $G_r=5.0$, $G_m=2.0$, $M=1.0$, $P_r=0.71$, $S_o=2.0$, $S_c=0.6$ and $E_c=0.5$.
- Table 4.4. Numerical values proportional to τ and J_w for $v_o=1.0$, $G_r=5.0$, $G_m=2.0$, $M=1.0$, $P_m=1.0$, $P_r=0.71$, $S_c=0.6$ and $E_c=0.5$.
- Table 4.5. Numerical values proportional to τ and J_w for $v_o=1.0$, $G_r=5.0$, $G_m=2.0$, $M=1.0$, $P_m=1.0$, $P_r=0.71$, $S_o=2.0$, and $S_c=0.6$.
- Table 4.6. Numerical values proportional to τ and J_w for $v_o=1.0$, $G_m=2.0$, $M=1.0$, $P_m=1.0$, $P_r=0.71$, $S_o=2.0$, $S_c=0.6$ and $E_c=0.5$.
- Table 4.7. Numerical values proportional to τ and J_w for $v_o=1.0$, $G_r=5.0$, $G_m=2.0$, $M=1.0$, $P_m=1.0$, $S_o=2.0$, $S_c=0.6$ and $E_c=0.5$ as fixed.
- Table 4.8. Numerical values proportional to τ and J_w for $v_o=1.0$, $G_r=5.0$, $G_m=2.0$, $M=1.0$, $P_m=1.0$, $P_r=0.71$, $S_o=2.0$, and $E_c=0.5$.

Steady case

page 93-94

- Table 5.1. Numerical values proportional to τ and J_w for $G_r=5.0$, $G_m=2.0$, $M=1.0$, $P_m=1.0$, $S_o=2.0$, $S_c=0.6$ and $E_c=0.2$.
- Table 5.2. Numerical values proportional to τ and J_w for $f_w=2.0$, $G_r=5.0$, $G_m=2.0$, $P_m=1.0$, $S_o=2.0$, $S_c=0.6$ and $E_c=0.2$.
- Table 5.3. Numerical values proportional to τ and J_w for $f_w=2.0$, $G_r=5.0$, $G_m=2.0$, $M=1.0$, $S_o=2.0$, $S_c=0.6$ and $E_c=0.2$.
- Table 5.4. Numerical values proportional to τ and J_w for $f_w=2.0$, $G_r=5.0$, $G_m=2.0$, $M=1.0$, $P_m=1.0$, $S_c=0.6$ and $E_c=0.2$.
- Table 5.5. Numerical values proportional to τ and J_w for $f_w=2.0$, $G_r=5.0$, $G_m=2.0$, $M=1.0$, $P_m=1.0$, $S_o=2.0$ and $S_c=0.6$.
- Table 5.6. Numerical values proportional to τ and J_w for $f_w=2.0$, $G_m=2.0$, $M=1.0$, $P_m=1.0$, $S_o=2.0$, $S_c=0.6$ and $E_c=0.2$.
- Table 5.7. Numerical values proportional to τ and J_w for $f_w=2.0$, $G_r=5.0$, $G_m=2.0$, $M=1.0$, $P_m=1.0$, $S_o=2.0$ and $E_c=0.2$.

Chapter 1

Some Available Information on MHD

1.1. Magnetohydrodynamics (MHD)

Magnetohydrodynamics (MHD) is the branch of magneto fluid dynamics, which deals with the flow of electrically conducting fluid in electric and magnetic field. Probably, the largest advancement towards an understanding of such phenomena comes from the field of astrophysics. It has long been suspected that most of the matter in the universe is in the form of plasma or highly ionized gaseous state and much of the basic knowledge in the area of electromagnetic fluid dynamics evolved from these studies. The field of MHD consists of the study of a continuous, electrically conducting fluid under the influence electromagnetic fields. Originally, MHD included only the study of partially ionized gases as well as the other names have been suggested, such as magneto fluid mechanics or magneto aerodynamics, but the original nomenclature has persisted. The essential requirement for problem to be analyzed under the law of MHD is that the continuum approach be applicable.

There are many natural phenomena and engineering problems susceptible to MHD analysis. It is useful in astrophysics because much of the universe is filled with widely spaced charged particles and permeated by magnetic fields and so the continuum assumption becomes applicable. Engineers employ MHD principles in the design of heat exchangers, pumps and flow meters; in solving space vehicle propulsion, control and reentry problem; in designing communications and radar system; in creating novel power generating systems, and in developing confinement schemes for controlled fusion.

The MHD in the generation of electrical power with the flow of electrically conducting fluid through a transverse magnetic field is one of the most important applications. Recently, these experiments with ionized gases have been performed with the hope of producing power on large

scale in stationary plants with large magnetic fields. Generation of MHD power on a smaller scale is of interest of space applications.

Generally we known that, to convert the heat energy in to the electricity, several intermediate transformations are necessary. Each of these steps means a loss of energy. This naturally limits the over all efficiency, reliability and compactness of the conversion process. Method for the direct conversion to energy is now increasingly receiving attention. Of these, the fuel converts the chemical energy of fuel directly into electrical energy; fusion energy utilizes the energy released when two hydrogen molecules fuse into a heavier one, and thermoelectrically power generation uses a thermocouple. MHD power generation is another new process that has received worldwide attention.

The principal MHD effects were first demonstrated in the experiments of Faraday & Ritchie. Faraday (1832) find out experiments with flow of mercury in glass tubes placed between poles of a magnet and discovered that a voltage was induced across the tube by the motion of the mercury across the magnetic field, perpendicular to the direction of flow and to the magnetic field. Faraday observed that the current generated by this induced voltage interacted with the magnetic field to slow down the motion of the fluid, and he was aware of the fact that the current produced its own magnetic fluid that obeyed Ampere's right-hand rule and thus, in turn distorted the field of magnet.

Ritchie contemporary of Faraday, discovered in 1832 that when an electric field was applied to a conducting fluid perpendicularly to a magnetic field, it pumped the fluid in a direction perpendicular to both fields. Faraday also suggested that electrical power could be generated in a load circuit by the interaction of a flowing conducting fluid and a magnetic field.

The first astronomical application of the MHD theory occurred in 1899, when Bigalow suggested that the sun as a gigantic magnetic system. It remained, however, for Alfven(1942) to make a most significant contribution by discovering MHD waves in the sun. These waves are produced by disturbances which propagate simultaneously in the conducting fluid and the magnetic field. The analogy that explains the generation of an Alfven wave is that of a harp string plucked while submerged in a fluid. The string provides the elastic force and the fluid provides the inertia force, and they combine to propagate a perturbing wave through the fluid and the string.

In summary, MHD phenomena result from the mutual effect of a magnetic field and conducting fluid flowing across it. Thus, an electromagnetic force is produced in a fluid flowing across a transverse magnetic field, and the resulting current and magnetic field combine to produce a force that resists the fluid's motion. The current also generates its own magnetic field which

distorts the original magnetic field. An opposing or pumping force on the fluid can be produced by applying an electric field perpendicularly to the magnetic field. Disturbance in either the magnetic field or the fluid can propagate in both to produce MHD waves, as well as upstream and downstream-wake phenomena. The science of MHD is the detailed study of these phenomena, which occur in nature and are produced in engineering devices.

1.2. Some Useful Dimensionless Parameters

Reynolds number (R_e)

The Reynolds number R_e is the most important parameter of the fluid dynamics of a viscous fluid, which is defined by the following ratio

$$R_e = \frac{\text{inertia force}}{\text{viscous force}} = \frac{\text{mass} \times \text{acceleration}}{\text{shear stress} \times \text{cross sectional area}} = \frac{\rho L^3 \times \frac{U}{T}}{\mu \times \frac{U}{L} \times L^2} = \frac{\rho L U}{\mu} = \frac{L U}{\nu}$$

where, L and U denotes the characteristic length and velocity respectively and $\nu = \frac{\mu}{\rho}$ is the kinematic viscosity (μ is the viscosity and ρ is the density).

For if R_e is small, the viscous force will be predominant and the effect of viscosity will be felt in the whole flow field. On the other hand if R_e is large the inertia force will be predominant and in such case the effect of viscosity to be confined in a thin layer, near to the solid wall or other restricted region, which is known as boundary layer. However if R_e is very large, the flow ceases to be laminar and becomes turbulent. The Reynolds number at which transition from laminar to turbulent occurs is known as critical Reynolds number.

Reynolds in 1883 found that for flow in a circular pipe becomes turbulent when R_e exceeds the critical value 2300,

$$\text{i.e. } R_e = \left[\frac{\bar{U} d}{\nu} \right]_{\text{crit}} = 2300$$

where \bar{U} is the mean velocity and ' d ' is the diameter of the pipe.

When the viscous force is pre-dominating force, Reynolds number must be similar for dynamic similarity of two flows.

Prandtl number (P_r)

The Prandtl number P_r is the ratio of the kinematic viscosity to the thermal diffusivity and is defined by

$$P_r = \frac{\nu}{a} = \frac{\frac{\mu}{\rho}}{\frac{k}{\rho c_p}} = \frac{\mu c_p}{k}$$

where c_p is the specific heat at constant pressure and k is the thermal conductivity. The value of $\frac{k}{\rho c_p}$ is the thermal diffusivity due to the heat conduction. The smaller value of $\frac{k}{\rho c_p}$ is, the narrower is the region which affected by the heat conduction and it is known as the thermal boundary layer. The value of $\nu = \frac{\mu}{\rho}$ show the effect of viscosity of the fluid. Thus the Prandtl number shows that the relative importance of heat conduction and viscosity of a fluid. Evidently P_r varies from fluid to fluid. For air $P_r = 0.72$ (approx.), for water at 15.5°C , $P_r = 7.00$ (approx.), for mercury $P_r = 0.044$, but for high viscous fluid it may be very large, e.g. for glycerin $P_r = 7250$.

Magnetic Force number (M)

The magnetic force number is the ratio of the magnetic force to the inertia force and is defined by $M = \frac{\text{magnetic force}}{\text{inertia force}} = \frac{\mu_e^3 H_o^2 \sigma' L}{\rho U}$

Schmidt number (S_c)

The Schmidt number is the ratio of the viscous diffusivity to the chemical molecular diffusivity and is defined by $S_c = \frac{\text{viscous diffusivity}}{\text{chemical molecular diffusivity}} = \frac{\nu}{D_m}$

Grashof number (G_r)

The Grashof number is defined by $G_r = \frac{g\beta L^3 \nabla T}{\nu^2 T}$

and is a measure of the relative importance of the buoyancy and viscous forces. The larger it is, stronger is the convective current.

Modified Grashof number (G_m)

The Modified Grashof number is defined by $G_m = \frac{g\beta^* L^3 \nabla C}{\nu^2}$

Soret number (S_o)

The Soret number is defined by $S_o = \frac{D_m K_T (T_w - T_\infty)}{T_m \nu (C_w - C_\infty)}$

Magnetic diffusivity (P_m)

The magnetic diffusivity is defined by $P_m = \mu_e \sigma' \nu$

Eckert number (E_c)

The Eckert number is defined by $E_c = \frac{kU_0}{\sigma q c_p}$

1.3. MHD Boundary Layer and Related Transfer Phenomena

Boundary layer phenomena occur when the viscous effect may be considered to be confined in a very thin layer near to the boundaries and the non-dimensional diffusion parameter such as the Reynolds number, the Peclet number and the magnetic Reynolds number are very large. The boundary layers are then the velocity and thermal (or magnetic) boundary layers and each of its thickness is inversely proportional to the square root of the associated diffusion number. Prandtl observed, in classical fluid dynamics boundary layer theory, from experimental flows that for large Reynolds number, the viscosity and the thermal conductivity appreciably influences the flow only near a wall. When distance measurements in the flow direction are compared with a characteristic dimension in that direction, transverse measurement compared with the boundary layer thickness and velocities compared with the free stream velocity, the Navier-Stokes and energy equations can be considerably simplified neglecting small quantities. The flow directional component equations only remain and pressure is then only a function of the flow direction and can be determined from the non-viscous flow solution. Also the number of viscous term is reduced to the dominant term and the heat conduction flow direction is negligible.

There are two types of MHD boundary layer flows, by considering the limiting cases of a very large and a negligible small magnetic Reynolds number. When the magnetic Reynolds number is large; the magnetic boundary layer thickness is small and is of nearly the same size of the viscous and thermal boundary layers and then the equations of the MHD boundary layer must be solved simultaneously. On the other hand, when the magnetic Reynolds number is very small and the magnetic field is oriented in an arbitrary direction relative to a confining surface; the flow direction component of the magnetic interaction and the corresponding joule heating is only a function of the transverse magnetic field component and the local velocity in the flow direction. Changes in the transverse magnetic boundary layer are negligible. The thickness of the magnetic boundary layer is very large and the induced magnetic field is negligible. In this case the magnetic field moves with the flow and is called frozen mass.

1.4. MHD and Heat Transfer

With the advent of hypersonic flight, the field of MHD, as defined above, which has attracted the interest of aerodynamists and associated largely with liquid metal pumping. It is possible to alter the flow and the heat transfer around high velocity vehicles provided that the air is sufficiently ionized. Furthermore, the invention of high temperature facilities such as the shock tube plasma jet has provided laboratory sources of flowing ionized gas, which provide an incentive for the study of plasma accelerators and generators. As a result of this, many of the classical problems of fluid mechanics have been reinvestigated. Some of these analyses arose out of the natural tendency of scientists to search a new subject. In this case it was the academic problem of solving the equations of fluid mechanics with a new body force and another source of dissipation in the energy equation. Some time there were no practical applications for these results. As for example, natural convection MHD flows have been of interest to the engineering community only since the investigations, directly applicable to the problems in geophysics and astrophysics. But it was in the field of aerodynamic heating that the largest interest was awakened. Rossow (1957) presented the first paper on this subject. His result for incompressible constant property flat plate boundary layer flow indicated that the skin friction and heat transfer were reduced substantially when a transverse magnetic field was applied to the fluid. This encouraged a multitude analysis for every imaginable type of aerodynamic flow, and most of the research centered on the stagnation point, where in hypersonic flight, the highest degree of ionization could be expected. The result of these studies were sometimes contradictory concerning the amount by which the heat transfer would be reduced (some of this was due to misinterpretations and invalid comparison). Eventually, however, it was concluded that the field strength, necessary to provide sufficient shielding against heat fluxes during atmospheric flight, were not competitive (in terms of weight) with other method of cooling (Sutton and Gloersen, 1961). However the invention of new light weight super conducting magnets has revived interests in the problem of providing heat protection during the very high velocity re-entry from orbital and super orbital flight (Levy and Petschek, 1962).

1.5. Free Convection

In the studies related to heat transfer, considerable effort has been directed towards the convective mode, in which the relative motion of the fluid provides an additional mechanism for the transfer of energy and material, the latter being a more important consideration in cases where mass transfer, due to a concentration difference, occurs. Convection is inevitably coupled with the conductive mechanisms, since, although the fluid motion modifies the transport process, the eventual transfer of energy from one fluid element to another in its neighborhood is thorough

conduction. Also, at the surface the process is predominantly that of conduction because the relative fluid motion is brought to zero at the surface. A study of the convective heat transfer therefore involves the mechanisms of conduction and sometimes those of radiative processes as well, coupled with that fluid flow. These make the study of this mode of heat or mass transfer very complex, although its importance in technology and in nature can hardly be exaggerated.

The heat transfer in convective mode is divided into two basic processes. If no externally induced flow is provided and flow arises naturally simply owing to the effect of a density difference, resulting from a temperature or concentration difference in a body force field, such as the gravitational field, the process is referred to the *natural convection*. On the other hand if the motion of the fluid is caused by an external agent such as the externally imposed flow of a fluid stream over a heated object, the process is termed as *force convection*. In the force convection, the fluid flow may be the result of, for instance, a fan, a blower, the wind or the motion of the heated object itself. Such problems are very frequently encountered in technology where the heat transfers to or from a body is often due to an imposed flow of a fluid at a different temperature from that of a body. On the other side, in the natural convection, the density difference gives rise to buoyancy effects, owing to which the flow is generated. A heated body cooling in ambient air generates such a flow in the region surrounding it. Similarly the buoyant flow arising from heat rejection to the atmosphere and to other ambient media, circulations arising in heated rooms, in the atmosphere, and in bodies of water, rise of buoyant flow to cause thermal stratification of the medium, as in temperature inversion and many other such heat transfer process in our natural environment, as well as in many technological applications, are included in the area of natural convection. The flow may also arise owing to concentration differences such as those caused by salinity differences in the sea and by composition differences in chemical processing unit, and these cause a natural convection mass transfer.

Practically some time both processes, natural and forced convection are important and heat transfer is by mixed convection, in which neither mode is truly predominant. The main difference between the two really lies in the word external. A heated body lying in still air loses energy by natural convection. But it also generates a buoyant flow above it and body placed in that flow is subjected to an external flow and it becomes necessary to determine the natural, as well as the forced convection effects and the regime in which the heat transfer mechanisms lie.

When MHD become a popular subject, it was normal that these flows would be investigated with the additional ponder motive body force as well as the buoyancy force. At a first glance there seems to be no practical applications for these MHD solutions, for most heat exchangers utilize

liquids, whose conductivity is so small that prohibitively large magnetic fields are necessary to influence the flow. But some nuclear power plants employ heat exchangers with liquid metal coolants, so the application of moderate magnetic fields to change the convection pattern appears feasible. Another classical natural convection problem is the thermal instability that occurs in a liquid heated from below. This subject is of natural interest to geophysicists and astrophysicists, although some applications might arise in boiling heat transfer.

The basic concepts involved in employing the boundary layer approximation to natural convection flows are very similar to those in forced flows. The main difference lies in the fact the pressure in the region beyond the boundary layer is hydrostatic instead of being imposed by an external flow, and that the velocity outside the layer is zero. However the basic treatment and analysis remain the same, the book by Schlichting (1968) is an excellent collection of the boundary layer analysis. There are several methods for the solution of the boundary layer equations namely the similarity variable method, the perturbation method, analytical method, numerical method etc. and their details are available in the books by Rosenberg (1969), Patanker and Spalding (1970) and Spalding (1977).

1.6. Heat and Mass Transfer

The basic heat and mass transfer problem is governed by the combined buoyancy effects arising from the simultaneous diffusion of thermal energy and chemical species. Therefore the equations of continuity, momentum, energy, mass diffusion are coupled through the buoyancy terms alone, if there are other effects, such as the Soret and Duffor effects, they are neglected. This would again be valid for low species concentration levels. These additional effects have also been considered in several investigations, for example, the work of the Caldwell (1974), Groot and Mozur (1962), Hurel and Jakeman (1971) and Legros, et al. (1968).

Somers (1956) considered combined buoyancy mechanisms for flow adjacent to a wet isothermal vertical surface in an unsaturated environment. Uniform temperature and uniform species concentration at the surface were assumed and an integral analysis was carried out to obtain the result which is expected to be valid for Pr and Sc values around 1.0 with one buoyancy effect being small compared with the other. Adams and McFadden (1966) presented experimental measurements of heat and mass transfer parameters, with opposed buoyancy effects. Gebhart and Pera (1971) studied laminar vertical natural convection flows resulting from the combined buoyancy mechanisms in terms of similarity solutions.

Nanousis and Goudas (1979) have studied the effects of mass transfer on free convection problem in the Stokes problem for an infinite vertical limiting surface. Georgantopolous and Nanousis (1980) have considered the effects of the mass transfer on free convection flow of an electrically conducting viscous fluid (e.g. of a stellar atmosphere, of star) in the presence of transverse magnetic field. Solution for the velocity and skin friction in closed form are obtained with the help of the Laplace transformation technique, and the results obtained for the various values of the parameters S_c , P_r and M are given in graphical form. Raptis and Kafoussias (1982) presented the analysis of free convection and mass transfer steady hydro magnetic flow of an electrically conducting viscous incompressible fluid, through a porous medium, occupying a semi infinite region of the space bounded by an infinite vertical porous plate under the action of transverse magnetic field. Agrawal et al. (1983) have investigated the effect of Hall current on the combined effect of thermal and mass diffusion of an electrically conducting liquid past an infinite vertical porous plate, when the free stream oscillates about constant non zero mean. The velocity and temperature distributions are shown on graphs for different values of parameters.

1.7. Thermal Diffusion

In the above mentioned studies heat and mass transfer occur simultaneously in a moving fluid, where the relations between the fluxes and driving potentials are of more complicated nature. In general the thermal diffusion effects is of a small order of magnitude, described by Fourier or Flick's law, is often neglected in heat and mass transfer processes. Mass fluxes can also be created by temperature gradients and this is Soret or thermal diffusion effect. There are however, exceptions. The thermal diffusion effect for instance has been utilized for isotope separation and in mixtures between gases with very light molecular weight (H_2 , He) and of medium molecular weight (N_2 , air). Kafoussias (1992) studied the MHD free convection and mass transfer flow, past an infinite vertical plate moving on its own plane, taken into account the thermal diffusion when (i) the boundary surface is impulsively started moving in its own plane (I.S.P) and (ii) it is uniformly accelerated (U.A.P). The problem is solved with the help of Laplace transformation method and analytical expressions are given for the velocity field as well as for the skin friction for the above-mentioned two different cases. The effect of the velocity and skin friction of the various dimensionless parameters entering into the problem is discussed with the help of graph. For the both cases, it is seen from the figure that the effect of magnetic parameters M is to decrease the fluid (water) velocity inside the boundary layer. This influence of the magnetic field on the velocity field is more evident in the presence of the thermal diffusion. From the same figures it is also concluded that the fluid velocity rises due to greater thermal diffusion. Hence, the velocity field is considerably affected by the magnetic field and the thermal diffusion.

Nanousis(1992) extended the work of Kafoussias(1992) to the case of rotating fluid taking into account the Soret effect. The plate is assumed to be moving on its own plane with arbitrary velocity $U_o f(t')$, where U_o is a constant velocity and $f(t')$ is a non dimensional function of time t' . The solution of the problem is also obtained with the help of Laplace transformation technique. Analytical expression is given for the velocity field and for the skin friction for two different cases; **Case-I:** When the plate is impulsively started, moving on it own plane and **Case-II:** When the plate is uniformly accelerated, the effect on the velocity field and skin friction of various dimensionless parameters entering in to the problem, specially of the Soret number S_o , are discussed with the help of graphs. In the case of an impulsively started plate and uniformly accelerated plate, it is seen the primary velocity to increase with the increase of S_o and the magnetic parameter M . The mass fluxes can also be created by temperature gradients and this is the Soret or the thermal diffusion effect.

Chapter 2

The Basic Governing Equations

The generalized Continuity equation, Momentum equation, Energy equation, Magnetic induction equation, Concentration equation together with the Ohm's law and Maxwell equations form the basis of studying of magneto fluid dynamics (MFD). These equations are as follows:

Continuity equation for viscous compressible electrically conducting fluid is

$$\frac{\partial \rho}{\partial t} + \nabla \cdot (\rho \mathbf{q}) = 0 \quad (2.1)$$

where ρ the fluid density and \mathbf{q} is the fluid velocity.

For incompressible fluid ($\rho = \text{constant}$) the equation yields

$$\nabla \cdot \mathbf{q} = 0 \quad \text{where } \mathbf{q} = (u, v, w) \quad (2.1a)$$

Momentum equation for viscous compressible fluid is

$$\frac{d\mathbf{q}}{dt} = \mathbf{F} - \frac{1}{\rho} \nabla p + \nu \nabla^2 \mathbf{q} + \frac{\nu}{3} \nabla (\nabla \cdot \mathbf{q}) \quad (2.2)$$

For incompressible ($\nabla \cdot \mathbf{q} = 0$) the equation (2.2) yields

$$\frac{\partial \mathbf{q}}{\partial t} + (\mathbf{q} \cdot \nabla) \mathbf{q} = \mathbf{F} - \frac{1}{\rho} \nabla p + \nu \nabla^2 \mathbf{q} \quad (2.2a)$$

When the fluid moves through a magnetic field, then the equation (2.2a) becomes to be Magnetohydrodynamic (MHD) equation as

$$\frac{\partial \mathbf{q}}{\partial t} + (\mathbf{q} \cdot \nabla) \mathbf{q} = \mathbf{F} - \frac{1}{\rho} \nabla p + \nu \nabla^2 \mathbf{q} + \frac{\mu_e}{\rho} (\mathbf{J} \wedge \mathbf{H}) \quad (2.2b)$$

Magnetic induction equation for a viscous incompressible electrically conducting fluid is

$$\frac{\partial \mathbf{H}}{\partial t} + (\mathbf{q} \cdot \nabla) \mathbf{H} = (\mathbf{H} \cdot \nabla) \mathbf{q} + \frac{1}{\mu_e \sigma'} \nabla^2 \mathbf{H} \quad (2.3)$$

Energy equation for a viscous incompressible electrically conducting fluid is

$$\frac{\partial T}{\partial t} + (\mathbf{q} \cdot \nabla) T = \frac{k}{\rho c_p} \nabla^2 T + \frac{1}{\rho c_p} \phi + \frac{\mathbf{J}^2}{\rho c_p \sigma'} \quad (2.4)$$

The Concentration equation for a viscous incompressible electrically conducting fluid (in the absence of heat source, viscous dissipation and Joule heating term) is

$$\frac{\partial C}{\partial t} + (\mathbf{q} \cdot \nabla)C = D_m \nabla^2 C + \frac{D_m K_T}{T_m} \nabla^2 T \quad (2.5)$$

Generalized Ohm's law is of the form

$$\begin{aligned} \mathbf{J} &= \sigma'(\mathbf{E} + \mathbf{q} \wedge \mathbf{B}) - \frac{\sigma'}{en_e}(\mathbf{J} \wedge \mathbf{B} - \nabla P_e) \\ &= \sigma'(\mathbf{E} + \mathbf{q} \wedge \mathbf{B}) - \frac{\sigma'}{en_e} \mathbf{J} \wedge \mathbf{B} + \frac{\sigma'}{en_e} \nabla P_e \\ \Rightarrow \mathbf{J} + \frac{\sigma'}{en_e} \mathbf{J} \wedge \mathbf{B} &= \sigma'(\mathbf{E} + \mathbf{q} \wedge \mathbf{B}) + \frac{\sigma'}{en_e} \nabla P_e \end{aligned} \quad (2.6)$$

The Maxwell equation's are

$$\nabla \wedge \mathbf{H} = \mathbf{J} \quad (2.7a)$$

$$\nabla \wedge \mathbf{E} = 0 \quad (2.7b)$$

$$\nabla \cdot \mathbf{B} = 0 \quad (2.7c)$$

where, \mathbf{F} is the body force per unit mass, p is the fluid pressure, P_e is the pressure of electron, μ_e is the magnetic permeability, \mathbf{J} is the current density vector, \mathbf{B} is the magnetic field vector, \mathbf{E} is the electric field vector, \mathbf{H} is the magnetic field intensity, T is the fluid temperature, T_m is the mean fluid temperature, C is the species concentration variable, σ' is the electrical conductivity, e is the charge of electron, n_e is the number of density electron, c_p is the specific heat at constant pressure, k is the thermal conductivity, K_T is the thermal diffusion ratio and D_m is the coefficient of mass diffusivity.

Also φ denotes the dissipation function, involving the viscous stress and it represents the rate at which energy is being dissipated per unit volume through the action of viscosity. In fact the energy is dissipated in a viscous fluid in motion on account of internal friction and for incompressible fluid

$$\varphi = \mu \left[\left\{ \left(\frac{\partial u}{\partial x} \right)^2 + \left(\frac{\partial v}{\partial y} \right)^2 + \left(\frac{\partial w}{\partial z} \right)^2 \right\} + \left(\frac{\partial v}{\partial x} + \frac{\partial u}{\partial y} \right)^2 + \left(\frac{\partial w}{\partial y} + \frac{\partial v}{\partial z} \right)^2 + \left(\frac{\partial u}{\partial z} + \frac{\partial w}{\partial x} \right)^2 \right] \quad (2.8)$$

which is always positive, since all the terms are quadratic, where μ is the coefficient of viscosity.

Let us consider a heat and mass transfer by mixed convection flow of an incompressible electrically conducting viscous fluid past an electrically non-conducting vertical porous plate $y = 0$. Introducing the Cartesian co-ordinate system x -axis is chosen along the direction of flow and y -axis is normal to it. A uniform magnetic field is applied normal to the flow. In addition the analysis is based on the following assumption.

The magnetic Reynolds number of the flow is taken to be large so that the induced magnetic field is not negligible. The magnetic field is of the form:

$$\mathbf{H} = (H_x, H_y, 0)$$

The equation of the conservation of electric charge is $\nabla \cdot \mathbf{J} = 0$, where $\mathbf{J} = (J_x, J_y, 0)$, the direction of propagation is considered only along the y -axis and does not have any variation along the y -axis and the y derivative of \mathbf{J} namely $\frac{\partial J_y}{\partial y} = 0$, resulting in $J_y = \text{constant}$. Since the plate electrically non-conducting, this constant is zero and hence $J_y = 0$ everywhere in the flow.

The divergence equation of Maxwell equations is $\nabla \cdot \mathbf{H} = 0$

which gives $\frac{\partial H_y}{\partial y} = 0 \Rightarrow H_y = \text{constant} = H_0$ (say) So $\mathbf{H} = (H_x, H_0, 0)$

Now, from equation (2.7a) we have,

$$\begin{aligned} \mathbf{J} &= \nabla \wedge \mathbf{H} \\ &= \begin{vmatrix} \hat{i} & \hat{j} & \hat{k} \\ \frac{\partial}{\partial x} & \frac{\partial}{\partial y} & \frac{\partial}{\partial z} \\ H_x & H_0 & 0 \end{vmatrix} \\ &= \hat{i} \left(0 - \frac{\partial H_0}{\partial z} \right) - \hat{j} \left(0 - \frac{\partial H_x}{\partial z} \right) + \hat{k} \left(\frac{\partial H_0}{\partial x} - \frac{\partial H_x}{\partial y} \right) \\ &= \hat{i} (0 - 0) - \hat{j} \left(0 - \frac{\partial H_x}{\partial z} \right) + \hat{k} \left(0 - \frac{\partial H_x}{\partial y} \right) \\ \Rightarrow \mathbf{J} &= \left(0, \frac{\partial H_x}{\partial z}, -\frac{\partial H_x}{\partial y} \right) \end{aligned} \quad (2.9)$$



$$\begin{aligned}
\text{Therefore } \frac{\mu_e}{\rho} (\mathbf{J} \wedge \mathbf{H}) &= \frac{\mu_e}{\rho} \begin{vmatrix} \hat{i} & \hat{j} & \hat{k} \\ 0 & \frac{\partial H_x}{\partial z} & -\frac{\partial H_x}{\partial y} \\ H_x & H_0 & 0 \end{vmatrix} \\
&= \frac{\mu_e}{\rho} \left[\hat{i} \left(0 + H_0 \frac{\partial H_x}{\partial y} \right) - \hat{j} \left(0 + H_x \frac{\partial H_x}{\partial y} \right) + \hat{k} \left(0 - H_x \frac{\partial H_x}{\partial z} \right) \right] \\
&= \frac{\mu_e}{\rho} \left(H_0 \frac{\partial H_x}{\partial y}, -H_x \frac{\partial H_x}{\partial y}, -H_x \frac{\partial H_x}{\partial z} \right)
\end{aligned} \tag{2.10}$$

$$\text{Also } \mathbf{F} = (F_x, F_y, F_z) \tag{2.11}$$

Thus the momentum equation (2.2b) can be written in the Cartesian form with the help of equations (2.10) and (2.11) as

$$\frac{\partial u}{\partial t} + u \frac{\partial u}{\partial x} + v \frac{\partial u}{\partial y} + w \frac{\partial u}{\partial z} = F_x - \frac{1}{\rho} \frac{\partial P}{\partial x} + \nu \left(\frac{\partial^2 u}{\partial x^2} + \frac{\partial^2 u}{\partial y^2} + \frac{\partial^2 u}{\partial z^2} \right) + \frac{\mu_e}{\rho} H_0 \frac{\partial H_x}{\partial y} \tag{2.12a}$$

$$\frac{\partial v}{\partial t} + u \frac{\partial v}{\partial x} + v \frac{\partial v}{\partial y} + w \frac{\partial v}{\partial z} = F_y - \frac{1}{\rho} \frac{\partial P}{\partial y} + \nu \left(\frac{\partial^2 v}{\partial x^2} + \frac{\partial^2 v}{\partial y^2} + \frac{\partial^2 v}{\partial z^2} \right) - \frac{\mu_e}{\rho} H_x \frac{\partial H_x}{\partial y} \tag{2.12b}$$

$$\frac{\partial w}{\partial t} + u \frac{\partial w}{\partial x} + v \frac{\partial w}{\partial y} + w \frac{\partial w}{\partial z} = F_z - \frac{1}{\rho} \frac{\partial P}{\partial z} + \nu \left(\frac{\partial^2 w}{\partial x^2} + \frac{\partial^2 w}{\partial y^2} + \frac{\partial^2 w}{\partial z^2} \right) - \frac{\mu_e}{\rho} H_x \frac{\partial H_x}{\partial z} \tag{2.12c}$$

$$\text{Again } \mathbf{H} = (H_x, H_0, 0)$$

$$\text{and } \mathbf{q} \cdot \nabla = u \frac{\partial}{\partial x} + v \frac{\partial}{\partial y} + w \frac{\partial}{\partial z}$$

$$\begin{aligned}
\therefore (\mathbf{q} \cdot \nabla) \mathbf{H} &= \left(u \frac{\partial}{\partial x} + v \frac{\partial}{\partial y} + w \frac{\partial}{\partial z} \right) (\hat{i} H_x + \hat{j} H_0 + \hat{k} 0) \\
&= \hat{i} \left(u \frac{\partial H_x}{\partial x} + v \frac{\partial H_x}{\partial y} + w \frac{\partial H_x}{\partial z} \right) + \hat{j} \left(u \frac{\partial H_0}{\partial x} + v \frac{\partial H_0}{\partial y} + w \frac{\partial H_0}{\partial z} \right) + \hat{k} 0 \\
&= \hat{i} \left(u \frac{\partial H_x}{\partial x} + v \frac{\partial H_x}{\partial y} + w \frac{\partial H_x}{\partial z} \right) + 0 + 0 \quad \left[\because \frac{\partial H_0}{\partial x} = \frac{\partial H_0}{\partial y} = \frac{\partial H_0}{\partial z} = 0 \right] \\
&= \hat{i} \left(u \frac{\partial H_x}{\partial x} + v \frac{\partial H_x}{\partial y} + w \frac{\partial H_x}{\partial z} \right)
\end{aligned} \tag{2.13}$$

$$\text{Again } (\mathbf{H} \cdot \nabla) \mathbf{q} = \left[(\hat{i} H_x + \hat{j} H_0 + \hat{k} 0) \cdot \left(\hat{i} \frac{\partial}{\partial x} + \hat{j} \frac{\partial}{\partial y} + \hat{k} \frac{\partial}{\partial z} \right) \right] (\hat{i} u + \hat{j} v + \hat{k} w)$$

$$\begin{aligned}\Rightarrow (\mathbf{H} \cdot \nabla) \mathbf{q} &= \left(H_x \frac{\partial}{\partial x} + H_o \frac{\partial}{\partial y} + 0 \right) (\hat{i}u + \hat{j}v + \hat{k}w) \\ &= \hat{i} \left(H_x \frac{\partial u}{\partial x} + H_o \frac{\partial u}{\partial y} \right) + \hat{j} \left(H_x \frac{\partial v}{\partial x} + H_o \frac{\partial v}{\partial y} \right) + \hat{k} \left(H_x \frac{\partial w}{\partial x} + H_o \frac{\partial w}{\partial y} \right)\end{aligned}\quad (2.14)$$

$$\begin{aligned}\text{Also } \frac{1}{\mu_e \sigma'} \nabla^2 \mathbf{H} &= \frac{1}{\mu_e \sigma'} \left(\frac{\partial^2}{\partial x^2} + \frac{\partial^2}{\partial y^2} + \frac{\partial^2}{\partial z^2} \right) (\hat{i}H_x + \hat{j}H_o + \hat{k}0) \\ &= \frac{1}{\mu_e \sigma'} \left[\hat{i} \left(\frac{\partial^2 H_x}{\partial x^2} + \frac{\partial^2 H_x}{\partial y^2} + \frac{\partial^2 H_x}{\partial z^2} \right) + \hat{j} \left(\frac{\partial^2 H_o}{\partial x^2} + \frac{\partial^2 H_o}{\partial y^2} + \frac{\partial^2 H_o}{\partial z^2} \right) + \hat{k}0 \right] \\ &= \frac{1}{\mu_e \sigma'} \left[\hat{i} \left(\frac{\partial^2 H_x}{\partial x^2} + \frac{\partial^2 H_x}{\partial y^2} + \frac{\partial^2 H_x}{\partial z^2} \right) + \hat{j}0 + \hat{k}0 \right] \\ &= \frac{1}{\mu_e \sigma'} \left(\frac{\partial^2 H_x}{\partial x^2} + \frac{\partial^2 H_x}{\partial y^2} + \frac{\partial^2 H_x}{\partial z^2}, 0, 0 \right)\end{aligned}\quad (2.15)$$

Thus the magnetic induction equation (2.3) yields

$$\frac{\partial H_x}{\partial t} + u \frac{\partial H_x}{\partial x} + v \frac{\partial H_x}{\partial y} + w \frac{\partial H_x}{\partial z} = H_x \frac{\partial u}{\partial x} + H_o \frac{\partial u}{\partial y} + \frac{1}{\mu_e \sigma'} \left(\frac{\partial^2 H_x}{\partial x^2} + \frac{\partial^2 H_x}{\partial y^2} + \frac{\partial^2 H_x}{\partial z^2} \right)\quad (2.16a)$$

$$0 = H_x \frac{\partial v}{\partial x} + H_o \frac{\partial v}{\partial y}\quad (2.16b)$$

$$0 = H_x \frac{\partial w}{\partial x} + H_o \frac{\partial w}{\partial y}\quad (2.16c)$$

$$\text{Again, } \mathbf{J} = \nabla \wedge \mathbf{H} = \left(0, \frac{\partial H_x}{\partial z}, -\frac{\partial H_x}{\partial y} \right)$$

$$\therefore \mathbf{J}^2 = \left[\left(\frac{\partial H_x}{\partial z} \right)^2 + \left(-\frac{\partial H_x}{\partial y} \right)^2 \right]$$

$$\therefore \frac{\mathbf{J}^2}{\rho c_p \sigma'} = \frac{1}{\rho c_p \sigma'} \left[\left(\frac{\partial H_x}{\partial z} \right)^2 + \left(\frac{\partial H_x}{\partial y} \right)^2 \right]\quad (2.17)$$

Thus the energy equation (2.4) become

$$\frac{\partial T}{\partial t} + u \frac{\partial T}{\partial x} + v \frac{\partial T}{\partial y} + w \frac{\partial T}{\partial z} = \frac{k}{\rho c_p} \left(\frac{\partial^2 T}{\partial x^2} + \frac{\partial^2 T}{\partial y^2} + \frac{\partial^2 T}{\partial z^2} \right) + \frac{1}{\rho c_p} \varphi + \frac{1}{\rho c_p \sigma'} \left[\left(\frac{\partial H_x}{\partial z} \right)^2 + \left(\frac{\partial H_x}{\partial y} \right)^2 \right]\quad (2.18)$$

$$\text{where } \varphi = \mu \left[\left(\frac{\partial u}{\partial x} \right)^2 + \left(\frac{\partial v}{\partial y} \right)^2 + \left(\frac{\partial w}{\partial z} \right)^2 \right] + \left(\frac{\partial v}{\partial x} + \frac{\partial u}{\partial y} \right)^2 + \left(\frac{\partial w}{\partial y} + \frac{\partial v}{\partial z} \right)^2 + \left(\frac{\partial u}{\partial z} + \frac{\partial w}{\partial x} \right)^2$$

and the species concentration equation (2.5) become

$$\frac{\partial C}{\partial t} + u \frac{\partial C}{\partial x} + v \frac{\partial C}{\partial y} + w \frac{\partial C}{\partial z} = D_m \left(\frac{\partial^2 C}{\partial x^2} + \frac{\partial^2 C}{\partial y^2} + \frac{\partial^2 C}{\partial z^2} \right) + \frac{D_m K_T}{T_m} \left(\frac{\partial^2 T}{\partial x^2} + \frac{\partial^2 T}{\partial y^2} + \frac{\partial^2 T}{\partial z^2} \right) \quad (2.19)$$

Thus in three dimensional cartesian coordinate system the continuity equation, the momentum equation, the magnetic induction equation and the species concentration equation become

Continuity equation
$$\frac{\partial u}{\partial x} + \frac{\partial v}{\partial y} + \frac{\partial w}{\partial z} = 0 \quad (2.20)$$

Momentum equation

$$\frac{\partial u}{\partial t} + u \frac{\partial u}{\partial x} + v \frac{\partial u}{\partial y} + w \frac{\partial u}{\partial z} = F_x - \frac{1}{\rho} \frac{\partial P}{\partial x} + \nu \left(\frac{\partial^2 u}{\partial x^2} + \frac{\partial^2 u}{\partial y^2} + \frac{\partial^2 u}{\partial z^2} \right) + \frac{\mu_e}{\rho} H_o \frac{\partial H_x}{\partial y} \quad (2.21a)$$

$$\frac{\partial v}{\partial t} + u \frac{\partial v}{\partial x} + v \frac{\partial v}{\partial y} + w \frac{\partial v}{\partial z} = F_y - \frac{1}{\rho} \frac{\partial P}{\partial y} + \nu \left(\frac{\partial^2 v}{\partial x^2} + \frac{\partial^2 v}{\partial y^2} + \frac{\partial^2 v}{\partial z^2} \right) - \frac{\mu_e}{\rho} H_x \frac{\partial H_x}{\partial y} \quad (2.21b)$$

$$\frac{\partial w}{\partial t} + u \frac{\partial w}{\partial x} + v \frac{\partial w}{\partial y} + w \frac{\partial w}{\partial z} = F_z - \frac{1}{\rho} \frac{\partial P}{\partial z} + \nu \left(\frac{\partial^2 w}{\partial x^2} + \frac{\partial^2 w}{\partial y^2} + \frac{\partial^2 w}{\partial z^2} \right) - \frac{\mu_e}{\rho} H_x \frac{\partial H_x}{\partial z} \quad (2.21c)$$

Magnetic induction equation

$$\frac{\partial H_x}{\partial t} + u \frac{\partial H_x}{\partial x} + v \frac{\partial H_x}{\partial y} + w \frac{\partial H_x}{\partial z} = H_x \frac{\partial u}{\partial x} + H_o \frac{\partial u}{\partial y} + \frac{1}{\mu_e \sigma'} \left(\frac{\partial^2 H_x}{\partial x^2} + \frac{\partial^2 H_x}{\partial y^2} + \frac{\partial^2 H_x}{\partial z^2} \right) \quad (2.22a)$$

$$0 = H_x \frac{\partial v}{\partial x} + H_o \frac{\partial v}{\partial y} \quad (2.22b)$$

$$0 = H_x \frac{\partial w}{\partial x} + H_o \frac{\partial w}{\partial y} \quad (2.22c)$$

Energy equation

$$\frac{\partial T}{\partial t} + u \frac{\partial T}{\partial x} + v \frac{\partial T}{\partial y} + w \frac{\partial T}{\partial z} = \frac{k}{\rho c_p} \left(\frac{\partial^2 T}{\partial x^2} + \frac{\partial^2 T}{\partial y^2} + \frac{\partial^2 T}{\partial z^2} \right) + \frac{1}{\rho c_p} \varphi + \frac{1}{\rho c_p \sigma'} \left[\left(\frac{\partial H_x}{\partial z} \right)^2 + \left(\frac{\partial H_x}{\partial y} \right)^2 \right] \quad (2.23)$$

where $\varphi = \mu \left[\left(\frac{\partial u}{\partial x} \right)^2 + \left(\frac{\partial v}{\partial y} \right)^2 + \left(\frac{\partial w}{\partial z} \right)^2 \right] + \left(\frac{\partial v}{\partial x} + \frac{\partial u}{\partial y} \right)^2 + \left(\frac{\partial w}{\partial y} + \frac{\partial v}{\partial z} \right)^2 + \left(\frac{\partial u}{\partial z} + \frac{\partial w}{\partial x} \right)^2 \right]$

Concentration equation

$$\frac{\partial C}{\partial t} + u \frac{\partial C}{\partial x} + v \frac{\partial C}{\partial y} + w \frac{\partial C}{\partial z} = D_m \left(\frac{\partial^2 C}{\partial x^2} + \frac{\partial^2 C}{\partial y^2} + \frac{\partial^2 C}{\partial z^2} \right) + \frac{D_m K_T}{T_m} \left(\frac{\partial^2 T}{\partial x^2} + \frac{\partial^2 T}{\partial y^2} + \frac{\partial^2 T}{\partial z^2} \right) \quad (2.24)$$

The next section deals with the specific problem.

Case-I

Let us consider an unsteady heat and mass transfer by mixed convection flow of an electrically conducting viscous fluid past an infinite vertical porous plate $y = 0$. The flow is also assumed to be in x -direction which is taken along the plate in upward direction and y -axis is normal to it. The temperature and species concentration at the plate are instantly raised from T_w and C_w to T_∞ and C_∞ respectively. Which are thereafter maintained as constant, where T_∞ and C_∞ the temperature and species concentration of the uniform flow respectively. A uniform magnetic field strength \mathbf{H} is applied to the plate to be acting along the y -axis, which is electrically non-conducting.

In the heat and mass transfer by mixed convection flow along the vertical plate, the body force and the pressure gradient along the direction is

$$g\beta(T - T_\infty) + g\beta^*(C - C_\infty) \quad (2.25)$$

where g is the acceleration due to the gravitation, β is the coefficient of volume expansion, β^* is the volumetric coefficient expansion with concentration.

With reference to the above assumptions, the continuity equation (2.20), the momentum equations (2.21a)-(2.21c), the magnetic induction equations (2.22a)-(2.22c), the energy equation (2.23) and the species concentration equation (2.24) become:

$$\text{Continuity equation} \quad \frac{\partial u}{\partial x} + \frac{\partial v}{\partial y} + \frac{\partial w}{\partial z} = 0 \quad (2.26)$$

Momentum equation

$$\frac{\partial u}{\partial t} + u \frac{\partial u}{\partial x} + v \frac{\partial u}{\partial y} + w \frac{\partial u}{\partial z} = g\beta(T - T_\infty) + g\beta^*(C - C_\infty) + \nu \left(\frac{\partial^2 u}{\partial x^2} + \frac{\partial^2 u}{\partial y^2} + \frac{\partial^2 u}{\partial z^2} \right) + \frac{\mu_e}{\rho} H_o \frac{\partial H_x}{\partial y} \quad (2.27a)$$

$$\frac{\partial v}{\partial t} + u \frac{\partial v}{\partial x} + v \frac{\partial v}{\partial y} + w \frac{\partial v}{\partial z} = \nu \left(\frac{\partial^2 v}{\partial x^2} + \frac{\partial^2 v}{\partial y^2} + \frac{\partial^2 v}{\partial z^2} \right) - \frac{\mu_e}{\rho} H_x \frac{\partial H_x}{\partial y} \quad (2.27b)$$

$$\frac{\partial w}{\partial t} + u \frac{\partial w}{\partial x} + v \frac{\partial w}{\partial y} + w \frac{\partial w}{\partial z} = \nu \left(\frac{\partial^2 w}{\partial x^2} + \frac{\partial^2 w}{\partial y^2} + \frac{\partial^2 w}{\partial z^2} \right) - \frac{\mu_e}{\rho} H_x \frac{\partial H_x}{\partial z} \quad (2.27c)$$

Magnetic induction equation

$$\frac{\partial H_x}{\partial t} + u \frac{\partial H_x}{\partial x} + v \frac{\partial H_x}{\partial y} + w \frac{\partial H_x}{\partial z} = H_x \frac{\partial u}{\partial x} + H_o \frac{\partial u}{\partial y} + \frac{1}{\mu_e \sigma'} \left(\frac{\partial^2 H_x}{\partial x^2} + \frac{\partial^2 H_x}{\partial y^2} + \frac{\partial^2 H_x}{\partial z^2} \right) \quad (2.28a)$$

$$0 = H_x \frac{\partial v}{\partial x} + H_o \frac{\partial v}{\partial y} \quad (2.28b)$$

$$0 = H_x \frac{\partial w}{\partial x} + H_o \frac{\partial w}{\partial y} \quad (2.28c)$$

Energy equation

$$\frac{\partial T}{\partial t} + u \frac{\partial T}{\partial x} + v \frac{\partial T}{\partial y} + w \frac{\partial T}{\partial z} = \frac{k}{\rho c_p} \left(\frac{\partial^2 T}{\partial x^2} + \frac{\partial^2 T}{\partial y^2} + \frac{\partial^2 T}{\partial z^2} \right) + \frac{1}{\rho c_p} \varphi + \frac{1}{\rho c_p \sigma'} \left[\left(\frac{\partial H_x}{\partial z} \right)^2 + \left(\frac{\partial H_x}{\partial y} \right)^2 \right] \quad (2.29)$$

$$\text{where } \varphi = \mu \left[\left\{ \left(\frac{\partial u}{\partial x} \right)^2 + \left(\frac{\partial v}{\partial y} \right)^2 + \left(\frac{\partial w}{\partial z} \right)^2 \right\} + \left(\frac{\partial v}{\partial x} + \frac{\partial u}{\partial y} \right)^2 + \left(\frac{\partial w}{\partial y} + \frac{\partial v}{\partial z} \right)^2 + \left(\frac{\partial u}{\partial z} + \frac{\partial w}{\partial x} \right)^2 \right]$$

Concentration equation

$$\frac{\partial C}{\partial t} + u \frac{\partial C}{\partial x} + v \frac{\partial C}{\partial y} + w \frac{\partial C}{\partial z} = D_m \left(\frac{\partial^2 C}{\partial x^2} + \frac{\partial^2 C}{\partial y^2} + \frac{\partial^2 C}{\partial z^2} \right) + \frac{D_m K_T}{T_m} \left(\frac{\partial^2 T}{\partial x^2} + \frac{\partial^2 T}{\partial y^2} + \frac{\partial^2 T}{\partial z^2} \right) \quad (2.30)$$

Since the plate occupying the plane $y=0$ is of infinite extent and the fluid motion is unsteady, so all the physical quantities will depend only upon y and t . Thus the given governing equations (2.26)-(2.30) reduced to one dimensional equations, which are as follows

$$\text{Continuity equation} \quad \frac{\partial v}{\partial y} = 0 \quad (2.31)$$

Momentum equation

$$\frac{\partial u}{\partial t} + v \frac{\partial u}{\partial y} = g\beta(T - T_\infty) + g\beta^*(C - C_\infty) + \nu \frac{\partial^2 u}{\partial y^2} + \frac{\mu_e}{\rho} H_o \frac{\partial H_x}{\partial y} \quad (2.32a)$$

$$\frac{\partial v}{\partial t} + v \frac{\partial v}{\partial y} = \nu \frac{\partial^2 v}{\partial y^2} - \frac{\mu_e}{\rho} H_x \frac{\partial H_x}{\partial y} \quad (2.32b)$$

Magnetic induction equation

$$\frac{\partial H_x}{\partial t} + v \frac{\partial H_x}{\partial y} = H_o \frac{\partial u}{\partial y} + \frac{1}{\mu_e \sigma'} \frac{\partial^2 H_x}{\partial y^2} \quad (2.33a)$$

$$0 = H_o \frac{\partial v}{\partial y} \quad (2.33b)$$

Energy equation

$$\frac{\partial T}{\partial t} + v \frac{\partial T}{\partial y} = \frac{k}{\rho c_p} \frac{\partial^2 T}{\partial y^2} + \frac{\mu}{\rho c_p} \left[\left(\frac{\partial u}{\partial y} \right)^2 + \left(\frac{\partial v}{\partial y} \right)^2 \right] + \frac{1}{\rho c_p \sigma'} \left(\frac{\partial H_x}{\partial y} \right)^2 \quad (2.34)$$

Concentration equation

$$\frac{\partial C}{\partial t} + v \frac{\partial C}{\partial y} = D_m \frac{\partial^2 C}{\partial y^2} + \frac{D_m K_T}{T_m} \frac{\partial^2 T}{\partial y^2} \quad (2.35)$$

Since the magnetic Reynolds number of the flow be large so that the viscosity of the fluid be small. Let δ be the small thickness of the boundary layer and $\varepsilon \ll 1$ be the order of magnitude of δ i. e. $O(\delta) = \varepsilon$, then we can write

$$O(y) = \varepsilon, \quad O(v) = \varepsilon, \quad O(H_o) = \varepsilon$$

$$\text{Also we assume that} \quad O(u) = 1, \quad O(t) = 1, \quad O(H_x) = 1,$$

Hence

$$\begin{aligned} O\left(\frac{\partial u}{\partial t}\right) &= 1, & O\left(\frac{\partial u}{\partial y}\right) &= \frac{1}{\varepsilon}, & O\left(\frac{\partial^2 u}{\partial y^2}\right) &= \frac{1}{\varepsilon^2}, & O\left(\frac{\partial H_x}{\partial y}\right) &= \frac{1}{\varepsilon}, \\ O\left(\frac{\partial v}{\partial t}\right) &= \varepsilon, & O\left(\frac{\partial v}{\partial y}\right) &= 1, & O\left(\frac{\partial^2 v}{\partial y^2}\right) &= \frac{1}{\varepsilon} \\ O\left(\frac{\partial H_x}{\partial t}\right) &= 1 & O\left(\frac{\partial^2 H_x}{\partial y^2}\right) &= \frac{1}{\varepsilon^2} \end{aligned}$$

within the boundary layer.

Then the equations (2.31)—(2.33c) with order become

$$\text{Continuity equation} \quad \frac{\partial v}{\partial y} = 0 \quad (2.36)$$

1

Momentum equation

$$\frac{\partial u}{\partial t} + v \frac{\partial u}{\partial y} = g\beta(T - T_\infty) + g\beta^*(C - C_\infty) + \nu \frac{\partial^2 u}{\partial y^2} + \frac{\mu_e}{\rho} H_o \frac{\partial H_x}{\partial y} \quad (2.37a)$$

$$1 \quad \varepsilon \quad \frac{1}{\varepsilon} \quad \frac{1}{\varepsilon^2} \quad \varepsilon \quad \frac{1}{\varepsilon}$$

$$\frac{\partial v}{\partial t} + v \frac{\partial v}{\partial y} = \nu \frac{\partial^2 v}{\partial y^2} - \frac{\mu_e}{\rho} H_x \frac{\partial H_x}{\partial y} \quad (2.37b)$$

$$\varepsilon \quad \varepsilon \quad 1 \quad \frac{1}{\varepsilon} \quad \frac{1}{\varepsilon}$$

Magnetic induction equation

$$\frac{\partial H_x}{\partial t} + v \frac{\partial H_x}{\partial y} = H_o \frac{\partial u}{\partial y} + \frac{1}{\mu_e \sigma'} \frac{\partial^2 H_x}{\partial y^2} \quad (2.38a)$$

$$1 \quad \varepsilon \quad \frac{1}{\varepsilon} \quad \varepsilon \quad \frac{1}{\varepsilon} \quad \frac{1}{\varepsilon^2}$$

$$0 = H_0 \frac{\partial v}{\partial y} \quad (2.38b)$$

$\varepsilon \quad 1$

Again let δ_T be the thermal boundary layer thickness and let $\varepsilon \ll 1$ be also the order of δ_T , i.e. $O(\delta_T) = \varepsilon$. Then we can write, $O(y) = \varepsilon, O(v) = \varepsilon$. Also we can write $O(T) = 1, O(C) = 1, O(x) = 1$ and $O(u) = 1$.

Hence

$$\begin{aligned} O\left(\frac{\partial T}{\partial t}\right) &= 1, & O\left(\frac{\partial T}{\partial y}\right) &= \frac{1}{\varepsilon}, & O\left(\frac{\partial^2 T}{\partial y^2}\right) &= \frac{1}{\varepsilon^2}, \\ O\left(\frac{\partial C}{\partial t}\right) &= 1, & O\left(\frac{\partial C}{\partial y}\right) &= \frac{1}{\varepsilon}, & O\left(\frac{\partial^2 C}{\partial y^2}\right) &= \frac{1}{\varepsilon^2} \end{aligned}$$

within the boundary layer.

Then the equations (2.34)—(2.35) with order become

Energy equation

$$\frac{\partial T}{\partial t} + v \frac{\partial T}{\partial y} = \frac{k}{\rho c_p} \frac{\partial^2 T}{\partial y^2} + \frac{\mu}{\rho c_p} \left[\left(\frac{\partial u}{\partial y} \right)^2 + \left(\frac{\partial v}{\partial y} \right)^2 \right] + \frac{1}{\rho c_p \sigma'} \left(\frac{\partial H_x}{\partial y} \right)^2 \quad (2.39)$$

$1 \quad \varepsilon \frac{1}{\varepsilon} \quad \frac{1}{\varepsilon^2} \quad \frac{1}{\varepsilon^2} \quad 1 \quad \frac{1}{\varepsilon^2}$

Concentration equation

$$\frac{\partial C}{\partial t} + v \frac{\partial C}{\partial y} = D_m \frac{\partial^2 C}{\partial y^2} + \frac{D_m K_T}{T_m} \frac{\partial^2 T}{\partial y^2} \quad (2.40)$$

$1 \quad \varepsilon \frac{1}{\varepsilon} \quad \frac{1}{\varepsilon^2} \quad \frac{1}{\varepsilon^2}$

Again we have to find that $O(g\beta(T - T_\infty)) = 1, O(g\beta^*(C - C_\infty)) = 1, O\left(\frac{\mu_e}{\rho}\right) = 1, O(v) = \varepsilon^2,$

$$O\left(\frac{1}{\mu_e \sigma'}\right) = \varepsilon^2, \quad O\left(\frac{k}{\rho c_p}\right) = \varepsilon^2, \quad O(D_m) = \varepsilon^2, \quad O\left(\frac{D_m K_T}{T_m}\right) = \varepsilon^2, \quad O\left(\frac{v}{c_p}\right) = \varepsilon^2, \quad O\left(\frac{1}{\rho c_p \sigma'}\right) = \varepsilon^2$$

Since the viscosity is very small, so neglecting the small order terms. Thus we have to from equations (2.36)—(2.40) yields

$$\frac{\partial v}{\partial y} = 0 \quad (2.41)$$

$$\frac{\partial u}{\partial t} + v \frac{\partial u}{\partial y} = g\beta(T - T_\infty) + g\beta^*(C - C_\infty) + \nu \frac{\partial^2 u}{\partial y^2} + \frac{\mu_e}{\rho} H_o \frac{\partial H_x}{\partial y} \quad (2.42)$$

$$\frac{\partial H_x}{\partial t} + v \frac{\partial H_x}{\partial y} = H_o \frac{\partial u}{\partial y} + \frac{1}{\mu_e \sigma'} \frac{\partial^2 H_x}{\partial y^2} \quad (2.43)$$

$$\frac{\partial T}{\partial t} + v \frac{\partial T}{\partial y} = \frac{k}{\rho c_p} \frac{\partial^2 T}{\partial y^2} + \frac{\nu}{c_p} \left(\frac{\partial u}{\partial y} \right)^2 + \frac{1}{\rho c_p \sigma'} \left(\frac{\partial H_x}{\partial y} \right)^2 \quad (2.44)$$

$$\frac{\partial C}{\partial t} + v \frac{\partial C}{\partial y} = D_m \frac{\partial^2 C}{\partial y^2} + \frac{D_m K_T}{T_m} \frac{\partial^2 T}{\partial y^2} \quad (2.45)$$

and the boundary conditions for the problem are

$$\left. \begin{array}{l} t > 0, \quad u = U_o(t), \quad v = v(t), \quad \frac{\partial T}{\partial y} = -\frac{q}{k}, \quad \frac{\partial C}{\partial y} = -\frac{m}{D_m}, \quad H_x = H_w \quad \text{at } y = 0 \\ t > 0, \quad u = 0, \quad T \rightarrow T_\infty, \quad C \rightarrow C_\infty, \quad H_x \rightarrow 0 \quad \text{as } y \rightarrow \infty \end{array} \right\} \quad (2.46)$$

where H_x is the induced magnetic field, H_w is the induced magnetic field at the plate and m is the coefficient of mass flux per unite area.

Case-II

Let us consider a steady heat and mass transfer by mixed convection flow of an electrically conducting viscous fluid past a semi-infinite vertical porous plate $y = 0$. The flow is also assumed to be in x -direction which is taken along the plate in upward direction and y -axis is normal to it. The detailed descriptions of the present problem are similar to those of **Case-I**.

In the heat and mass transfer by mixed convection flow along the vertical plate, the body force and pressure gradient along the direction is

$$g\beta(T - T_\infty) + g\beta^*(C - C_\infty) \quad (2.47)$$

where g is the acceleration due to the gravitation,

β is the coefficient of volume expansion,

β^* is the volumetric coefficient expansion with concentration.

With reference to the above assumptions, the continuity equation (2.20), the momentum equations (2.21a)-(2.21c), the magnetic induction equations (2.22a)-(2.22c), the energy equation (2.23) and the species concentration equation (2.24) become:

$$\text{Continuity equation} \quad \frac{\partial u}{\partial x} + \frac{\partial v}{\partial y} + \frac{\partial w}{\partial z} = 0 \quad (2.48)$$

Momentum equation

$$u \frac{\partial u}{\partial x} + v \frac{\partial u}{\partial y} + w \frac{\partial u}{\partial z} = g\beta(T - T_\infty) + g\beta^*(C - C_\infty) + \nu \left(\frac{\partial^2 u}{\partial x^2} + \frac{\partial^2 u}{\partial y^2} + \frac{\partial^2 u}{\partial z^2} \right) + \frac{\mu_e}{\rho} H_0 \frac{\partial H_x}{\partial y} \quad (2.49a)$$

$$u \frac{\partial v}{\partial x} + v \frac{\partial v}{\partial y} + w \frac{\partial v}{\partial z} = \nu \left(\frac{\partial^2 v}{\partial x^2} + \frac{\partial^2 v}{\partial y^2} + \frac{\partial^2 v}{\partial z^2} \right) - \frac{\mu_e}{\rho} H_x \frac{\partial H_x}{\partial y} \quad (2.49b)$$

$$u \frac{\partial w}{\partial x} + v \frac{\partial w}{\partial y} + w \frac{\partial w}{\partial z} = \nu \left(\frac{\partial^2 w}{\partial x^2} + \frac{\partial^2 w}{\partial y^2} + \frac{\partial^2 w}{\partial z^2} \right) - \frac{\mu_e}{\rho} H_x \frac{\partial H_x}{\partial z} \quad (2.49c)$$

Magnetic induction equation

$$u \frac{\partial H_x}{\partial x} + v \frac{\partial H_x}{\partial y} + w \frac{\partial H_x}{\partial z} = H_x \frac{\partial u}{\partial x} + H_0 \frac{\partial u}{\partial y} + \frac{1}{\mu_e \sigma'} \left(\frac{\partial^2 H_x}{\partial x^2} + \frac{\partial^2 H_x}{\partial y^2} + \frac{\partial^2 H_x}{\partial z^2} \right) \quad (2.50a)$$

$$0 = H_x \frac{\partial v}{\partial x} + H_0 \frac{\partial v}{\partial y} \quad (2.50b)$$

$$0 = H_x \frac{\partial w}{\partial x} + H_0 \frac{\partial w}{\partial y} \quad (2.50c)$$

Energy equation

$$\frac{\partial T}{\partial t} + u \frac{\partial T}{\partial x} + v \frac{\partial T}{\partial y} + w \frac{\partial T}{\partial z} = \frac{k}{\rho c_p} \left(\frac{\partial^2 T}{\partial x^2} + \frac{\partial^2 T}{\partial y^2} + \frac{\partial^2 T}{\partial z^2} \right) + \frac{1}{\rho c_p} \phi + \frac{1}{\rho c_p \sigma'} \left[\left(\frac{\partial H_x}{\partial z} \right)^2 + \left(\frac{\partial H_x}{\partial y} \right)^2 \right] \quad (2.51)$$

$$\text{where } \phi = \mu \left[\left(\frac{\partial u}{\partial x} \right)^2 + \left(\frac{\partial v}{\partial y} \right)^2 + \left(\frac{\partial w}{\partial z} \right)^2 \right] + \left(\frac{\partial v}{\partial x} + \frac{\partial u}{\partial y} \right)^2 + \left(\frac{\partial w}{\partial y} + \frac{\partial v}{\partial z} \right)^2 + \left(\frac{\partial u}{\partial z} + \frac{\partial w}{\partial x} \right)^2$$

Concentration equation

$$\frac{\partial C}{\partial t} + u \frac{\partial C}{\partial x} + v \frac{\partial C}{\partial y} + w \frac{\partial C}{\partial z} = D_m \left(\frac{\partial^2 C}{\partial x^2} + \frac{\partial^2 C}{\partial y^2} + \frac{\partial^2 C}{\partial z^2} \right) + \frac{D_m K_T}{T_m} \left(\frac{\partial^2 T}{\partial x^2} + \frac{\partial^2 T}{\partial y^2} + \frac{\partial^2 T}{\partial z^2} \right) \quad (2.52)$$

Since the plate occupying the plane $y = 0$ is of semi-infinite extent and the fluid motion is steady, so all the physical quantities will depend only upon x and y . Thus the given governing equations (2.48)-(2.52) reduced to two dimensional equations, which are as follows:

$$\text{Continuity equation} \quad \frac{\partial u}{\partial x} + \frac{\partial v}{\partial y} = 0 \quad (2.53)$$

Momentum equation

$$u \frac{\partial u}{\partial x} + v \frac{\partial u}{\partial y} = g\beta(T - T_\infty) + g\beta^*(C - C_\infty) + \nu \left(\frac{\partial^2 u}{\partial x^2} + \frac{\partial^2 u}{\partial y^2} \right) + \frac{\mu_e}{\rho} H_0 \frac{\partial H_x}{\partial y} \quad (2.54a)$$

$$u \frac{\partial v}{\partial x} + v \frac{\partial v}{\partial y} = \nu \left(\frac{\partial^2 v}{\partial x^2} + \frac{\partial^2 v}{\partial y^2} \right) - \frac{\mu_e}{\rho} H_x \frac{\partial H_x}{\partial y} \quad (2.54b)$$

Magnetic induction equation

$$u \frac{\partial H_x}{\partial x} + v \frac{\partial H_x}{\partial y} = H_x \frac{\partial u}{\partial x} + H_o \frac{\partial u}{\partial y} + \frac{1}{\mu_e \sigma'} \left(\frac{\partial^2 H_x}{\partial x^2} + \frac{\partial^2 H_x}{\partial y^2} \right) \quad (2.55a)$$

$$0 = H_x \frac{\partial v}{\partial x} + H_o \frac{\partial v}{\partial y} \quad (2.55b)$$

Energy equation

$$u \frac{\partial T}{\partial x} + v \frac{\partial T}{\partial y} = \frac{k}{\rho c_p} \left(\frac{\partial^2 T}{\partial x^2} + \frac{\partial^2 T}{\partial y^2} \right) + \frac{\mu}{\rho c_p} \left[\left(\frac{\partial u}{\partial x} \right)^2 + \left(\frac{\partial v}{\partial y} \right)^2 + \left(\frac{\partial v}{\partial x} + \frac{\partial u}{\partial y} \right)^2 \right] + \frac{1}{\rho c_p \sigma'} \left(\frac{\partial H_x}{\partial y} \right)^2 \quad (2.56)$$

Concentration equation

$$u \frac{\partial C}{\partial x} + v \frac{\partial C}{\partial y} = D_m \left(\frac{\partial^2 C}{\partial x^2} + \frac{\partial^2 C}{\partial y^2} \right) + \frac{D_m K_T}{T_m} \left(\frac{\partial^2 T}{\partial x^2} + \frac{\partial^2 T}{\partial y^2} \right) \quad (2.57)$$

Since the magnetic Reynolds number of the flow be large so that the viscosity of the fluid be small. Let δ be the small thickness of the boundary layer and $\varepsilon \ll 1$ be the order of magnitude of δ i. e. $O(\delta) = \varepsilon$, then we can write

$$O(y) = \varepsilon, \quad O(v) = \varepsilon, \quad O(H_o) = \varepsilon$$

Also we assume that $O(u) = 1, \quad O(x) = 1, \quad O(H_x) = 1,$

Hence

$$\begin{aligned} O\left(\frac{\partial u}{\partial x}\right) &= 1, & O\left(\frac{\partial^2 u}{\partial x^2}\right) &= 1, & O\left(\frac{\partial u}{\partial y}\right) &= \frac{1}{\varepsilon}, & O\left(\frac{\partial^2 u}{\partial y^2}\right) &= \frac{1}{\varepsilon^2}, & O\left(\frac{\partial H_x}{\partial y}\right) &= \frac{1}{\varepsilon}, \\ O\left(\frac{\partial v}{\partial x}\right) &= \varepsilon, & O\left(\frac{\partial^2 v}{\partial x^2}\right) &= \varepsilon, & O\left(\frac{\partial v}{\partial y}\right) &= 1, & O\left(\frac{\partial^2 v}{\partial y^2}\right) &= \frac{1}{\varepsilon} \\ O\left(\frac{\partial H_x}{\partial x}\right) &= 1 & O\left(\frac{\partial^2 H_x}{\partial x^2}\right) &= 1 & O\left(\frac{\partial H_x}{\partial y}\right) &= \frac{1}{\varepsilon}, & O\left(\frac{\partial^2 H_x}{\partial y^2}\right) &= \frac{1}{\varepsilon^2} \end{aligned}$$

within the boundary layer.

Then the equations (2.53)—(2.55c) with order become

$$\text{Continuity equation} \quad \frac{\partial u}{\partial x} + \frac{\partial v}{\partial y} = 0 \quad (2.58)$$

$$1 \quad 1$$

Momentum equation

$$u \frac{\partial u}{\partial x} + v \frac{\partial u}{\partial y} = g\beta(T - T_\infty) + g\beta^*(C - C_\infty) + \nu \left(\frac{\partial^2 u}{\partial x^2} + \frac{\partial^2 u}{\partial y^2} \right) + \frac{\mu_e}{\rho} H_o \frac{\partial H_x}{\partial y} \quad (2.59a)$$

$$1 \quad 1 \quad \varepsilon \quad \frac{1}{\varepsilon} \quad 1 \quad \frac{1}{\varepsilon^2} \quad \varepsilon \quad \frac{1}{\varepsilon}$$

$$u \frac{\partial v}{\partial x} + v \frac{\partial v}{\partial y} = \nu \left(\frac{\partial^2 v}{\partial x^2} + \frac{\partial^2 v}{\partial y^2} \right) - \frac{\mu_e}{\rho} H_x \frac{\partial H_x}{\partial y} \quad (2.59b)$$

$$1 \quad \varepsilon \quad \varepsilon \quad 1 \quad \varepsilon \quad \frac{1}{\varepsilon} \quad \frac{1}{\varepsilon}$$

Magnetic induction equation

$$u \frac{\partial H_x}{\partial x} + v \frac{\partial H_x}{\partial y} = H_x \frac{\partial u}{\partial x} + H_o \frac{\partial u}{\partial y} + \frac{1}{\mu_e \sigma'} \left(\frac{\partial^2 H_x}{\partial x^2} + \frac{\partial^2 H_x}{\partial y^2} \right) \quad (2.60a)$$

$$1 \quad 1 \quad \varepsilon \quad \frac{1}{\varepsilon} \quad 1 \quad 1 \quad \varepsilon \quad \frac{1}{\varepsilon} \quad 1 \quad \frac{1}{\varepsilon^2}$$

$$0 = H_x \frac{\partial v}{\partial x} + H_o \frac{\partial v}{\partial y} \quad (2.60b)$$

$$1 \quad \varepsilon \quad \varepsilon \quad 1$$

Again let δ_T be the thermal boundary layer thickness and let $\varepsilon \ll 1$ be also the order of δ_T , i.e. $O(\delta_T) = \varepsilon$. Then we can write, $O(y) = \varepsilon$, $O(v) = \varepsilon$. Also we assume that $O(T) = 1$, $O(C) = 1$, $O(x) = 1$ and $O(u) = 1$.

Hence

$$\begin{aligned} O\left(\frac{\partial T}{\partial x}\right) &= 1, & O\left(\frac{\partial^2 T}{\partial x^2}\right) &= 1, & O\left(\frac{\partial T}{\partial y}\right) &= \frac{1}{\varepsilon}, & O\left(\frac{\partial^2 T}{\partial y^2}\right) &= \frac{1}{\varepsilon^2}, \\ O\left(\frac{\partial C}{\partial x}\right) &= 1, & O\left(\frac{\partial^2 C}{\partial x^2}\right) &= 1, & O\left(\frac{\partial C}{\partial y}\right) &= \frac{1}{\varepsilon}, & O\left(\frac{\partial^2 C}{\partial y^2}\right) &= \frac{1}{\varepsilon^2} \end{aligned}$$

within the boundary layer

Then the equations (2.56)—(2.57) with order become

Energy equation

$$u \frac{\partial T}{\partial x} + v \frac{\partial T}{\partial y} = \frac{k}{\rho_p} \left(\frac{\partial^2 T}{\partial x^2} + \frac{\partial^2 T}{\partial y^2} \right) + \frac{\mu}{\rho_p} \left[\left(\frac{\partial u}{\partial x} \right)^2 + \left(\frac{\partial v}{\partial y} \right)^2 + \left(\frac{\partial v}{\partial x} + \frac{\partial u}{\partial y} \right)^2 \right] + \frac{1}{\rho_p \sigma'} \left(\frac{\partial H_x}{\partial y} \right)^2 \quad (2.61)$$

$$1 \quad 1 \quad \varepsilon \quad \frac{1}{\varepsilon} \quad 1 \quad \frac{1}{\varepsilon^2} \quad 1 \quad 1 \quad \varepsilon^2 \quad \frac{1}{\varepsilon^2} \quad \frac{1}{\varepsilon^2}$$

Concentration equation

$$u \frac{\partial C}{\partial x} + v \frac{\partial C}{\partial y} = D_m \left(\frac{\partial^2 C}{\partial x^2} + \frac{\partial^2 C}{\partial y^2} \right) + \frac{D_m K_T}{T_m} \left(\frac{\partial^2 T}{\partial x^2} + \frac{\partial^2 T}{\partial y^2} \right) \quad (2.62)$$

$$1 \quad 1 \quad \varepsilon \quad \frac{1}{\varepsilon} \quad 1 \quad \frac{1}{\varepsilon^2} \quad 1 \quad \frac{1}{\varepsilon^2}$$

Again we have to find that $O(g\beta(T - T_\infty)) = 1$, $O(g\beta^*(C - C_\infty)) = 1$, $O\left(\frac{\mu_e}{\rho}\right) = 1$, $O(v) = \varepsilon^2$,

$$O\left(\frac{1}{\mu_e \sigma'}\right) = \varepsilon^2, \quad O\left(\frac{k}{\rho c_p}\right) = \varepsilon^2, \quad O(D_m) = \varepsilon^2, \quad O\left(\frac{D_m K_T}{T_m}\right) = \varepsilon^2, \quad O\left(\frac{v}{c_p}\right) = \varepsilon^2 \text{ and } O\left(\frac{1}{\rho c_p \sigma'}\right) = \varepsilon^2$$

Since the viscosity is very small, so neglecting the small order terms. Thus we have to from equations (2.58)—(2.62) yields

$$\frac{\partial u}{\partial x} + \frac{\partial v}{\partial y} = 0 \quad (2.63)$$

$$u \frac{\partial u}{\partial x} + v \frac{\partial u}{\partial y} = g\beta(T - T_\infty) + g\beta^*(C - C_\infty) + v \frac{\partial^2 u}{\partial y^2} + \frac{\mu_e}{\rho} H_o \frac{\partial H_x}{\partial y} \quad (2.64)$$

$$u \frac{\partial H_x}{\partial x} + v \frac{\partial H_x}{\partial y} = H_x \frac{\partial u}{\partial x} + H_o \frac{\partial u}{\partial y} + \frac{1}{\mu_e \sigma'} \frac{\partial^2 H_x}{\partial y^2} \quad (2.65)$$

$$u \frac{\partial T}{\partial x} + v \frac{\partial T}{\partial y} = \frac{k}{\rho c_p} \frac{\partial^2 T}{\partial y^2} + \frac{v}{c_p} \left(\frac{\partial u}{\partial y} \right)^2 + \frac{1}{\rho c_p \sigma'} \left(\frac{\partial H_x}{\partial y} \right)^2 \quad (2.66)$$

$$u \frac{\partial C}{\partial x} + v \frac{\partial C}{\partial y} = D_m \frac{\partial^2 C}{\partial y^2} + \frac{D_m K_T}{T_m} \frac{\partial^2 T}{\partial y^2} \quad (2.67)$$

and the boundary conditions for the problem are

$$\left. \begin{aligned} u = U_o, \quad v = v(x), \quad \frac{\partial T}{\partial y} = -\frac{q}{k}, \quad \frac{\partial C}{\partial y} = -\frac{m}{D_m}, \quad H_x = H_w \quad \text{at } y = 0 \\ u = 0, \quad T \rightarrow T_\infty, \quad C \rightarrow C_\infty, \quad H_x \rightarrow 0 \quad \text{as } y \rightarrow \infty \end{aligned} \right\} \quad (2.68)$$

where H_x is the induced magnetic field, H_w is the induced magnetic field at the plate and m is the coefficient of mass flux per unite area.

Chapter 3

The Calculation Technique

The set of ordinary coupled non-linear differential equations with the boundary conditions are very difficult to solve analytically. Hence we adopt numerical procedures to obtain solutions. To solve our problem we will use a standard initial value solver namely the sixth order Runge Kutta method along with Nachtsheim-Swigert iteration technique.

Nachtsheim-Swigert iteration technique

To solved the boundary layer equations by using Nachtsheim-Swigert iteration technique, if there are three asymptotic boundary conditions then there will have three unknown surface conditions $f''(0)$, $H'(0)$, $\theta'(0)$.

Within the context of the initial value method and Nachtsheim-Swigert iteration technique the outer boundary conditions may be functionally represented as

$$f'(\eta_{\max}) = f'(f''(0), H'(0), \theta'(0)) = \delta_1 \quad (3.1)$$

$$H(\eta_{\max}) = H(f''(0), H'(0), \theta'(0)) = \delta_2 \quad (3.2)$$

$$\theta(\eta_{\max}) = \theta(f''(0), H'(0), \theta'(0)) = \delta_3 \quad (3.3)$$

with the asymptotic convergence criteria is given by

$$f''(\eta_{\max}) = f''(f''(0), H'(0), \theta'(0)) = \delta_4 \quad (3.4)$$

$$H'(\eta_{\max}) = H'(f''(0), H'(0), \theta'(0)) = \delta_5 \quad (3.5)$$

$$\theta'(\eta_{\max}) = \theta'(f''(0), H'(0), \theta'(0)) = \delta_6 \quad (3.6)$$

Let us choose, $f''(0) = g_1$, $H'(0) = g_2$, $\theta'(0) = g_3$

and expanding first order Taylor series expansion after using the above equations (3.1)-(3.6), yields

$$f'(\eta_{\max}) = f'_c(\eta_{\max}) + \frac{\partial f'}{\partial g_1} \Delta g_1 + \frac{\partial f'}{\partial g_2} \Delta g_2 + \frac{\partial f'}{\partial g_3} \Delta g_3 = \delta_1 \quad (3.7)$$

$$H(\eta_{\max}) = H_c(\eta_{\max}) + \frac{\partial H}{\partial g_1} \Delta g_1 + \frac{\partial H}{\partial g_2} \Delta g_2 + \frac{\partial H}{\partial g_3} \Delta g_3 = \delta_2 \quad (3.8)$$

$$\theta(\eta_{\max}) = \theta_c(\eta_{\max}) + \frac{\partial \theta}{\partial g_1} \Delta g_1 + \frac{\partial \theta}{\partial g_2} \Delta g_2 + \frac{\partial \theta}{\partial g_3} \Delta g_3 = \delta_3 \quad (3.9)$$

$$f''(\eta_{\max}) = f_c''(\eta_{\max}) + \frac{\partial f''}{\partial g_1} \Delta g_1 + \frac{\partial f''}{\partial g_2} \Delta g_2 + \frac{\partial f''}{\partial g_3} \Delta g_3 = \delta_4 \quad (3.10)$$

$$H'(\eta_{\max}) = H'_c(\eta_{\max}) + \frac{\partial H'}{\partial g_1} \Delta g_1 + \frac{\partial H'}{\partial g_2} \Delta g_2 + \frac{\partial H'}{\partial g_3} \Delta g_3 = \delta_5 \quad (3.11)$$

$$\theta'(\eta_{\max}) = \theta'_c(\eta_{\max}) + \frac{\partial \theta'}{\partial g_1} \Delta g_1 + \frac{\partial \theta'}{\partial g_2} \Delta g_2 + \frac{\partial \theta'}{\partial g_3} \Delta g_3 = \delta_6 \quad (3.12)$$

where subscript 'c' indicates the value of the function at η_{\max} determined from the trial integration. Solution of these equation in a least square sense requires determining the minimum value of the error as

$$E = \delta_1^2 + \delta_2^2 + \delta_3^2 + \delta_4^2 + \delta_5^2 + \delta_6^2 \quad (3.13)$$

with respect to g_1 , g_2 and g_3 .

Now differentiating equation (3.13) with respect to g_1 , g_2 and g_3 , we get

$$\delta_1 \frac{\partial \delta_1}{\partial g_1} + \delta_2 \frac{\partial \delta_2}{\partial g_1} + \delta_3 \frac{\partial \delta_3}{\partial g_1} + \delta_4 \frac{\partial \delta_4}{\partial g_1} + \delta_5 \frac{\partial \delta_5}{\partial g_1} + \delta_6 \frac{\partial \delta_6}{\partial g_1} = 0 \quad (3.14)$$

$$\delta_1 \frac{\partial \delta_1}{\partial g_2} + \delta_2 \frac{\partial \delta_2}{\partial g_2} + \delta_3 \frac{\partial \delta_3}{\partial g_2} + \delta_4 \frac{\partial \delta_4}{\partial g_2} + \delta_5 \frac{\partial \delta_5}{\partial g_2} + \delta_6 \frac{\partial \delta_6}{\partial g_2} = 0 \quad (3.15)$$

$$\delta_1 \frac{\partial \delta_1}{\partial g_3} + \delta_2 \frac{\partial \delta_2}{\partial g_3} + \delta_3 \frac{\partial \delta_3}{\partial g_3} + \delta_4 \frac{\partial \delta_4}{\partial g_3} + \delta_5 \frac{\partial \delta_5}{\partial g_3} + \delta_6 \frac{\partial \delta_6}{\partial g_3} = 0 \quad (3.16)$$

Now using the equations (3.7)-(3.12) in the equation (3.14), we get

$$\begin{aligned} & \left[f'_c + \frac{\partial f'}{\partial g_1} \Delta g_1 + \frac{\partial f'}{\partial g_2} \Delta g_2 + \frac{\partial f'}{\partial g_3} \Delta g_3 \right] \frac{\partial f'}{\partial g_1} + \left[H_c + \frac{\partial H}{\partial g_1} \Delta g_1 + \frac{\partial H}{\partial g_2} \Delta g_2 + \frac{\partial H}{\partial g_3} \Delta g_3 \right] \frac{\partial H}{\partial g_1} \\ & + \left[\theta_c + \frac{\partial \theta}{\partial g_1} \Delta g_1 + \frac{\partial \theta}{\partial g_2} \Delta g_2 + \frac{\partial \theta}{\partial g_3} \Delta g_3 \right] \frac{\partial \theta}{\partial g_1} + \left[f_c'' + \frac{\partial f''}{\partial g_1} \Delta g_1 + \frac{\partial f''}{\partial g_2} \Delta g_2 + \frac{\partial f''}{\partial g_3} \Delta g_3 \right] \frac{\partial f''}{\partial g_1} \\ & + \left[H'_c + \frac{\partial H'}{\partial g_1} \Delta g_1 + \frac{\partial H'}{\partial g_2} \Delta g_2 + \frac{\partial H'}{\partial g_3} \Delta g_3 \right] \frac{\partial H'}{\partial g_1} + \left[\theta'_c + \frac{\partial \theta'}{\partial g_1} \Delta g_1 + \frac{\partial \theta'}{\partial g_2} \Delta g_2 + \frac{\partial \theta'}{\partial g_3} \Delta g_3 \right] \frac{\partial \theta'}{\partial g_1} = 0 \\ \Rightarrow & \left[\left(\frac{\partial f'}{\partial g_1} \right)^2 + \left(\frac{\partial H}{\partial g_1} \right)^2 + \left(\frac{\partial \theta}{\partial g_1} \right)^2 + \left(\frac{\partial f''}{\partial g_1} \right)^2 + \left(\frac{\partial H'}{\partial g_1} \right)^2 + \left(\frac{\partial \theta'}{\partial g_1} \right)^2 \right] \Delta g_1 \\ & + \left[\frac{\partial f'}{\partial g_2} \frac{\partial f'}{\partial g_1} + \frac{\partial H}{\partial g_2} \frac{\partial H}{\partial g_1} + \frac{\partial \theta}{\partial g_2} \frac{\partial \theta}{\partial g_1} + \frac{\partial f''}{\partial g_2} \frac{\partial f''}{\partial g_1} + \frac{\partial H'}{\partial g_2} \frac{\partial H'}{\partial g_1} + \frac{\partial \theta'}{\partial g_2} \frac{\partial \theta'}{\partial g_1} \right] \Delta g_2 \end{aligned}$$

$$\begin{aligned}
& + \left[\frac{\partial f'}{\partial g_3} \frac{\partial f'}{\partial g_1} + \frac{\partial H}{\partial g_3} \frac{\partial H}{\partial g_1} + \frac{\partial \theta}{\partial g_3} \frac{\partial \theta}{\partial g_1} + \frac{\partial f''}{\partial g_3} \frac{\partial f''}{\partial g_1} + \frac{\partial H'}{\partial g_3} \frac{\partial H'}{\partial g_1} + \frac{\partial \theta'}{\partial g_3} \frac{\partial \theta'}{\partial g_1} \right] \Delta g_3 \\
& = - \left[f'_c \frac{\partial f'}{\partial g_1} + H_c \frac{\partial H}{\partial g_1} + \theta_c \frac{\partial \theta}{\partial g_1} + f''_c \frac{\partial f''}{\partial g_1} + H'_c \frac{\partial H'}{\partial g_1} + \theta'_c \frac{\partial \theta'}{\partial g_1} \right] \quad (3.17)
\end{aligned}$$

Similarly by using the equations (3.7)-(3.12) in the equation (3.15), we get

$$\begin{aligned}
& \left[\frac{\partial f'}{\partial g_1} \frac{\partial f'}{\partial g_2} + \frac{\partial H}{\partial g_1} \frac{\partial H}{\partial g_2} + \frac{\partial \theta}{\partial g_1} \frac{\partial \theta}{\partial g_2} + \frac{\partial f''}{\partial g_1} \frac{\partial f''}{\partial g_2} + \frac{\partial H'}{\partial g_1} \frac{\partial H'}{\partial g_2} + \frac{\partial \theta'}{\partial g_1} \frac{\partial \theta'}{\partial g_2} \right] \Delta g_1 \\
& + \left[\left(\frac{\partial f'}{\partial g_2} \right)^2 + \left(\frac{\partial H}{\partial g_2} \right)^2 + \left(\frac{\partial \theta}{\partial g_2} \right)^2 + \left(\frac{\partial f''}{\partial g_2} \right)^2 + \left(\frac{\partial H'}{\partial g_2} \right)^2 + \left(\frac{\partial \theta'}{\partial g_2} \right)^2 \right] \Delta g_2 \\
& + \left[\frac{\partial f'}{\partial g_3} \frac{\partial f'}{\partial g_2} + \frac{\partial H}{\partial g_3} \frac{\partial H}{\partial g_2} + \frac{\partial \theta}{\partial g_3} \frac{\partial \theta}{\partial g_2} + \frac{\partial f''}{\partial g_3} \frac{\partial f''}{\partial g_2} + \frac{\partial H'}{\partial g_3} \frac{\partial H'}{\partial g_2} + \frac{\partial \theta'}{\partial g_3} \frac{\partial \theta'}{\partial g_2} \right] \Delta g_3 \\
& = - \left[f'_c \frac{\partial f'}{\partial g_2} + H_c \frac{\partial H}{\partial g_2} + \theta_c \frac{\partial \theta}{\partial g_2} + f''_c \frac{\partial f''}{\partial g_2} + H'_c \frac{\partial H'}{\partial g_2} + \theta'_c \frac{\partial \theta'}{\partial g_2} \right] \quad (3.18)
\end{aligned}$$

and

$$\begin{aligned}
& \left[\frac{\partial f'}{\partial g_1} \frac{\partial f'}{\partial g_3} + \frac{\partial H}{\partial g_1} \frac{\partial H}{\partial g_3} + \frac{\partial \theta}{\partial g_1} \frac{\partial \theta}{\partial g_3} + \frac{\partial f''}{\partial g_1} \frac{\partial f''}{\partial g_3} + \frac{\partial H'}{\partial g_1} \frac{\partial H'}{\partial g_3} + \frac{\partial \theta'}{\partial g_1} \frac{\partial \theta'}{\partial g_3} \right] \Delta g_1 \\
& + \left[\frac{\partial f'}{\partial g_2} \frac{\partial f'}{\partial g_3} + \frac{\partial H}{\partial g_2} \frac{\partial H}{\partial g_3} + \frac{\partial \theta}{\partial g_2} \frac{\partial \theta}{\partial g_3} + \frac{\partial f''}{\partial g_2} \frac{\partial f''}{\partial g_3} + \frac{\partial H'}{\partial g_2} \frac{\partial H'}{\partial g_3} + \frac{\partial \theta'}{\partial g_2} \frac{\partial \theta'}{\partial g_3} \right] \Delta g_2 \\
& + \left[\left(\frac{\partial f'}{\partial g_3} \right)^2 + \left(\frac{\partial H}{\partial g_3} \right)^2 + \left(\frac{\partial \theta}{\partial g_3} \right)^2 + \left(\frac{\partial f''}{\partial g_3} \right)^2 + \left(\frac{\partial H'}{\partial g_3} \right)^2 + \left(\frac{\partial \theta'}{\partial g_3} \right)^2 \right] \Delta g_3 \\
& = - \left[f'_c \frac{\partial f'}{\partial g_3} + H_c \frac{\partial H}{\partial g_3} + \theta_c \frac{\partial \theta}{\partial g_3} + f''_c \frac{\partial f''}{\partial g_3} + H'_c \frac{\partial H'}{\partial g_3} + \theta'_c \frac{\partial \theta'}{\partial g_3} \right] \quad (3.19)
\end{aligned}$$

We can write the equations (3.17)-(3.19) in system of linear equations in the following form as:

$$a_{11} \Delta g_1 + a_{12} \Delta g_2 + a_{13} \Delta g_3 = b_{11} \quad (3.20)$$

$$a_{21} \Delta g_1 + a_{22} \Delta g_2 + a_{23} \Delta g_3 = b_{22} \quad (3.21)$$

$$a_{31} \Delta g_1 + a_{32} \Delta g_2 + a_{33} \Delta g_3 = b_{33} \quad (3.22)$$

where

$$a_{11} = \left(\frac{\partial f'}{\partial g_1} \right)^2 + \left(\frac{\partial H}{\partial g_1} \right)^2 + \left(\frac{\partial \theta}{\partial g_1} \right)^2 + \left(\frac{\partial f''}{\partial g_1} \right)^2 + \left(\frac{\partial H'}{\partial g_1} \right)^2 + \left(\frac{\partial \theta'}{\partial g_1} \right)^2$$

$$a_{22} = \left(\frac{\partial f'}{\partial g_2} \right)^2 + \left(\frac{\partial H}{\partial g_2} \right)^2 + \left(\frac{\partial \theta}{\partial g_2} \right)^2 + \left(\frac{\partial f''}{\partial g_2} \right)^2 + \left(\frac{\partial H'}{\partial g_2} \right)^2 + \left(\frac{\partial \theta'}{\partial g_2} \right)^2$$

$$a_{33} = \left(\frac{\partial f'}{\partial g_3} \right)^2 + \left(\frac{\partial H}{\partial g_3} \right)^2 + \left(\frac{\partial \theta}{\partial g_3} \right)^2 + \left(\frac{\partial f''}{\partial g_3} \right)^2 + \left(\frac{\partial H'}{\partial g_3} \right)^2 + \left(\frac{\partial \theta'}{\partial g_3} \right)^2$$

$$\begin{aligned}
a_{12} = a_{21} &= \frac{\partial f'}{\partial g_1} \frac{\partial f'}{\partial g_2} + \frac{\partial H}{\partial g_1} \frac{\partial H}{\partial g_2} + \frac{\partial \theta}{\partial g_1} \frac{\partial \theta}{\partial g_2} + \frac{\partial f''}{\partial g_1} \frac{\partial f''}{\partial g_2} + \frac{\partial H'}{\partial g_1} \frac{\partial H'}{\partial g_2} + \frac{\partial \theta'}{\partial g_1} \frac{\partial \theta'}{\partial g_2} \\
a_{13} = a_{31} &= \frac{\partial f'}{\partial g_1} \frac{\partial f'}{\partial g_3} + \frac{\partial H}{\partial g_1} \frac{\partial H}{\partial g_3} + \frac{\partial \theta}{\partial g_1} \frac{\partial \theta}{\partial g_3} + \frac{\partial f''}{\partial g_1} \frac{\partial f''}{\partial g_3} + \frac{\partial H'}{\partial g_1} \frac{\partial H'}{\partial g_3} + \frac{\partial \theta'}{\partial g_1} \frac{\partial \theta'}{\partial g_3} \\
a_{23} = a_{32} &= \frac{\partial f'}{\partial g_2} \frac{\partial f'}{\partial g_3} + \frac{\partial H}{\partial g_2} \frac{\partial H}{\partial g_3} + \frac{\partial \theta}{\partial g_2} \frac{\partial \theta}{\partial g_3} + \frac{\partial f''}{\partial g_2} \frac{\partial f''}{\partial g_3} + \frac{\partial H'}{\partial g_2} \frac{\partial H'}{\partial g_3} + \frac{\partial \theta'}{\partial g_2} \frac{\partial \theta'}{\partial g_3} \\
b_{11} &= - \left[f'_c \frac{\partial f'}{\partial g_1} + H_c \frac{\partial H}{\partial g_1} + \theta_c \frac{\partial \theta}{\partial g_1} + f''_c \frac{\partial f''}{\partial g_1} + H'_c \frac{\partial H'}{\partial g_1} + \theta'_c \frac{\partial \theta'}{\partial g_1} \right] \\
b_{22} &= - \left[f'_c \frac{\partial f'}{\partial g_2} + H_c \frac{\partial H}{\partial g_2} + \theta_c \frac{\partial \theta}{\partial g_2} + f''_c \frac{\partial f''}{\partial g_2} + H'_c \frac{\partial H'}{\partial g_2} + \theta'_c \frac{\partial \theta'}{\partial g_2} \right] \\
b_{33} &= - \left[f'_c \frac{\partial f'}{\partial g_3} + H_c \frac{\partial H}{\partial g_3} + \theta_c \frac{\partial \theta}{\partial g_3} + f''_c \frac{\partial f''}{\partial g_3} + H'_c \frac{\partial H'}{\partial g_3} + \theta'_c \frac{\partial \theta'}{\partial g_3} \right]
\end{aligned}$$

Now solving the equations (3.20)-(3.22) by Cramer's rule, we have

$$\Delta g_1 = \frac{\det A_1}{\det A}, \quad \Delta g_2 = \frac{\det A_2}{\det A} \quad \text{and} \quad \Delta g_3 = \frac{\det A_3}{\det A}$$

where

$$\begin{aligned}
\det A &= \begin{vmatrix} a_{11} & a_{12} & a_{13} \\ a_{21} & a_{22} & a_{23} \\ a_{31} & a_{32} & a_{33} \end{vmatrix} & \det A_1 &= \begin{vmatrix} b_{11} & a_{12} & a_{13} \\ b_{22} & a_{22} & a_{23} \\ b_{33} & a_{32} & a_{33} \end{vmatrix} \\
\det A_2 &= \begin{vmatrix} a_{11} & b_{11} & a_{13} \\ a_{21} & b_{22} & a_{23} \\ a_{31} & b_{33} & a_{33} \end{vmatrix} & \det A_3 &= \begin{vmatrix} a_{11} & a_{12} & b_{11} \\ a_{21} & a_{22} & b_{22} \\ a_{31} & a_{32} & b_{33} \end{vmatrix}
\end{aligned}$$

Then we obtain the missing (unspecified) values as

$$\left. \begin{aligned}
g_1 &\leftarrow g_1 + \Delta g_1 \\
g_2 &\leftarrow g_2 + \Delta g_2 \\
g_3 &\leftarrow g_3 + \Delta g_3
\end{aligned} \right\} \quad (3.23)$$

Thus adopting this type of numerical technique as described above, a computer program was set up for the solution of the basic non-linear differential equations of our problem where the integration technique was adopted as the sixth order Runge Kutta method of integration. Based on the integration done with the above numerical technique, the results obtained are in the appropriate section.

Chapter 4

Unsteady heat and mass transfer by mixed convection flow from a vertical porous plate with induced magnetic field, constant heat and mass fluxes

4.1. Introduction

Many transport processes can be found in various ways in both nature and technology, in which the heat and mass transfer by mixed convection flow occur due to the buoyancy force caused by thermal diffusion (temperature difference), mass diffusion (concentration difference). The heat and mass transfer by mixed convection flow has great significance in stellar, planetary, magnetosphere studied and also in the field of aeronautics, chemical engineering and electronics. In many engineering application heat and mass transfer process in fluid condensing or boiling at a solid surface play a decisive role. Boiling and condensing are characteristic for many separation processes in chemical engineering. As examples of this type of process, the evaporation, condensation, distillation, rectification absorption of a fluid should all be mentioned (Baehr and Stephan, 1998).

Magneto fluid dynamics (MFD) is the study of flow of electrically conducting fluid in electric and magnetic field. It unifies in a common framework the electromagnetic & fluid dynamic theories to yield descriptions of the concurrent effects of magnetic field on the flow and the flow on the magnetic field. Magneto fluid dynamics deals with an electrically conducting fluid whereas its subtopics; Magnetohydrodynamics (MHD) and Magneto Gas dynamics (MGD) are specifically concerned with electrically conducting liquids & ionized compressible gases.

The problem of laminar natural convection flow in channels with wall temperature and heat transfer of fluid has been studied by Ostrach (1952). The natural convection flow along a vertical isothermal plate is a classical problem of fluid mechanics that has been solved with the similarity

method by Ostrach(1953). Combined natural and forced convection laminar flow with and without heat source has been studied extensively by Ostrach(1953,1954,1955).

Kawase and Ulbrecht(1984) and Martynenko et al.(1984) investigated the free convection flow past an infinite vertical plate with constant suction. It was assumed that the plate temperature oscillates in such way that its amplitude is small. Weiss et al.(1994), further extended the problem of natural convection on a vertical flat plate. Free convection heat transfer on a vertical semi-infinite plate was studied by Berezovsky et al.(1977). Mollendorf and Grebhart(1974) studied the natural convection resulting from the combined buoyancy effect of the thermal and mass diffusion. Lin and Wu (1995,1997) have analyzed the problem of simultaneous heat and mass transfer with the entire range of buoyancy ratio for most practical chemical species in dilute and aqueous solutions.

MHD is currently undergoing a period of great enlargement and differentiation of subject matter. The MHD heat and mass transfer flow of a viscous incompressible fluid past an infinite vertical porous plate under oscillatory suction velocity normal to the plate was investigated by Singh et al. (2003). The problem of combined heat and mass transfer of an electrically conducting fluid in MHD natural convection adjacent to a vertical surface was analyzed by Chen (2004). All the above works are related to the stationary vertical surface; however, the flow past a continuously moving surface has many applications in manufacturing processes. Such processes are hot rolling, the metal and plastic extrusion, continuous casting, glass fiber production and paper production (Altan et al., 1979).

Soundalgekar and Ramana Murty (1980) studied the heat transfer flow past a continuous moving plate with variable temperature. Sami and Al-Sanea(2004) studied the steady laminar flow and heat transfer characteristics of a continuously moving vertical sheet of extruded material. Very recently an analytical study of the combined heat and mass transfer by laminar mixed convection flow of an incompressible electrically conducting viscous fluid past an electrically non-conducting continuously moving infinite vertical porous plate under the action of a uniform transverse magnetic with constant heat flux and induced magnetic field is done by Chaudhary and Sharma (2006).

Hence our aim is to investigate the heat and mass transfer by mixed convection flows from a vertical porous plate with induced magnetic field, constant heat and mass fluxes. This problem is solved numerically in case of one-dimensional unsteady flow. The Governing equations of the problem contain the partial differential equations, which are transformed by similarity transformation in to a system of ordinary coupled non-linear differential equations and are

solved numerically by the sixth order Runge Kutta method along with the Nachtsheim-Swigert iteration technique. The obtained solutions are shown graphically as well as in tabular form.

4.2. The Governing Equations

Let us consider an unsteady MHD heat and mass transfer by mixed convection flow of an electrically conducting viscous fluid past an infinite vertical porous plate $y = 0$. The flow is also assumed to be in x -direction which is taken along the plate in upward direction and y -axis is normal to it. The temperature and species concentration at the plate are instantly raised from T_w and C_w to T_∞ and C_∞ respectively. Which are thereafter maintained as constant, where T_∞ and C_∞ the temperature and species concentration of the uniform flow respectively. A uniform magnetic field strength \mathbf{H} is applied to the plate to be acting along the y -axis, which is electrically non-conducting. We assumed that the magnetic Reynolds number of the flow be large enough so that the induced magnetic field is not negligible. The induced magnetic field is of the form $\mathbf{H} = (H_x, H_0, 0)$. The equation of the conservation of electric charge is $\nabla \cdot \mathbf{J} = 0$, where $\mathbf{J} = (J_x, J_y, J_z)$, the direction of propagation is considered only along the y -axis and does not have any variation along the y -axis and the derivative of \mathbf{J} with respect to y namely $\frac{\partial J_y}{\partial y} = 0$, resulting in $J_y = \text{constant}$. Since the plate is electrically non-conducting, this constant is zero and hence $J_y = 0$ every where in the flow.

With reference to the generalized equation describe in **Case-I** of *Chapter-2*, the one-dimensional problem under the above assumptions and Boussinesq approximation can be put in the following form,

$$\frac{\partial v}{\partial y} = 0 \quad (4.1)$$

$$\frac{\partial u}{\partial t} + v \frac{\partial u}{\partial y} = g\beta(T - T_\infty) + g\beta^*(C - C_\infty) + \nu \frac{\partial^2 u}{\partial y^2} + \frac{\mu_e}{\rho} H_0 \frac{\partial H_x}{\partial y} \quad (4.2)$$

$$\frac{\partial H_x}{\partial t} + v \frac{\partial H_x}{\partial y} = H_0 \frac{\partial u}{\partial y} + \frac{1}{\mu_e \sigma'} \frac{\partial^2 H_x}{\partial y^2} \quad (4.3)$$

$$\frac{\partial T}{\partial t} + v \frac{\partial T}{\partial y} = \frac{k}{\rho c_p} \frac{\partial^2 T}{\partial y^2} + \frac{\nu}{c_p} \left(\frac{\partial u}{\partial y} \right)^2 + \frac{1}{\rho c_p \sigma'} \left(\frac{\partial H_x}{\partial y} \right)^2 \quad (4.4)$$

$$\frac{\partial C}{\partial t} + v \frac{\partial C}{\partial y} = D_m \frac{\partial^2 C}{\partial y^2} + \frac{D_m K_T}{T_m} \frac{\partial^2 T}{\partial y^2} \quad (4.5)$$

and the boundary conditions for the problem are

$$\left. \begin{aligned} t > 0, \quad u = U_o(t), \quad v = v(t), \quad \frac{\partial T}{\partial y} = -\frac{q}{k}, \quad \frac{\partial C}{\partial y} = -\frac{m}{D_m}, \quad H_x = H_w \quad \text{at } y = 0 \\ t > 0, \quad u = 0, \quad T \rightarrow T_\infty, \quad C \rightarrow C_\infty, \quad H_x \rightarrow 0 \quad \text{as } y \rightarrow \infty \end{aligned} \right\} \quad (4.6)$$

where u and v are the velocity components in x - and y -direction respectively, H_0 is the applied constant magnetic field, H_x is the induced magnetic field, H_w is the induced magnetic field at the plate, μ_e is the magnetic permeability, q is the constant heat flux per unit area, m is the constant mass flux per unit area, ν is the kinematic viscosity, g is the acceleration due to the gravity, ρ is the density, β is the coefficient of volume expansion, β^* is the volumetric coefficient expansion with concentration. T , and T_∞ are the temperature of the fluid inside the thermal boundary layer and the fluid temperature in the free stream respectively, while C and C_∞ are the corresponding concentration, c_p is the specific heat at constant pressure, T_m is the mean fluid temperature, K_T is the thermal diffusion ratio, D_m is the coefficient of mass diffusion and other symbols have their usual meaning.

4.3. Mathematical Formulation

In order to obtain the similarity solutions we introduce a similarity parameter σ as

$$\sigma = \sigma(t) \quad (4.7)$$

such that σ is the time dependent length scale. In term of this length scale a convenient solution of equation (4.1) considered to be

$$v(t) = -v_o \frac{\nu}{\sigma} \quad (4.8)$$

where the constant v_o represents a dimensionless normal velocity at the plate, which is positive for suction and negative for blowing.

Now we introduce the following dimensionless variable

$$\eta = \frac{y}{\sigma} \quad (4.9)$$

$$f(\eta) = \frac{u}{U_o} \quad (4.10)$$

$$\theta(\eta) = \frac{k}{q\sigma} (T - T_\infty) \quad (4.11)$$

$$\phi(\eta) = \frac{D_m}{m\sigma} (C - C_\infty) \quad (4.12)$$

$$H(\eta) = \frac{\sigma}{\nu} \sqrt{\frac{\mu_e}{\rho}} H_x \quad (4.13)$$

From equation (4.9) we have,

$$\frac{\partial \eta}{\partial t} = -\frac{\eta}{\sigma} \frac{\partial \sigma}{\partial t} \quad (4.14)$$

$$\frac{\partial \eta}{\partial y} = \frac{1}{\sigma} \quad (4.15)$$

From equations (4.10)-(4.13) we have,

$$u = U_o f(\eta) \quad (4.16)$$

$$T = T_\infty + \frac{q\sigma}{k} \theta(\eta) \quad (4.17)$$

$$C = C_\infty + \frac{m\sigma}{D_m} \phi(\eta) \quad (4.18)$$

$$H_x = \frac{\nu}{\sigma} \sqrt{\frac{\rho}{\mu_e}} H(\eta) \quad (4.19)$$

From equations (4.16)-(4.19) we have the following derivatives,

$$\frac{\partial u}{\partial t} = -\frac{U_o}{\sigma} \frac{\partial \sigma}{\partial t} \eta f'(\eta) \quad (4.20)$$

$$\frac{\partial u}{\partial y} = \frac{U_o}{\sigma} f'(\eta) \quad (4.21)$$

$$\frac{\partial^2 u}{\partial y^2} = \frac{U_o}{\sigma^2} f''(\eta) \quad (4.22)$$

$$\frac{\partial H_x}{\partial t} = -\frac{\nu}{\sigma^2} \sqrt{\frac{\rho}{\mu_e}} \frac{\partial \sigma}{\partial t} (\eta H' + H) \quad (4.23)$$

$$\frac{\partial H_x}{\partial y} = \frac{\nu}{\sigma^2} \sqrt{\frac{\rho}{\mu_e}} H'(\eta) \quad (4.24)$$

$$\frac{\partial^2 H_x}{\partial y^2} = \frac{\nu}{\sigma^3} \sqrt{\frac{\rho}{\mu_e}} H''(\eta) \quad (4.25)$$

$$\frac{\partial T}{\partial t} = -\frac{q}{k} \frac{\partial \sigma}{\partial t} (\eta \theta' - \theta) \quad (4.26)$$

$$\frac{\partial T}{\partial y} = \frac{q}{k} \theta'(\eta) \quad (4.27)$$

$$\frac{\partial^2 T}{\partial y^2} = \frac{q}{\sigma k} \theta''(\eta) \quad (4.28)$$

$$\frac{\partial C}{\partial t} = -\frac{m}{D_m} \frac{\partial \sigma}{\partial t} (\eta \phi' - \phi) \quad (4.29)$$

$$\frac{\partial C}{\partial y} = \frac{m}{D_m} \phi'(\eta) \quad (4.30)$$

$$\frac{\partial^2 C}{\partial y^2} = \frac{m}{\sigma D_m} \phi''(\eta) \quad (4.31)$$

Now substituting the equations (4.8)-(4.31) into the equation (4.2)-(4.5), and after simplification we get the following equations in terms of dimensionless variables

$$-\left[\frac{\sigma}{\nu} \frac{\partial \sigma}{\partial t} \eta + \nu_o \right] f' = f'' + G_r \theta + G_m \phi + MH' \quad (4.32)$$

$$H'' + P_m \left[\frac{\sigma}{\nu} \frac{\partial \sigma}{\partial t} \eta + \nu_o \right] H' + P_m \frac{\sigma}{\nu} \frac{\partial \sigma}{\partial t} H + MP_m f' = 0 \quad (4.33)$$

$$\theta'' + P_r \left[\frac{\sigma}{\nu} \frac{\partial \sigma}{\partial t} \eta + \nu_o \right] \theta' - P_r \frac{\sigma}{\nu} \frac{\partial \sigma}{\partial t} \theta + E_c P_r \left(f'^2 + \frac{1}{P_m} H'^2 \right) = 0 \quad (4.34)$$

$$\phi'' + S_c \left[\frac{\sigma}{\nu} \frac{\partial \sigma}{\partial t} \eta + \nu_o \right] \phi' - S_c \frac{\sigma}{\nu} \frac{\partial \sigma}{\partial t} \phi + S_o S_c \theta'' = 0 \quad (4.35)$$

where $G_r = \frac{q\sigma^3}{\nu U_o k} g\beta$ is the Grashof number,

$G_m = \frac{m\sigma^3}{\nu U_o D_m} g\beta^*$ is the modified Grashof number,

$M = \sqrt{\frac{\mu_e}{\rho}} \frac{H_o}{U_o}$ is the magnetic force number,

$P_m = \mu_e \sigma' \nu$ is the magnetic diffusivity number,

$P_r = \frac{\rho c_p \nu}{k}$ is the Prandtl number,

$E_c = \frac{k U_o}{\sigma q c_p}$ is the Eckert number.

$S_c = \frac{\nu}{D_m}$ is the Schmidt number,

and $S_o = \frac{D_m^2 q K_T}{T_m m \nu k}$ is the Soret number.

The equations (4.32)-(4.35) are similar except the term $\frac{\sigma}{\nu} \frac{\partial \sigma}{\partial t}$ where time t appears explicitly.

Thus the similarity condition requires that $\frac{\sigma}{\nu} \frac{\partial \sigma}{\partial t}$ in equations (4.32)-(4.35) must be constant

quantity. Hence following the work of Sattar and Alam (1994) one can try a class of solutions of the equation (4.32)-(4.35) by assuming that

$$\frac{\sigma}{\nu} \frac{\partial \sigma}{\partial t} = c \text{ (a constant)} \quad (4.36)$$

Now from equation (4.36) we have,

$$\sigma \partial \sigma = c \nu \partial t$$

by integrating $\frac{\sigma^2}{2} = c \nu t + k_1$ (k_1 is a constant)

Since when $t = 0$ then $\sigma = 0$, thus the integrating constant $k_1 = 0$, so that

$$\begin{aligned} \frac{\sigma^2}{2} &= c \nu t \\ \Rightarrow \sigma &= \sqrt{2c\nu t} \end{aligned} \quad (4.37)$$

It thus appear from (4.36) that by making a realistic choice of c to be equal to 2 in equation (4.37), the length scale become equal to $\sigma = 2\sqrt{\nu t}$ which exactly corresponds to the usual scaling factor considered for viscous unsteady boundary layer flows (Schlichting, 1968). Since σ is a scaling factor as well as a similarity parameter, any value of c in (4.37) would not change the nature of solution except that the scale would be different. Finally introducing $c = 2$ in equation (4.36) and (4.37), we have

$$\frac{\sigma}{\nu} \frac{\partial \sigma}{\partial t} = 2 \quad (4.38)$$

$$\therefore \frac{\sigma}{\nu} \frac{\partial \sigma}{\partial t} \eta + \nu_o = 2\eta + \nu_o = 2\left(\eta + \frac{\nu_o}{2}\right) = 2\xi \quad (4.39)$$

$$\text{where } \xi = \left(\eta + \frac{\nu_o}{2}\right) \quad (4.40)$$

Hence the equation (4.32)-(4.35), yields

$$f'' + 2\xi f' + G_r \theta + G_m \phi + MH' = 0 \quad (4.41)$$

$$H'' + 2\xi P_m H' + 2P_m H + MP_m f' = 0 \quad (4.42)$$

$$\theta'' + 2\xi P_r \theta' - 2P_r \theta + E_c P_r \left(f'^2 + \frac{1}{P_m} H'^2\right) = 0 \quad (4.43)$$

$$\phi'' + 2\xi S_c \phi' - 2S_c \phi + S_o S_c \theta'' = 0 \quad (4.44)$$

The corresponding boundary conditions are

$$\left. \begin{aligned} f = 1, \quad \theta' = -1, \quad \phi' = -1, \quad H = h \text{ (where } h = \frac{\sigma}{\nu} \sqrt{\frac{\mu_e}{\rho}} H_w = 1) \text{ at } \eta = 0 \\ f = 0, \quad \theta \rightarrow 0, \quad \phi \rightarrow 0, \quad H \rightarrow 0 \text{ as } \eta \rightarrow \infty \end{aligned} \right\} \quad (4.45)$$

In all the above equations prime denote the differentiation with respect to η . Hence the equations (4.41)-(4.44) give the dimensionless ordinary coupled non-linear differential equations.

4.4. Skin Friction Co-efficient and Current Density at the Plate

The quantities of chief physical interest are the local skin friction coefficient, and the Local Current density at the plate.

The shearing stress at the plate is generally known as the skin friction, the equation defining the local skin friction is

$$\tau = \mu \left(\frac{\partial u}{\partial y} \right)_{y=0} \quad \text{i.e. } \tau \propto f'(0)$$

The current density is generally expressed as $J = - \left(\frac{\partial H}{\partial y} \right)$ and hence the current density at the plate is $J_w \propto H'(0)$

The next section deals the solution technique of the problem.

4.5. Numerical Solution

The set of ordinary coupled non-linear differential equations (4.41)-(4.44) with the boundary conditions (4.45) for unsteady case are very difficult to solve analytically, so numerical procedures are adopted to obtain their solution. Here we use the standard initial value solver, namely the sixth order Runge Kutta method along with Nachtsheim-Swigert iteration technique.

In a Nachtsheim-Swigert iteration technique, the missing (unspecified) initial condition at the initial point of the interval is assumed and the differential equation is then integrated numerically as an initial value problem to the terminal point. The accuracy of the assumed missing initial condition is then checked by comparing the calculated value of the dependent variable at the terminal point with its given value there. If a difference exists, another value of the missing initial condition must be assumed and the process is repeated. This process is continued until the agreement between the calculated and the given condition at the terminal point is within the specified degree of accuracy. For this type of iterative approach, one naturally inquires whether or not there is a systematic way of finding each succeeding (assumed) value of the missing initial condition.

The Nachtsheim-Swigert iteration technique thus needs to be discussed elaborately. The boundary conditions (4.45) associated with the non-linear coupled ordinary differential equations (4.41)-(4.44) of the boundary layer type is of two point asymptotic class. Two point boundary

conditions have values of the depended variable specified at two different values of independent variable. Specification of an asymptotic boundary conditions implies that the first derivative (and higher derivatives of the boundary layer equations, if exist) of the dependent variable approaches to zero and the value of the velocity approaches to unity as the other specified value of the independent variable is approached. The method of numerical integration of two point asymptotic boundary value problem of the boundary layer type, the initial value method, requires that the problem be recast as an initial value problem. Thus it is necessary to set up as many boundary conditions as the surfaces there at infinity. The governing differential equations are then integrated with these assumed surface boundary conditions. If the required outer boundary conditions are satisfied, a solution has been achieved. However, this is not generally the case. Hence a method must be devised to logically estimate the new surface boundary conditions for the next trial integration. Asymptotic boundary value problems such as those governing boundary layer equations become more complicated by the fact that the outer boundary condition is specified at infinity. In the trial integration infinity is numerically approximated by some large value of the independent variable. There is no general method of estimating this value. Selecting too small a maximum value for the independent variable may not allow the solution to asymptotically converge to the required accuracy. Selecting a large value may result in slow convergence or even divergence of the trial integration. Selecting too large a value of the independent variable is expensive in terms of computer time. Nachtsheim-Swigert developed an iteration method, which overcomes these difficulties. Extensions of the Nachtsheim-Swigert iteration to the above system of differential equations (4.41)–(4.44) with boundary conditions are straight forward. In equation (4.45), there are four asymptotic boundary conditions and hence there will be four unknown surface conditions $f'(0)$, $H'(0)$, $\theta'(0)$, $\phi'(0)$

4.6. Results and Discussion

To study the physical situation of the problem, we have computed the numerical values of the velocity, induced magnetic field, current density, temperature and concentration within the boundary layer and also the skin friction and current density at the plate for different values of the suction parameter (v_o), the magnetic parameter (M), the Prandtl number (P_r), the Soret number (S_o), the Schmidt number (S_c), the Grashof number (G_r), the magnetic diffusivity parameter (P_m), the Eckert number (E_c) and for the fixed value of modified Grashof number (G_m). The values of G_r is taken to be large ($G_r=5.0$), since this value corresponds to a cooling problem that is generally encountered in nuclear engineering in connection with the cooling of reactors. The three values 0.71, 1.0 and 7.0 are considered for P_r (in particular, 0.71 represents air at 20°C, 1.0 corresponds to electrolyte solution such as salt water and 7.0 corresponds to

water at 20°C). The values 0.22, 0.30, 0.60 and 0.78 are also considered for S_c , which represents specific condition of the flow (in particular, 0.22 corresponds to hydrogen, while 0.30 corresponds to helium, 0.60 corresponds to water vapor that represents a diffusivity chemical species of most common interest in air and value 0.78 represents ammonia at temperature 25°C and 1 atmospheric pressure). The values of v_o , M , S_o , P_m , E_c and G_m are however chosen arbitrarily.

With the above mentioned parameters, the velocity profiles are presented in Figs. (4.2)-(4.9), the induced magnetic fields are presented in Figs. (4.10)-(4.17), the current density profiles are presented in Figs. (4.18)-(4.25), the temperature profiles are presented in Figs. (4.26)-(4.33) and the concentration profiles are presented in Figs. (4.34)-(4.41).

Fig.(4.2) shows the effect of the suction parameter v_o on the velocity field. This figure depicts that an increase in the suction parameter (v_o) leads to a decrease in the velocity. The usual stabilizing effect of the suction parameter on the boundary layer growth is also evident from this figure. The effect of the magnetic parameter (M) on the velocity field is shown in Fig.(4.3). It is observed from this figure that an increase in magnetic parameter (M) leads to an increase in the velocity. Also the stabilizing effect of M on the boundary layer growth is evident. It is observed from Fig (4.4) that the velocity increases within the interval $0 < \eta < 0.42$ (approx.) with the increase of P_m , whereas for roughly after $\eta > 0.45$ the velocity decreases with the increase of P_m . In Figs.(4.5), (4.6) and (4.7), the variation of the velocity field for different values of Soret number (S_o), Eckert number (E_c) and Grashof number (G_r) are shown respectively. It is observed from these figures that the velocity increases with the increase of S_o , E_c and G_r . In Figs (4.8) and (4.9), the variation of the velocity field for different values of P_r and S_c are shown respectively. From these figures, it is seen that the velocity decreases with the increase of P_r and S_c . It is seen from Figs.(4.2)-(4.9), the effect of the various parameters on the velocity profiles is more prominent when $\eta = 0.3$ (approximately). It is also seen from Fig.(4.9) that the velocity is more for hydrogen ($S_c = 0.22$ at temperature 25°C and 1 atmospheric pressure) than ammonia ($S_c = 0.78$ at temperature 25°C and 1 atmospheric pressure).

The effect of the suction parameter (v_o) on induced magnetic field are shown in Fig(4.10). It is observed from this figure that the induced magnetic field decreases within the interval $0 < \eta < 0.55$ (approx.), whereas after $\eta > 0.55$, the induced magnetic field increases with the increase of v_o . Figs.(4.11) and (4.12) show the effect of M and P_m on the induced magnetic field respectively. It is observed from Fig.(4.11) that the induced magnetic field has a large decreasing effect with the increase of M . The same effect is observed in case of magnetic diffusivity

parameter (P_m). In both cases decreasing effect is more prominent approximately at the point where, $\eta = 0.8$. The induced magnetic fields are shown in Figs.(4.13), (4.14) and (4.15) for different values of S_o , E_c or G_r . It is observed from these figures that the induced magnetic field decreases with the increase of S_o , E_c and G_r respectively. In Figs (4.16) and (4.17), the effects of Prandtl number (P_r) and Schimidt number (S_c) on the induced magnetic field are shown. It is observed from these figures that the induced magnetic field increases with the increase of P_r or S_c . It is seen from Fig.(4.17) that the induced magnetic field is more for ammonia ($S_c=0.78$ at temperature 25^0C and 1 atmospheric pressure) than hydrogen ($S_c =0.22$ at temperature 25^0C and 1 atmospheric pressure). In the above Figs.(4.10)-(4.17), it is seen that H becomes negative when $0.4 \leq \eta < 2.0$ approximately.

Fig.(4.18)-(4.25) show the effect of the above mentioned various parameters on the current density profiles. From Fig.(4.18), it is observed that the current density increases rapidly near the plate (approx. $\eta < 0.25$) and it has a decreasing effect within the interval $0.25 < \eta < 1$ with the increase of v_o . From this figure it is further observed that the current density again changes its pattern. Figs.(4.19) and (4.20) show that the current density increases rapidly near the plate(approx. $\eta < 0.64$), From the point where $\eta > 0.64$ the current density decreases with the increase of M or P_m . It is observed from Figs (4.21), (4.22) and (4.23) the current density has a quite minor increasing effects within the interval $0 < \eta < 0.8$ and from the point where $\eta > 0.8$ the current density decreases with the increase of S_o , E_c or G_r . In both Figs. (4.24) and (4.25), it is observed that the increase in P_r and S_c leads to a quite minor decreasing effect on the current density within the interval $0 < \eta < 0.8$ whereas it has a quite minor increasing effect after this interval. It is observed from Figs.(4.18)-(4.24), there is a back flow occurred in a considerable area of the boundary layer.

Figs.(4.26)-(4.33) show the effect of the above mentioned various parameters on the temperature profiles. Fig.(4.26) shows that the temperature decreases with the increase of v_o . The temperature rapidly increases towards the plate with the increase of M as found in Fig.(4.27). It is observed from the Fig.(4.28) that the temperature increases in the range $0 < \eta < 0.73$ (approx.) and further it has a quite minor decreasing effect after this interval with the increase of P_m . From Fig.(4.29), it is observed that the temperature has a minor increasing effect with the increase of S_o , whereas from Fig.(4.30), it is seen that the temperature has a large increasing effect towards the plate as E_c increases. From Fig.(4.31), it is observed that the temperature increases with increase in G_r . But in Figs.(4.32)-(4.33) leads to a decreasing effects of the temperature with increase of the

Prandtl number (P_r) and Schmidt number (S_c) respectively. It is also clear from Fig.(4.33) that the temperature is more for hydrogen ($S_c=0.22$) than ammonia ($S_c=0.78$).

The concentration profiles are shown in Figs.(4.34)-(4.41) for different values of v_o , M , P_m , S_o , E_c , G_r , P_r , and S_c . Fig.(4.34) shows that the concentration decreases with increase in the suction parameter (v_o). It is observed from Fig.(4.35) that the concentration increases close to the plate within the interval (approx. $0 < \eta < 0.48$), thereafter it has a decreasing effect with the increase of M . From Fig.(4.36), it is seen that the concentration has a minor decreasing effect within the interval $0 < \eta < 0.4$ and further it has a minor increasing effect within $0.4 < \eta < 1.5$, thereafter it has no effect with the increase of P_m . The concentration has a large increasing effect with the increase of S_o as shown in Fig.(4.37). It is seen from Fig.(4.38) that the decreasing effect of concentration occurs in the interval $0 < \eta < 0.55$ (approx.) and further it has a increasing effect from $\eta > 0.55$ with the increase of E_c , whereas from Fig.(4.39), the effects on the concentration for the different values of the Grashof number (G_r) are same as those of E_c . For the increasing value of P_r leads to a minor increasing effect on the concentration approximately in the interval $0 < \eta < 0.7$, thereafter it has a minor decreasing effect as shown in Fig(4.40). But Fig.(4.41) shows that the concentration increase with the increase of S_c . Also it is noticed from this figure that the concentration is more for hydrogen ($S_c=0.22$) than ammonia ($S_c=0.78$).

Finally the effects of the various parameters on the skin friction (τ) and the current density at the plate (J_w) are shown in Tables 4.1-4.8. It is observed from Table 4.1 that the skin friction (τ) decreases while the current density at the plate increases with the increase of suction parameter (v_o). In Tables 4.2-4.6, the skin friction and the current density at the plate are both increase with the increase of Magnetic parameter (M), Magnetic diffusivity (P_m), Soret number (S_o), Eckert number (E_c) and Grashof number (G_r) respectively. Whereas Tables 4.7 and 4.8 show that the skin friction and the current density at the plate (J_w) are both decrease with the increase of the Prandtl number (P_r) and Schmidt number (S_c) respectively.

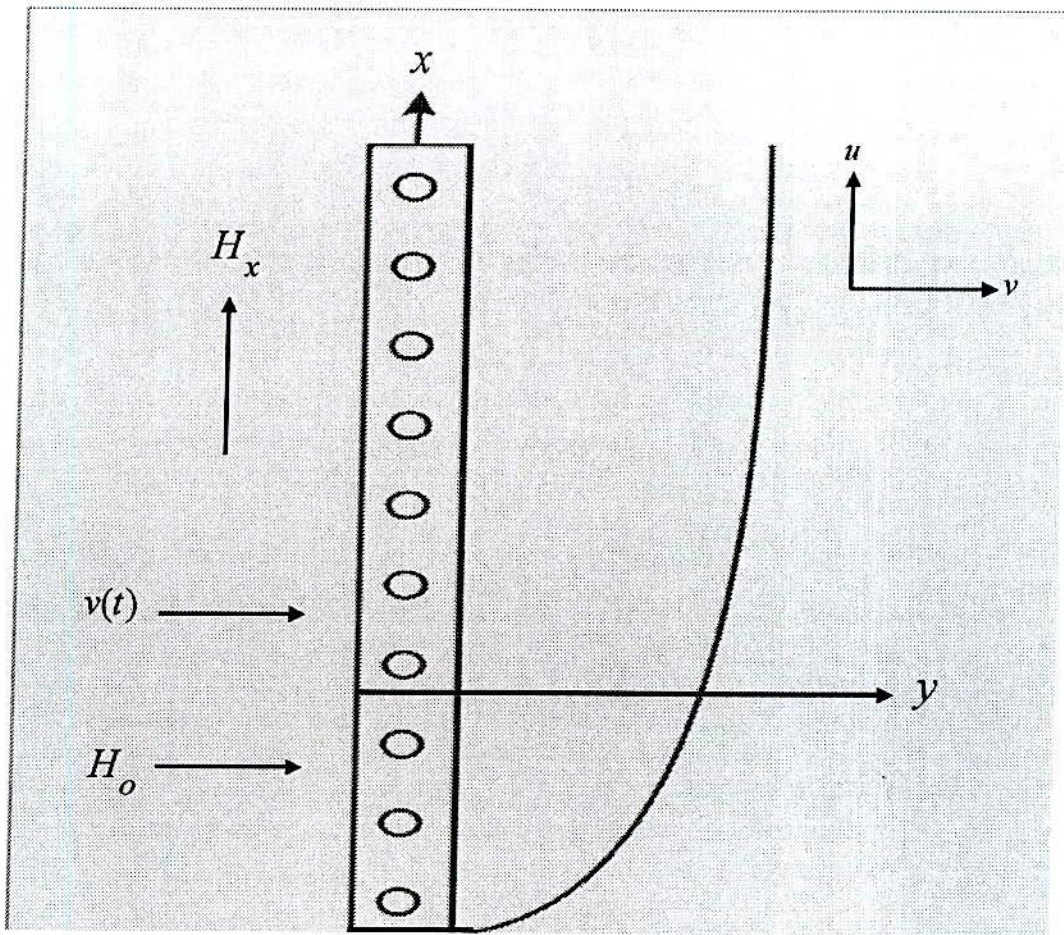


Fig. 4.1. Physical configuration and coordinate system.

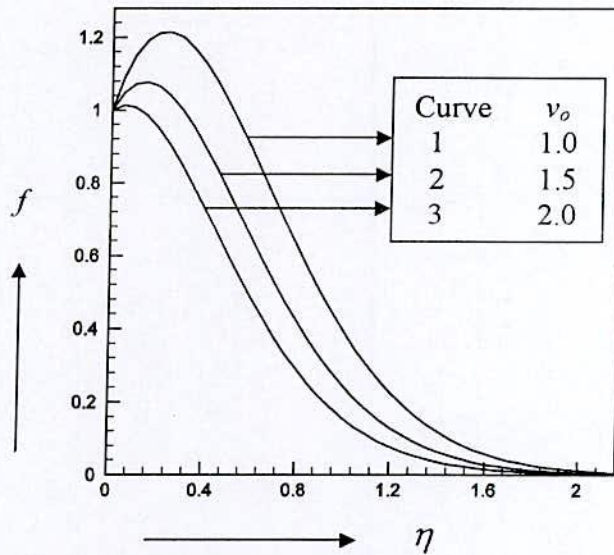


Fig. 4.2. Velocity profiles (f) for different values of v_o , taking $G_r=5.0$, $G_m=2.0$, $M=1.0$, $P_m=1.0$, $P_r=0.71$, $S_o=2.0$, $S_c=0.6$ and $E_c=0.5$ as fixed.

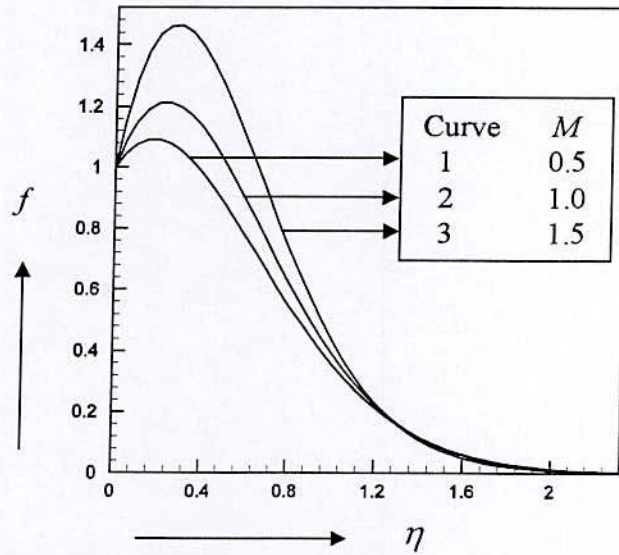


Fig. 4.3. Velocity profiles (f) for different values of M , taking $v_o=1.0$, $G_r=5.0$, $G_m=2.0$, $P_m=1.0$, $P_r=0.71$, $S_o=2.0$, $S_c=0.6$ and $E_c=0.5$ as fixed.

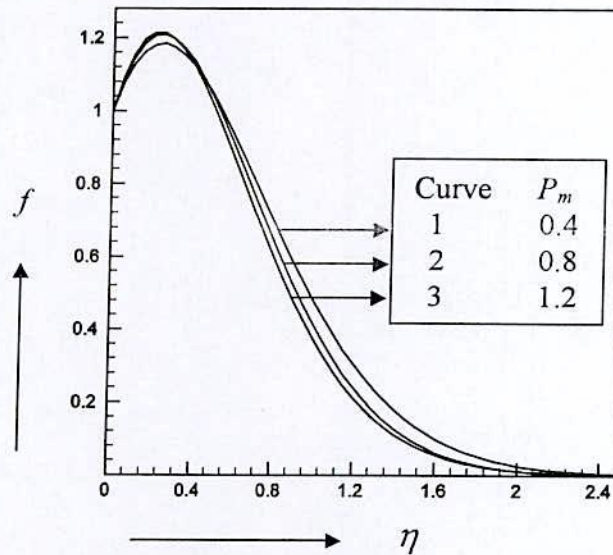


Fig. 4.4. Velocity profiles (f) for different values of P_m , taking $v_o=1.0$, $G_r=5.0$, $G_m=2.0$, $M=1.0$, $P_r=0.71$, $S_o=2.0$, $S_c=0.6$ and $E_c=0.5$ as fixed.

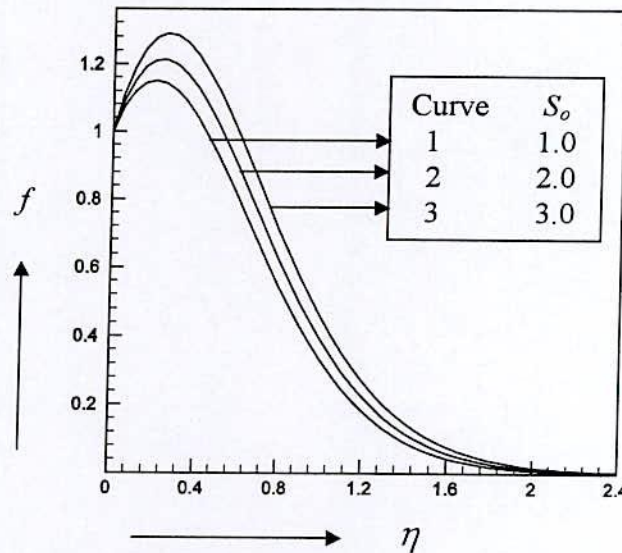


Fig. 4.5. Velocity profiles (f) for different values of S_o , taking $v_o=1.0$, $G_r=5.0$, $G_m=2.0$, $M=1.0$, $P_m=1.0$, $P_r=0.71$, $S_c=0.6$ and $E_c=0.5$ as fixed.

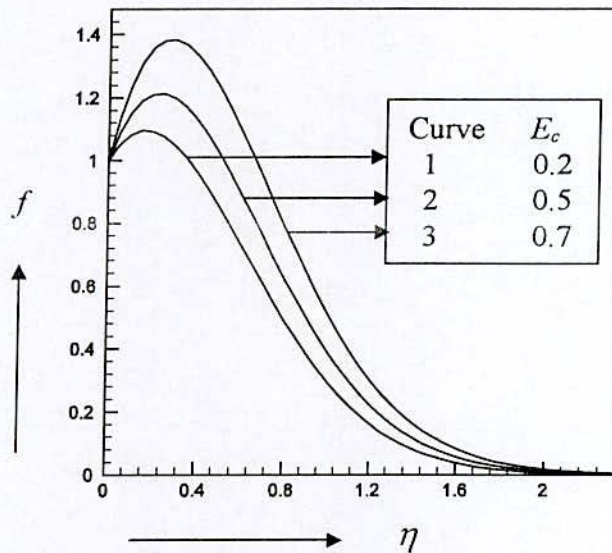


Fig. 4.6. Velocity profiles (f) for different values of E_c , taking $v_o=1.0$, $G_r=5.0$, $G_m=2.0$, $M=1.0$, $P_m=1.0$, $P_r=0.71$, $S_o=2.0$, and $S_c=0.6$ as fixed.

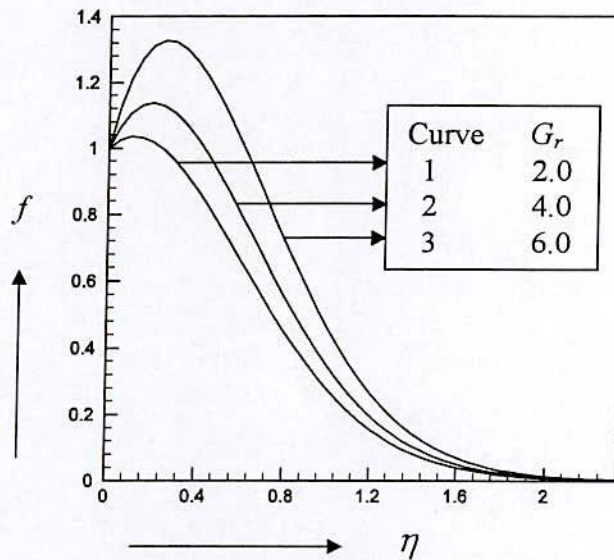


Fig. 4.7. Velocity profiles (f) for different values of G_r , taking $v_o=1.0$, $G_m=2.0$, $M=1.0$, $P_m=1.0$, $P_r=0.71$, $S_o=2.0$, $S_c=0.6$ and $E_c=0.5$ as fixed.

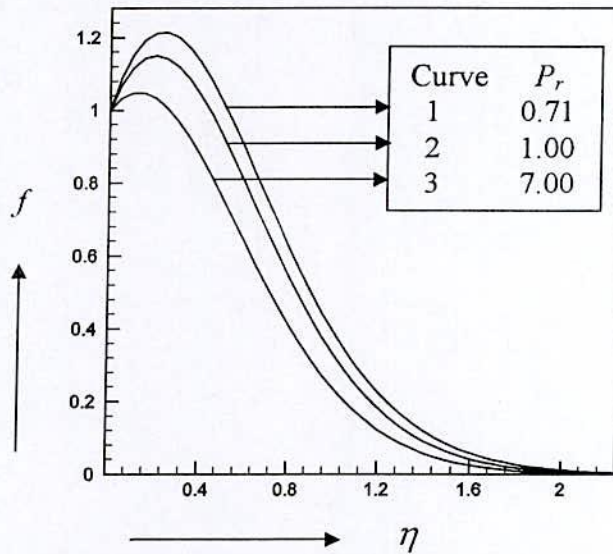


Fig. 4.8. Velocity profiles (f) for different values of P_r , taking $v_o=1.0$, $G_r=5.0$, $G_m=2.0$, $M=1.0$, $P_m=1.0$, $S_o=2.0$, $S_c=0.6$ and $E_c=0.5$ as fixed.

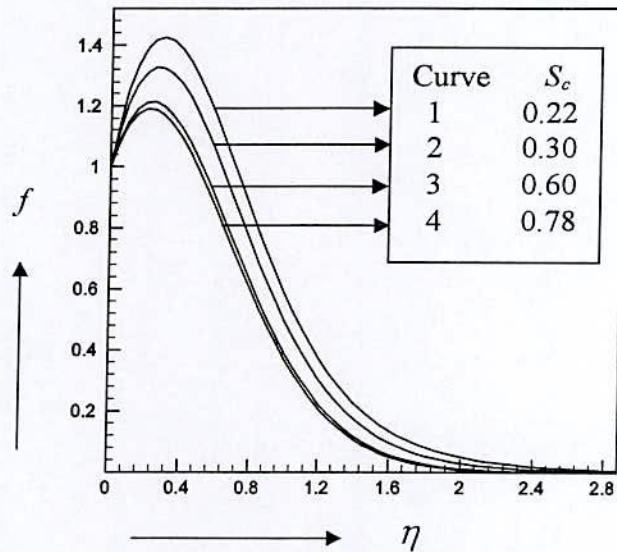


Fig. 4.9. Velocity profiles (f) for different values of S_c , taking $v_o=1.0$, $G_r=5.0$, $G_m=2.0$, $M=1.0$, $P_m=1.0$, $P_r=0.71$, $S_o=2.0$, and $E_c=0.5$ as fixed.

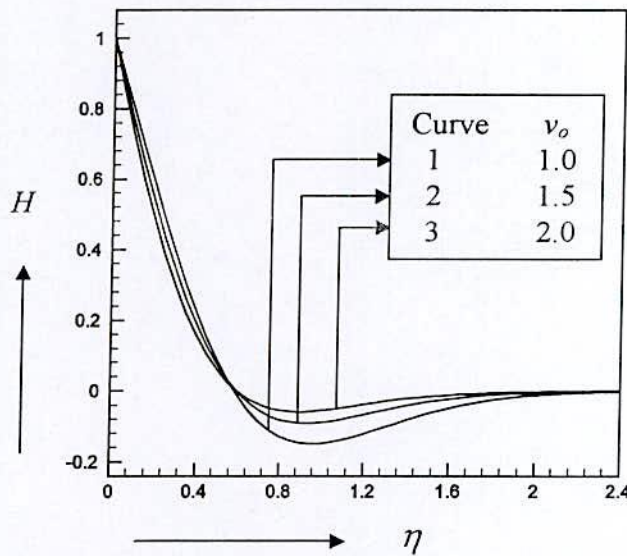


Fig. 4.10. Induced magnetic field (H) for different values of ν_o , taking $G_r=5.0$, $G_m=2.0$, $M=1.0$, $P_m=1.0$, $P_r=0.71$, $S_o=2.0$, $S_c=0.6$ and $E_c=0.5$ as fixed.

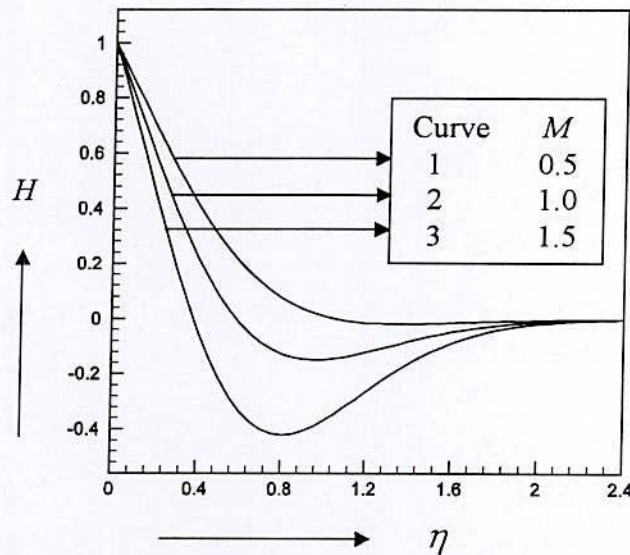


Fig. 4.11. Induced magnetic field (H) for different values of M , taking $\nu_o=1.0$, $G_r=5.0$, $G_m=2.0$, $P_m=1.0$, $P_r=0.71$, $S_o=2.0$, $S_c=0.6$ and $E_c=0.5$ as fixed.

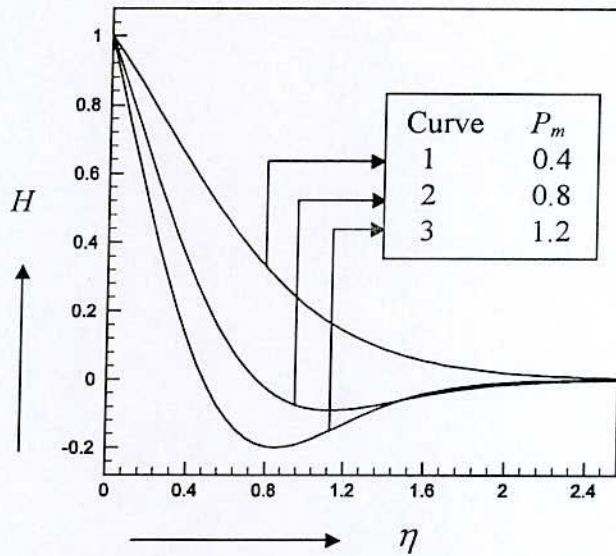


Fig. 4.12. Induced magnetic field (H) for different values of P_m , taking $\nu_o=1.0$, $G_r=5.0$, $G_m=2.0$, $M=1.0$, $P_r=0.71$, $S_o=2.0$, $S_c=0.6$ and $E_c=0.5$ as fixed.

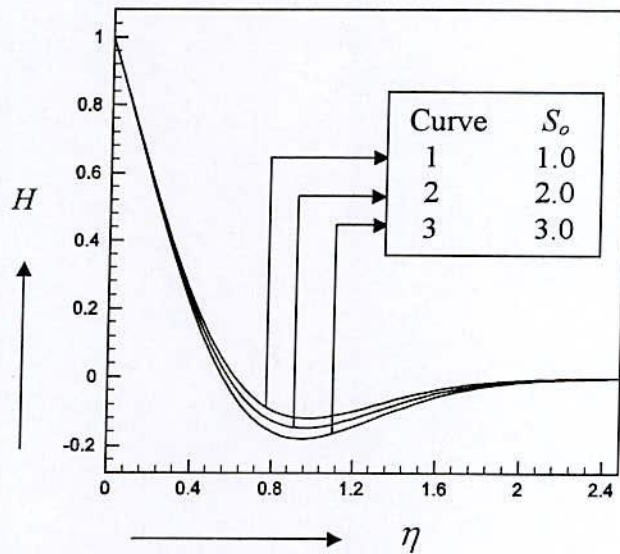


Fig. 4.13. Induced magnetic field (H) for different values of S_o , taking $\nu_o=1.0$, $G_r=5.0$, $G_m=2.0$, $M=1.0$, $P_m=1.0$, $P_r=0.71$, $S_c=0.6$ and $E_c=0.5$ as fixed.

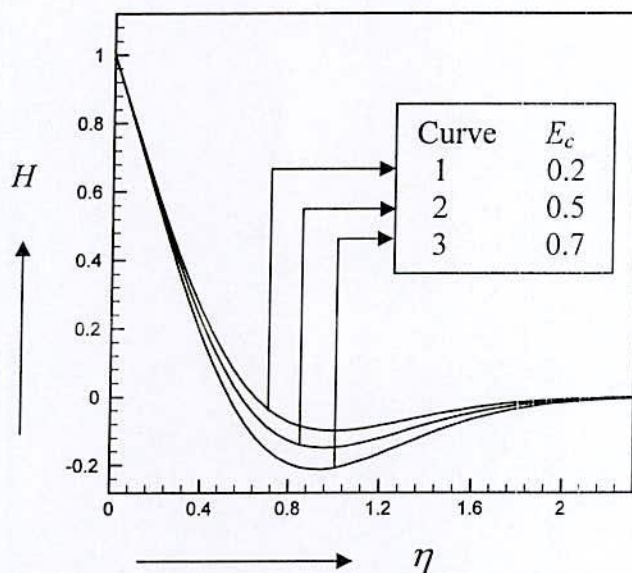


Fig.4.14. Induced magnetic field (H) for different values of E_c , taking $v_o=1.0$, $G_r=5.0$, $G_m=2.0$, $M=1.0$, $P_m=1.0$, $P_r=0.71$, $S_o=2.0$, and $S_c=0.6$ as fixed.

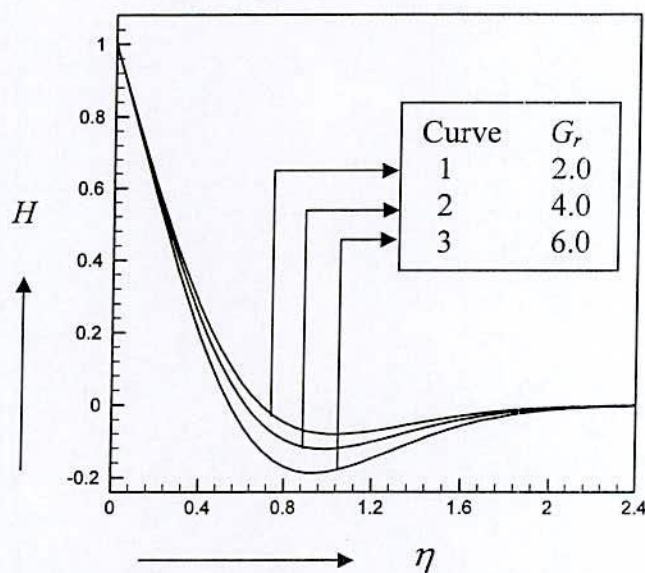


Fig. 4.15. Induced magnetic field (H) for different values of G_r , taking $v_o=1.0$, $G_m=2.0$, $M=1.0$, $P_m=1.0$, $P_r=0.71$, $S_o=2.0$, $S_c=0.6$ and $E_c=0.5$ as fixed.

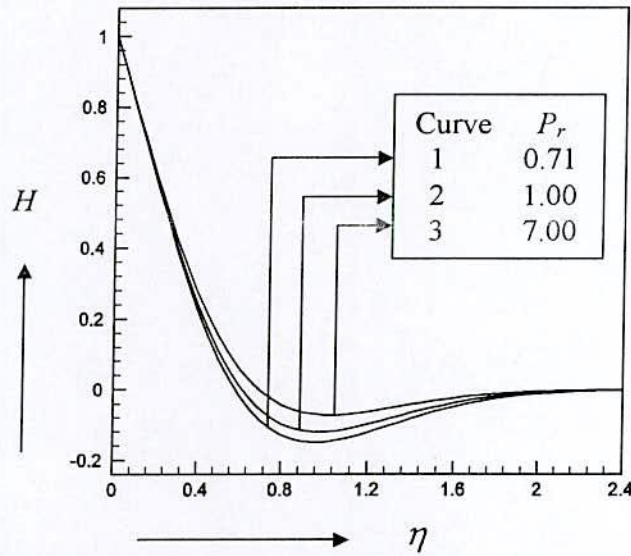


Fig. 4.16. Induced magnetic field (H) for different values of P_r , taking $\nu_o=1.0$, $G_r=5.0$, $G_m=2.0$, $M=1.0$, $P_m=1.0$, $S_o=2.0$, $S_c=0.6$ and $E_c=0.5$ as fixed.

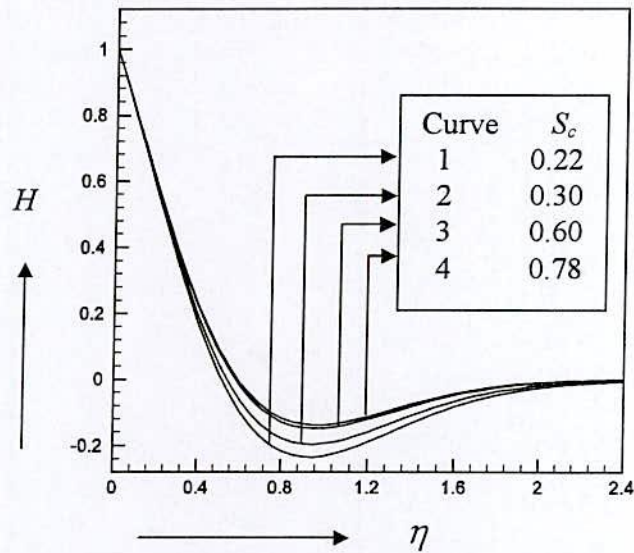


Fig.4.17. Induced magnetic field (H) for different values of S_c , taking $\nu_o=1.0$, $G_r=5.0$, $G_m=2.0$, $M=1.0$, $P_m=1.0$, $P_r=0.71$, $S_o=2.0$, and $E_c=0.5$ as fixed.

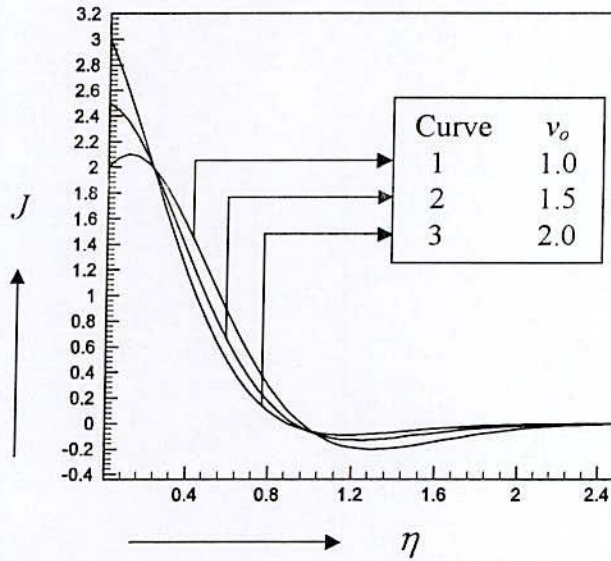


Fig. 4.18. Current density profiles (J) for different values of ν_o , taking $G_r=5.0$, $G_m=2.0$, $M=1.0$, $P_m=1.0$, $P_r=0.71$, $S_o=2.0$, $S_c=0.6$ and $E_c=0.5$ as fixed.

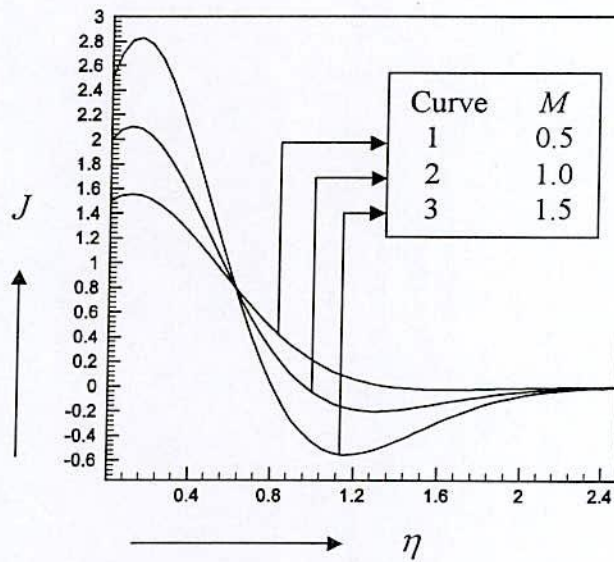


Fig. 4.19. Current density profiles (J) for different values of M , taking $\nu_o=1.0$, $G_r=5.0$, $G_m=2.0$, $P_m=1.0$, $P_r=0.71$, $S_o=2.0$, $S_c=0.6$ and $E_c=0.5$ as fixed.

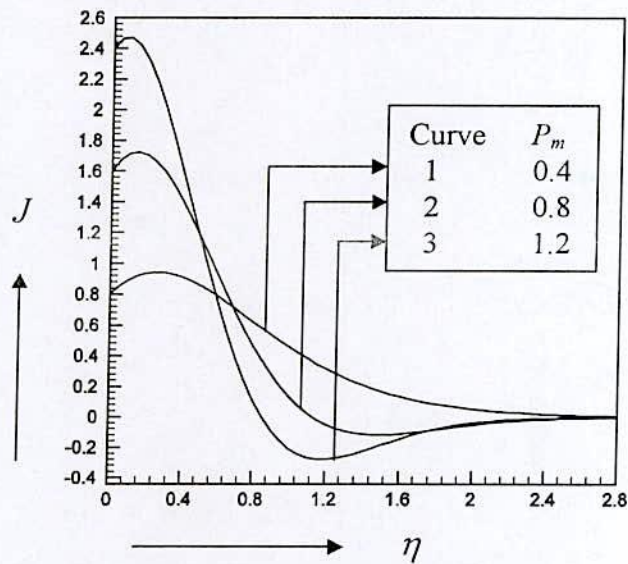


Fig. 4.20. Current density profiles (J) for different values of P_m , taking $v_o=1.0$, $G_r=5.0$, $G_m=2.0$, $M=1.0$, $P_r=0.71$, $S_o=2.0$, $S_c=0.6$ and $E_c=0.5$ as fixed.

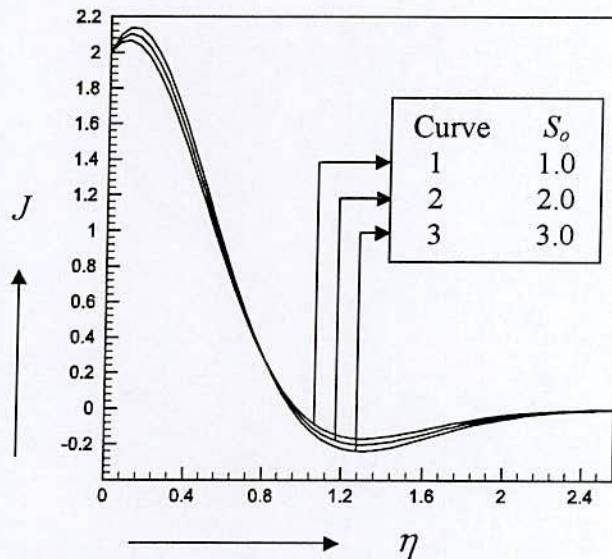


Fig. 4.21. Current density profiles (J) for different values of S_o , taking $v_o=1.0$, $G_r=5.0$, $G_m=2.0$, $M=1.0$, $P_m=1.0$, $P_r=0.71$, $S_c=0.6$ and $E_c=0.5$ as fixed.

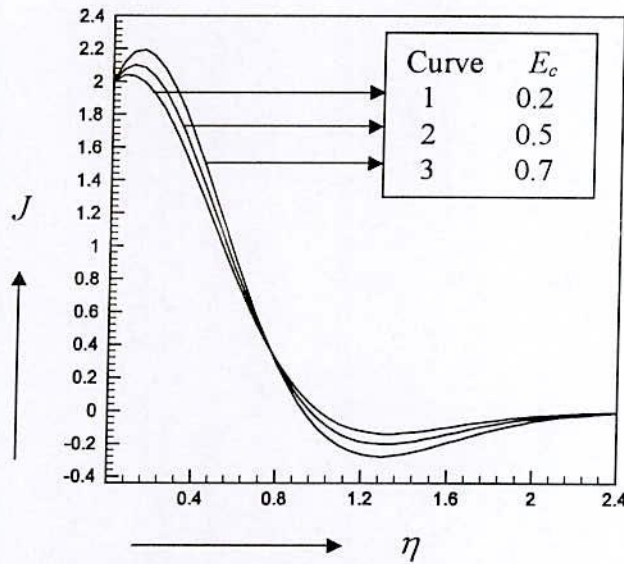


Fig. 4.22. Current density profiles (J) for different values of E_c , taking $\nu_o = 1.0$, $G_r = 5.0$, $G_m = 2.0$, $M = 1.0$, $P_m = 1.0$, $P_r = 0.71$, $S_o = 2.0$, and $S_c = 0.6$ as fixed.

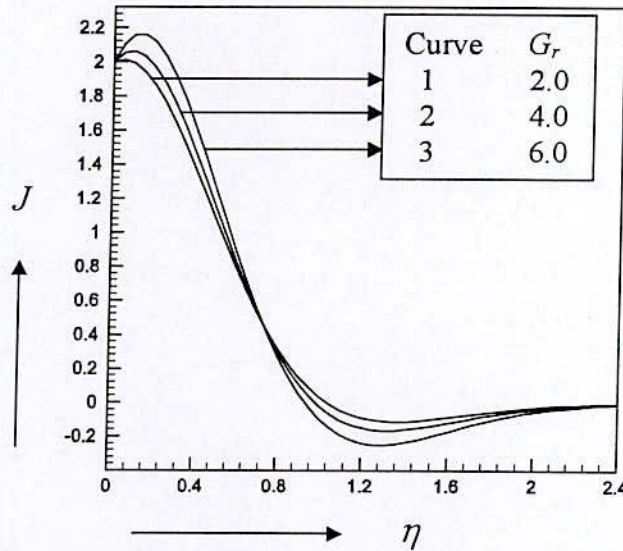


Fig. 4.23. Current density profiles (J) for different values of G_r , taking $\nu_o = 1.0$, $G_m = 2.0$, $M = 1.0$, $P_m = 1.0$, $P_r = 0.71$, $S_o = 2.0$, $S_c = 0.6$ and $E_c = 0.5$ as fixed.

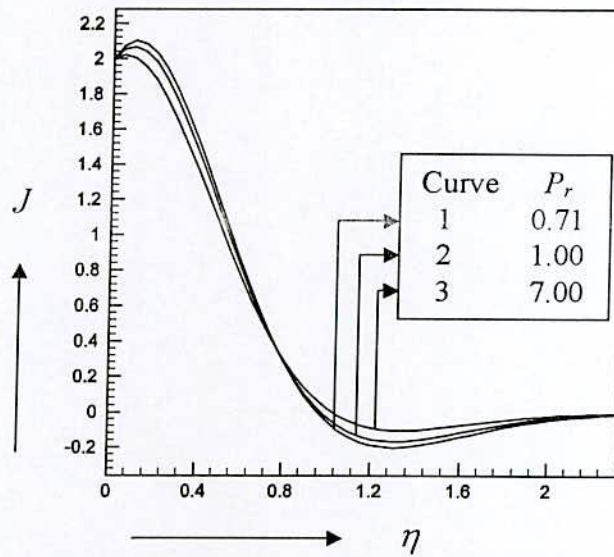


Fig. 4.24. Current density profiles (J) for different values of P_r , taking $\nu_o=1.0$, $G_r=5.0$, $G_m=2.0$, $M=1.0$, $P_m=1.0$, $S_o=2.0$, $S_c=0.6$ and $E_c=0.5$ as fixed.

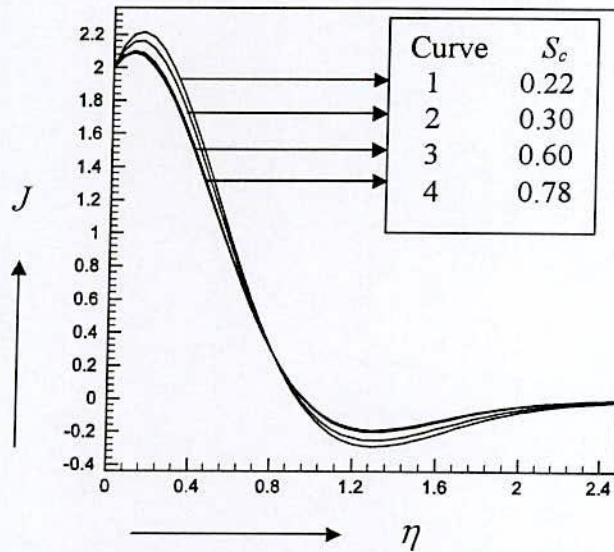


Fig. 4.25. Current density profiles (J) for different values of S_c , taking $\nu_o=1.0$, $G_r=5.0$, $G_m=2.0$, $M=1.0$, $P_m=1.0$, $P_r=0.71$, $S_o=2.0$, and $E_c=0.5$ as fixed.

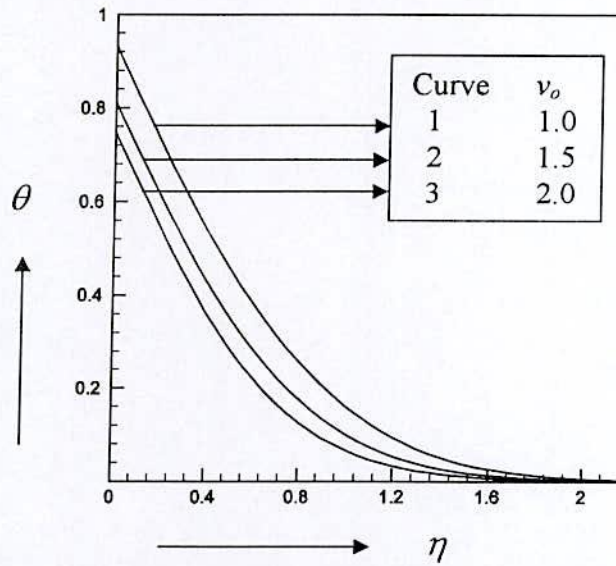


Fig. 4.26. Temperature profiles (θ) for different values of ν_0 , taking $G_r=5.0$, $G_m=2.0$, $M=1.0$, $P_m=1.0$, $P_r=0.71$, $S_o=2.0$, $S_c=0.6$ and $E_c=0.5$ as fixed.

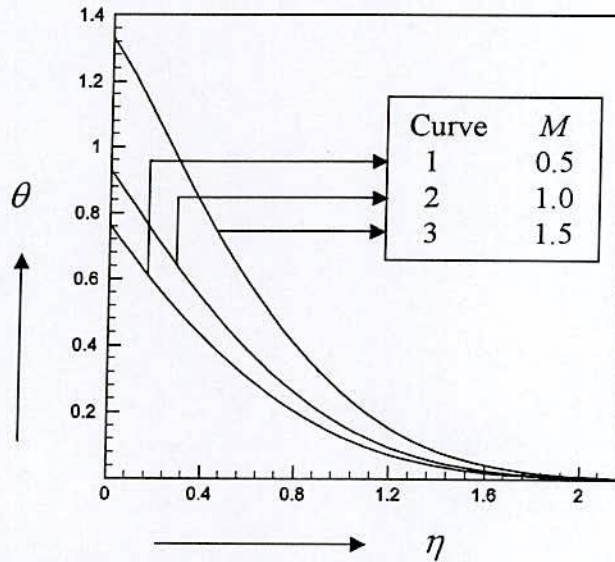


Fig. 4.27. Temperature profiles (θ) for different values of M , taking $\nu_0=1.0$, $G_r=5.0$, $G_m=2.0$, $P_m=1.0$, $P_r=0.71$, $S_o=2.0$, $S_c=0.6$ and $E_c=0.5$ as fixed.

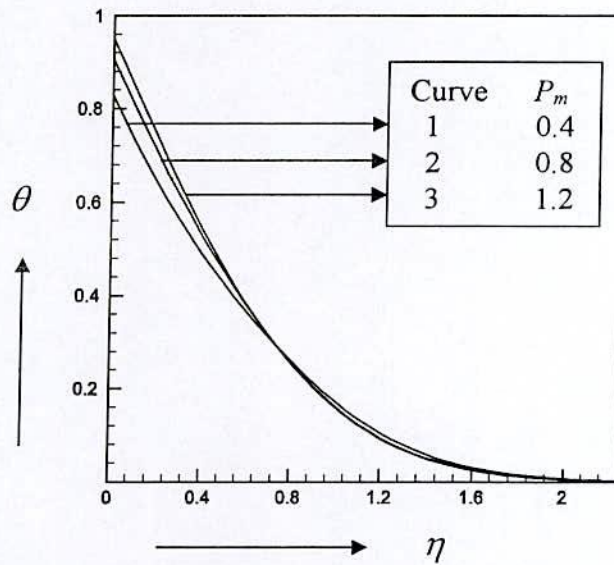


Fig. 4.28. Temperature profiles (θ) for different values of P_m , taking $\nu_o=1.0$, $G_r=5.0$, $G_m=2.0$, $M=1.0$, $P_r=0.71$, $S_o=2.0$, $S_c=0.6$ and $E_c=0.5$ as fixed.

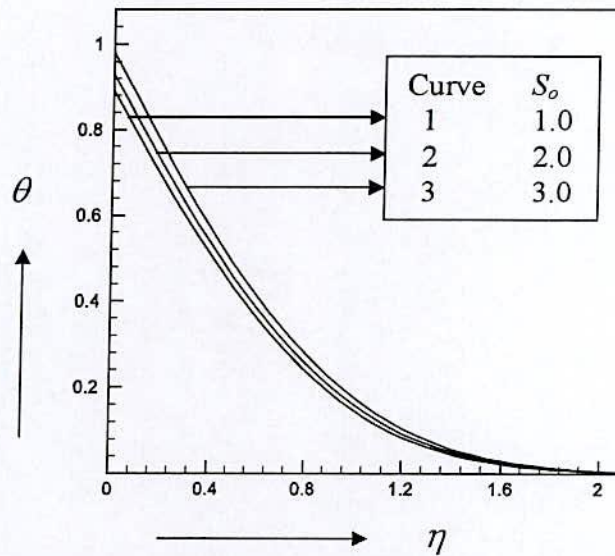


Fig. 4.29. Temperature profiles (θ) for different values of S_o , taking $\nu_o=1.0$, $G_r=5.0$, $G_m=2.0$, $M=1.0$, $P_m=1.0$, $P_r=0.71$, $S_c=0.6$ and $E_c=0.5$ as fixed.

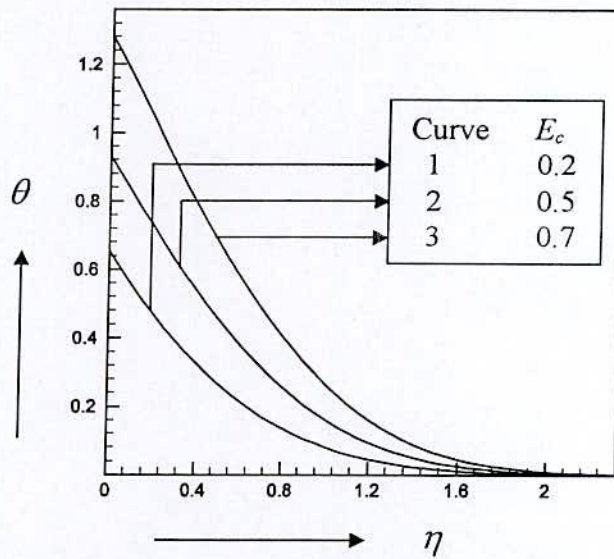


Fig. 4.30. Temperature profiles (θ) for different values of E_c , taking $\nu_o=1.0$, $G_r=5.0$, $G_m=2.0$, $M=1.0$, $P_m=1.0$, $P_r=0.71$, $S_o=2.0$, and $S_c=0.6$ as fixed.

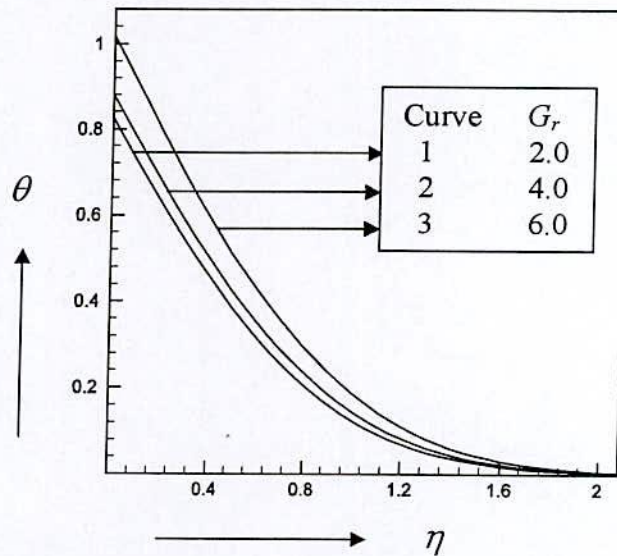


Fig. 4.31. Temperature profiles (θ) for different values of G_r , taking $\nu_o=1.0$, $G_m=2.0$, $M=1.0$, $P_m=1.0$, $P_r=0.71$, $S_o=2.0$, $S_c=0.6$ and $E_c=0.5$ as fixed.



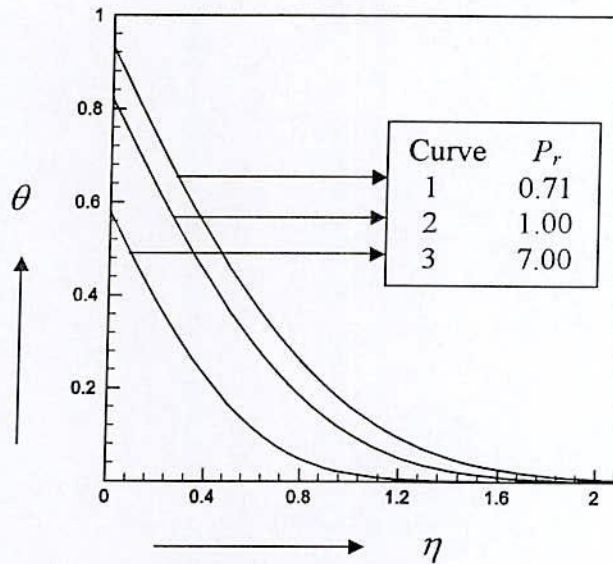


Fig. 4.32. Temperature profiles (θ) for different values of P_r , taking $\nu_o=1.0$, $G_r=5.0$, $G_m=2.0$, $M=1.0$, $P_m=1.0$, $S_o=2.0$, $S_c=0.6$ and $E_c=0.5$ as fixed.

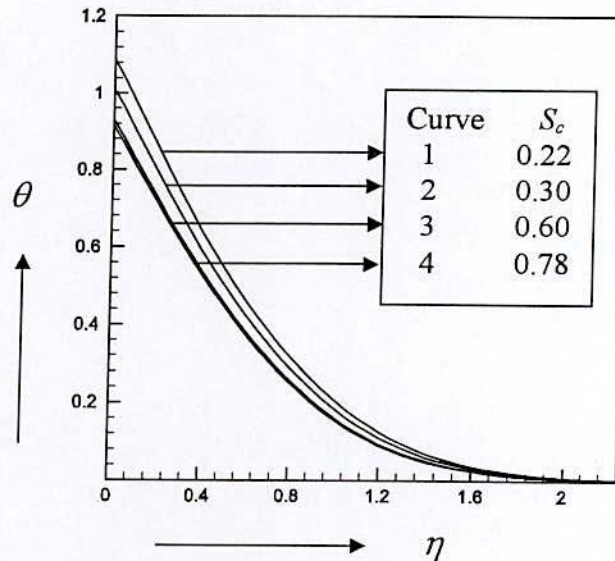


Fig. 4.33. Temperature profiles (θ) for different values of S_c , taking $\nu_o=1.0$, $G_r=5.0$, $G_m=2.0$, $M=1.0$, $P_m=1.0$, $P_r=0.71$, $S_o=2.0$, and $E_c=0.5$ as fixed.

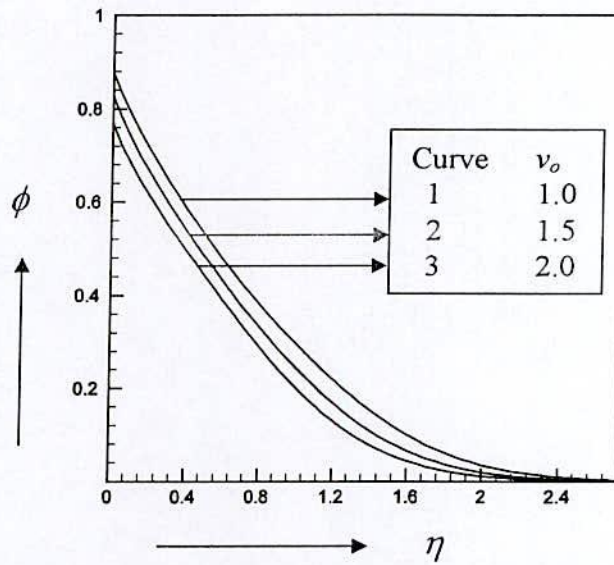


Fig. 4.34. Concentration profiles (ϕ) for different values of ν_o , taking $G_r=5.0$, $G_m=2.0$, $M=1.0$, $P_m=1.0$, $P_r=0.71$, $S_o=2.0$, $S_c=0.6$ and $E_c=0.5$ as fixed.

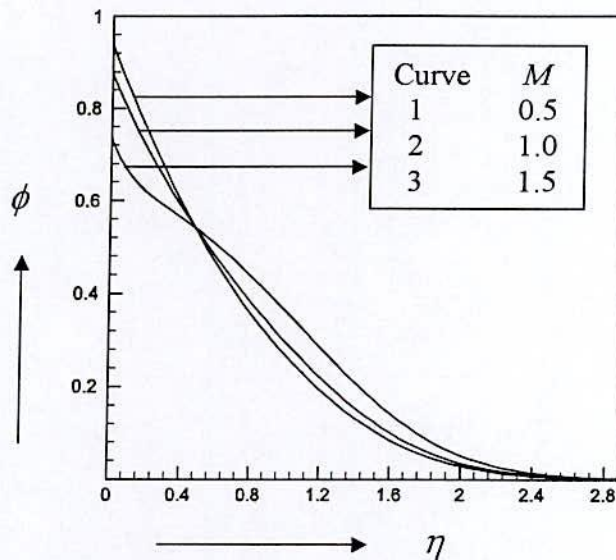


Fig. 4.35. Concentration profiles (ϕ) for different values of M , taking $\nu_o=1.0$, $G_r=5.0$, $G_m=2.0$, $P_m=1.0$, $P_r=0.71$, $S_o=2.0$, $S_c=0.6$ and $E_c=0.5$ as fixed.

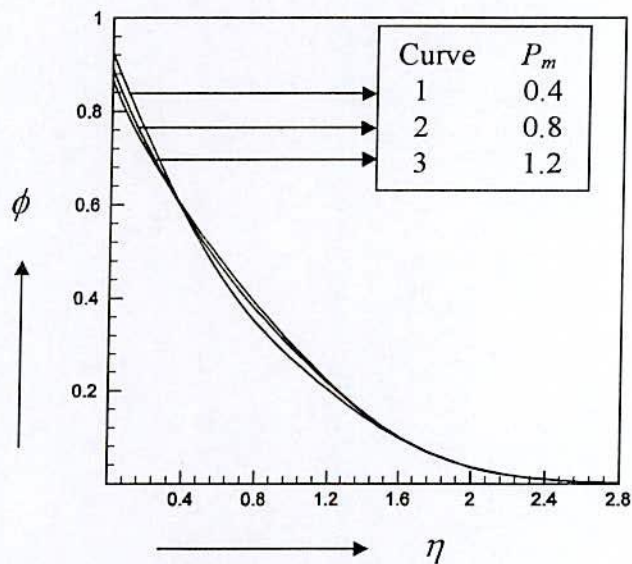


Fig. 4.36. Concentration profiles (ϕ) for different values of P_m , taking $\nu_o=1.0$, $G_r=5.0$, $G_m=2.0$, $M=1.0$, $P_r=0.71$, $S_o=2.0$, $S_c=0.6$ and $E_c=0.5$ as fixed.

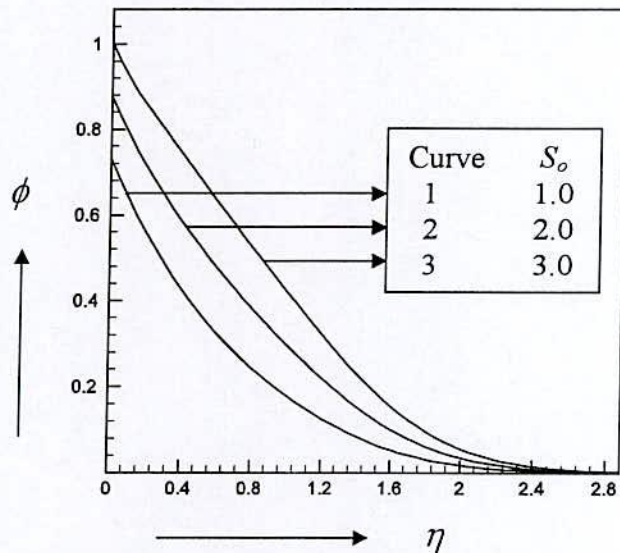


Fig. 4.37. Concentration profiles (ϕ) for different values of S_o , taking $\nu_o=1.0$, $G_r=5.0$, $G_m=2.0$, $M=1.0$, $P_m=1.0$, $P_r=0.71$, $S_c=0.6$ and $E_c=0.5$ as fixed.

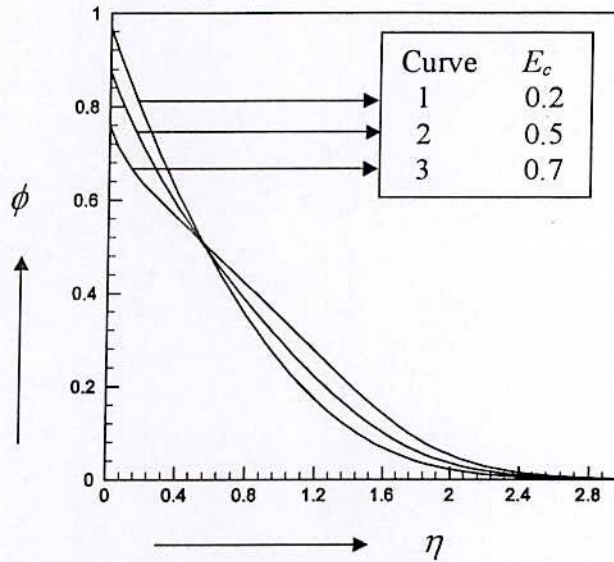


Fig. 4.38. Concentration profiles (ϕ) for different values of E_c , taking $\nu_o=1.0$, $G_r=5.0$, $G_m=2.0$, $M=1.0$, $P_m=1.0$, $P_r=0.71$, $S_o=2.0$, and $S_c=0.6$ as fixed.

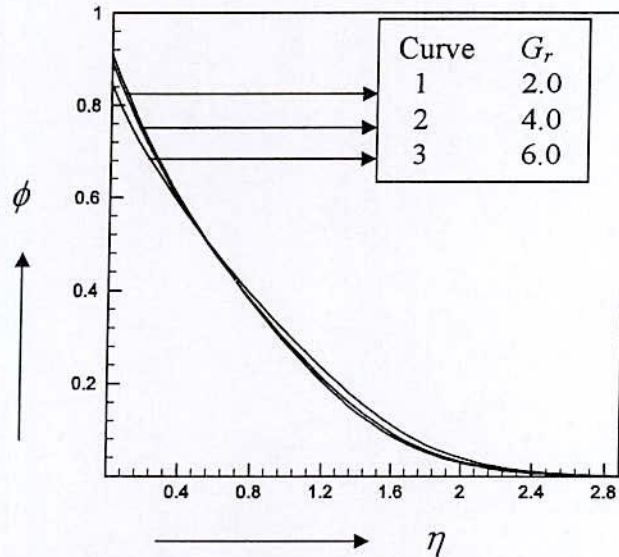


Fig. 4.39. Concentration profiles (ϕ) for different values of G_r , taking $\nu_o=1.0$, $G_m=2.0$, $M=1.0$, $P_m=1.0$, $P_r=0.71$, $S_o=2.0$, $S_c=0.6$ and $E_c=0.5$ as fixed.

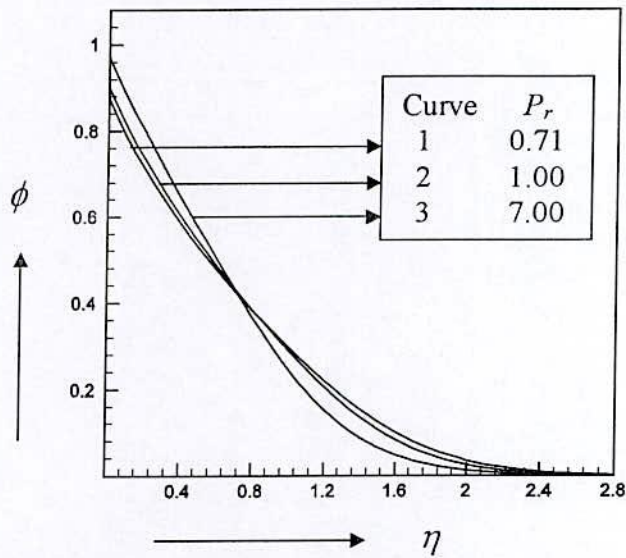


Fig. 4.40. Concentration profiles (ϕ) for different values of P_r , taking $v_o=1.0$, $G_r=5.0$, $G_m=2.0$, $M=1.0$, $P_m=1.0$, $S_o=2.0$, $S_c=0.6$ and $E_c=0.5$ as fixed.

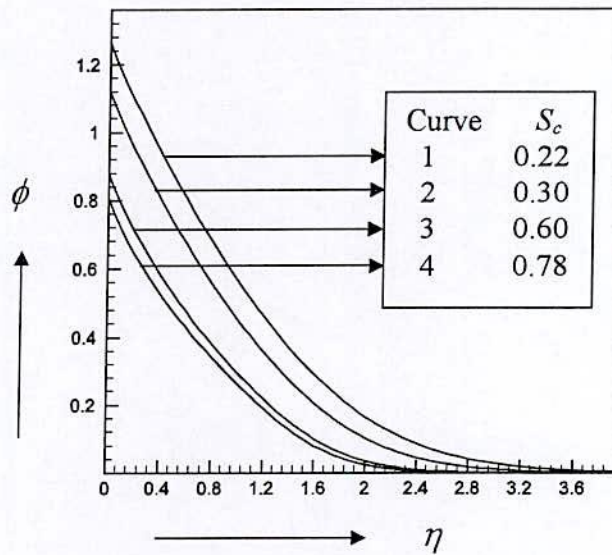


Fig. 4.41. Concentration profiles (ϕ) for different values of S_c , taking $v_o=1.0$, $G_r=5.0$, $G_m=2.0$, $M=1.0$, $P_m=1.0$, $P_r=0.71$, $S_o=2.0$, and $E_c=0.5$ as fixed.

Table 4.1. Numerical values proportional to τ and J_w for $G_r=5.0$, $G_m=2.0$, $M=1.0$, $P_m=1.0$, $P_r=0.71$, $S_o=2.0$, $S_c=0.6$ and $E_c=0.5$.

v_o	τ	J_w
1.00	2.0104592	1.9999696
1.50	1.1891806	2.4993759
2.00	0.4986988	2.9999856

Table 4.2. Numerical values proportional to τ and J_w for $v_o=1.0$, $G_r=5.0$, $G_m=2.0$, $P_m=1.0$, $P_r=0.71$, $S_o=2.0$, $S_c=0.6$ and $E_c=0.5$.

M	τ	J_w
0.50	1.1262961	1.5001152
1.00	2.0104592	1.9999696
1.50	3.6339727	2.4997521

Table 4.3. Numerical values proportional to τ and J_w for $v_o=1.0$, $G_r=5.0$, $G_m=2.0$, $M=1.0$, $P_r=0.71$, $S_o=2.0$, $S_c=0.6$ and $E_c=0.5$.

P_m	τ	J_w
0.40	1.6710856	0.8030961
0.80	1.9291178	1.5996509
1.20	2.0701131	2.4000924

Table 4.4. Numerical values proportional to τ and J_w for $v_o=1.0$, $G_r=5.0$, $G_m=2.0$, $M=1.0$, $P_m=1.0$, $P_r=0.71$, $S_c=0.6$ and $E_c=0.5$.

S_o	τ	J_w
1.0	1.6214634	2.0561243
2.0	2.0104592	2.0753115
3.0	2.4309134	2.0944394

Table 4.5. Numerical values proportional to τ and J_w for $v_o=1.0$, $G_r=5.0$, $G_m=2.0$, $M=1.0$, $P_m=1.0$, $P_r=0.71$, $S_o=2.0$, and $S_c=0.6$.

E_c	τ	J_w
0.20	1.2203901	2.0381327
0.50	2.0104592	2.0753115
0.70	2.9868018	2.1195070

Table:4.6. Numerical values proportional to τ and J_w for $v_o=1.0$, $G_m=2.0$, $M=1.0$, $P_m=1.0$, $P_r=0.71$, $S_o=2.0$, $S_c=0.6$ and $E_c=0.5$.

G_r	τ	J_w
2.0	0.6473006	2.0125380
4.0	1.4829989	2.0516683
6.0	2.7078323	2.1066295

Table 4.7. Numerical values proportional to τ and J_w for $v_o =1.0$, $G_r=5.0$, $G_m=2.0$, $M=1.0$, $P_m=1.0$, $S_o=2.0$, $S_c=0.6$ and $E_c=0.5$.

P_r	τ	J_w
0.71	2.0104592	2.0753116
1.00	1.6155200	2.0558877
7.00	0.8459845	2.0215634

Table 4.8. Numerical values proportional to τ and J_w for $v_o=1.0$, $G_r=5.0$, $G_m=2.0$, $M=1.0$, $P_m=1.0$, $P_r=0.71$, $S_o=2.0$, and $E_c=0.5$.

S_c	τ	J_w
0.22	3.1648616	2.0002390
0.30	2.6592434	2.0001581
0.60	2.0104592	1.9999696
0.78	1.8644322	1.9982135

Chapter 5

Steady heat and mass transfer by mixed convection flow from a vertical porous plate with induced magnetic field, constant heat and mass fluxes

5.1 Introduction

Heat and mass transfer in the presence of magnetic field, which is the subject matter of MHD has many different applications in engineering. Hot rolling, metal and plastic extrusion, continuous casting, glass fiber production, paper production etc are some processes where the concept of the flow past a continuously moving surface are applied. Researches in the related fields are ongoing. Recently the combined heat and mass transfer by laminar mixed convection flow of an incompressible electrically conducting viscous fluid past an electrically non-conducting continuously moving infinite vertical porous plate under the action of a uniform transverse magnetic with constant heat flux and induced magnetic field is studied analytically by Chaudhary and Sharma (2006).

Here heat and mass transfer by mixed convection flow from a vertical porous plate with induced magnetic field, constant heat and mass fluxes is investigated. This problem is solved numerically in case of two-dimensional steady flow. The Governing equations of the problem contain the partial differential equations, which are transformed by usual similarity transformation in to a system of ordinary coupled non-linear differential equations and are then solved numerically by the sixth order Runge Kutta method along with the Nachtsheim-Swigert iteration technique. The obtained solutions are shown graphically as well as in tabular form.

5.2. The Governing Equations

Let us consider a steady heat and mass transfer by mixed convection flow of an electrically conducting viscous fluid past a semi-infinite vertical porous plate $y = 0$. The flow is also

assumed to be in x-direction which is taken along the plate in upward direction and y-axis is normal to it. The detailed descriptions of the present problem are similar to those of *Chapter 4*.

With reference to the generalized equation described in **Case II** of *Chapter 2*, the two dimensional problem under the above assumptions and Boussinesq approximation can be put in the following form

$$\frac{\partial u}{\partial x} + \frac{\partial v}{\partial y} = 0 \quad (5.1)$$

$$u \frac{\partial u}{\partial x} + v \frac{\partial u}{\partial y} = g\beta(T - T_\infty) + g\beta^*(C - C_\infty) + \nu \frac{\partial^2 u}{\partial y^2} + \frac{\mu_e}{\rho} H_o \frac{\partial H_x}{\partial y} \quad (5.2)$$

$$u \frac{\partial H_x}{\partial x} + v \frac{\partial H_x}{\partial y} = H_x \frac{\partial u}{\partial x} + H_o \frac{\partial u}{\partial y} + \frac{1}{\mu_e \sigma'} \frac{\partial^2 H_x}{\partial y^2} \quad (5.3)$$

$$u \frac{\partial T}{\partial x} + v \frac{\partial T}{\partial y} = \frac{k}{\rho c_p} \frac{\partial^2 T}{\partial y^2} + \frac{\nu}{c_p} \left(\frac{\partial u}{\partial y} \right)^2 + \frac{1}{\rho c_p \sigma'} \left(\frac{\partial H_x}{\partial y} \right)^2 \quad (5.4)$$

$$u \frac{\partial C}{\partial x} + v \frac{\partial C}{\partial y} = D_m \frac{\partial^2 C}{\partial y^2} + \frac{D_m K_T}{T_m} \frac{\partial^2 T}{\partial y^2} \quad (5.5)$$

and the boundary conditions for the problem are

$$\left. \begin{aligned} u = U_o, \quad v = v(x), \quad \frac{\partial T}{\partial y} = -\frac{q}{k}, \quad \frac{\partial C}{\partial y} = -\frac{m}{D_m}, \quad H_x = H_w \quad \text{at } y = 0 \\ u = 0, \quad T \rightarrow T_\infty, \quad C \rightarrow C_\infty, \quad H_x \rightarrow 0 \quad \text{as } y \rightarrow \infty \end{aligned} \right\} \quad (5.6)$$

where u and v are the velocity components in x - and y -direction respectively, H_o is the applied constant magnetic field, H_x is the induced magnetic field, H_w is the induced magnetic field at the wall, μ_e is the magnetic permeability, q is the constant heat flux per unit area, m is the constant mass flux per unit area, ν is the kinematic viscosity, g is the acceleration due to the gravity, ρ is the density, β is the coefficient of volume expansion, β^* is the volumetric coefficient expansion with concentration. T and T_∞ are the temperature of the fluid inside the thermal boundary layer and the fluid temperature in the free stream respectively, while C and C_∞ are the corresponding concentration, c_p is the specific heat at constant pressure, T_m is the mean fluid temperature, K_T is the thermal diffusion ratio, D_m is the coefficient of mass diffusivity and other symbols have their usual meaning.

5.3 Mathematical Formulation

To solve the above system of equations (5.1)-(5.5) under the boundary conditions (5.6) we adopt the well-defined similarity technique to obtain the similarity solution.

For this purpose the following non-dimensional variables are introduced

$$\eta = y \sqrt{\frac{U_o}{2\nu x}} \quad (5.7)$$

$$f'(\eta) = \frac{u}{U_o} \quad (5.8)$$

$$\theta(\eta) = \frac{k(T - T_\infty)}{q} \sqrt{\frac{U_o}{2\nu x}} \quad (5.9)$$

$$\phi(\eta) = \frac{D_m(C - C_\infty)}{m} \sqrt{\frac{U_o}{2\nu x}} \quad (5.10)$$

$$H(\eta) = \sqrt{\frac{\mu_e}{\rho}} \sqrt{\frac{2x}{U_o \nu}} H_x \quad (5.11)$$

Now from equation (5.8),

$$u = U_o f' \quad (5.12)$$

and using this into the equation (5.1), yields

$$v = \sqrt{\frac{U_o \nu}{2x}} [\eta f'(\eta) - f(\eta)] \quad (5.13)$$

Also we have,
$$f_w = -v_o(x) \sqrt{\frac{2x}{U_o \nu}} \quad (5.14)$$

where f_w is the suction parameter or transpiration parameter.

Now from the equations (5.9)- (5.11), we get respectively,

$$T = T_\infty + \frac{q}{k} \sqrt{\frac{2\nu x}{U_o}} \theta(\eta) \quad (5.15)$$

$$C = C_\infty + \frac{m}{D_m} \sqrt{\frac{2\nu x}{U_o}} \phi(\eta) \quad (5.16)$$

$$H_x = \sqrt{\frac{\rho}{\mu_e}} \sqrt{\frac{U_o \nu}{2x}} H(\eta) \quad (5.17)$$

From equation (5.7) we have,

$$\frac{\partial \eta}{\partial x} = -\frac{\eta}{2x} \quad (5.18)$$

$$\frac{\partial \eta}{\partial y} = \sqrt{\frac{U_o}{2\nu x}} \quad (5.19)$$

Also from the equations (5.12) and (5.13) we have the following derivatives,

$$\frac{\partial u}{\partial x} = -\frac{U_o}{2x} \eta f''(\eta) \quad (5.20)$$

$$\frac{\partial u}{\partial y} = U_o \sqrt{\frac{U_o}{2\nu x}} f''(\eta) \quad (5.21)$$

$$\frac{\partial^2 u}{\partial y^2} = \frac{U_o^2}{2\nu x} f'''(\eta) \quad (5.22)$$

$$\frac{\partial v}{\partial y} = \frac{U_o}{2x} \eta f''(\eta) \quad (5.23)$$

Therefore equations (5.20) & (5.23) gives, $\frac{\partial u}{\partial x} + \frac{\partial v}{\partial y} = 0$, which shows that the continuity equation is satisfied.

Again from the equations (5.15)-(5.17) we have the following derivatives,

$$\frac{\partial H_x}{\partial x} = -\sqrt{\frac{\rho U_o \nu}{2x\mu_e}} \frac{1}{2x} (\eta H' + H) \quad (5.24)$$

$$\frac{\partial H_x}{\partial y} = \sqrt{\frac{\rho}{\mu_e}} \frac{U_o}{2x} H'(\eta) \quad (5.25)$$

$$\frac{\partial^2 H_x}{\partial y^2} = \sqrt{\frac{\rho U_o}{2\mu_e \nu x}} \frac{U_o}{2x} H''(\eta) \quad (5.26)$$

$$\frac{\partial T}{\partial x} = -\frac{q}{k} \sqrt{\frac{\nu}{2xU_o}} (\eta \theta' - \theta) \quad (5.27)$$

$$\frac{\partial T}{\partial y} = \frac{q}{k} \theta'(\eta) \quad (5.28)$$

$$\frac{\partial^2 T}{\partial y^2} = \frac{q}{k} \sqrt{\frac{U_o}{2\nu x}} \theta''(\eta) \quad (5.29)$$

$$\frac{\partial C}{\partial x} = -\frac{m}{D_m} \sqrt{\frac{\nu}{2xU_o}} (\eta \phi' - \phi) \quad (5.30)$$

$$\frac{\partial C}{\partial y} = \frac{m}{D_m} \phi'(\eta) \quad (5.31)$$

$$\frac{\partial^2 C}{\partial y^2} = \frac{m}{D_m} \sqrt{\frac{U_o}{2\nu x}} \phi''(\eta) \quad (5.32)$$

Now substituting the equations (5.11)- (5.32) into the equations (5.2)-(5.5), which gives the following dimensionless ordinary coupled non-linear differential equations

$$f''' + ff'' + G_r\theta + G_m\phi + MH' = 0 \quad (5.33)$$

$$H'' + P_m(f'H + fH') - P_m\eta Hf'' + MP_m f'' = 0 \quad (5.34)$$

$$\theta'' + P_r(f\theta' - f'\theta) + E_c P_r (f''^2 + \frac{1}{P_m} H'^2) = 0 \quad (5.35)$$

$$\phi'' + S_c(f\phi' - f'\phi) + S_o S_c \theta'' = 0 \quad (5.36)$$

with the corresponding boundary conditions

$$\left. \begin{aligned} f = f_w, f' = 1, \quad \theta' = -1, \quad \phi' = -1, \quad H = h = 1(\text{say}) \quad \text{at } \eta = 0 \\ f' = 0, \quad \theta \rightarrow 0, \quad \phi \rightarrow 0, \quad H \rightarrow 0 \quad \text{as } \eta \rightarrow \infty \end{aligned} \right\} \quad (5.37)$$

where, $G_r = g\beta \frac{q}{k} \sqrt{\frac{\nu(2x)^3}{U_o^5}}$ is the Grashof number,

$G_m = g\beta^* \frac{m}{D_m} \sqrt{\frac{\nu(2x)^3}{U_o^5}}$ is the Modified Grashof number,

$M = \sqrt{\frac{\mu_e}{\rho}} \frac{H_o}{U_o}$ is the magnetic force number.

$P_m = \mu_e \sigma' \nu$ is the magnetic diffusivity number,

$P_r = \frac{\rho c_p \nu}{k} = \frac{\mu c_p}{k}$ is the Prandtl number,

$E_c = \frac{k U_o^2}{q c_p} \sqrt{\frac{U_o}{2\nu x}}$ is the Eckert number,

$S_o = \frac{q D_m^2 K_T}{k \nu m T_m}$ is the Soret number,

and $S_c = \frac{\nu}{D_m}$ is the Schmidt number.

In all the above equations primes denote the differentiation with respect to η .

5.4. Skin Friction Co-efficient and Current Density at the Plate

The local skin friction coefficient and the local Current density at the plate are the quantities of chief physical interest.

The shearing stress at the plate is generally known as the skin friction, the equation defining the local skin friction is

$$\tau = \mu \left(\frac{\partial u}{\partial y} \right)_{y=0} \quad \text{i.e. } \tau \propto f''(0)$$

The current density is generally expressed as $J = -\frac{\partial H}{\partial y}$ and hence the current density at the plate is $J_w \propto H'(0)$

The next section deals the solution technique of the problem.

5.5. Numerical Solution

The set of ordinary coupled non-linear differential equations (5.33)-(5.36) with the boundary conditions (5.37) are very difficult to solve analytically. Hence we adopt a procedure to obtain the solution numerically. Here we use the standard initial value solver namely the sixth order Runge Kutta method along with Nachtsheim-Swigert iteration technique. The detailed descriptions of the procedure of the numerical solution of this problem are given in section 4.5 of *chapter 4*. In this problem there are four asymptotic boundary conditions and hence four unknown surface conditions $f''(0)$, $H'(0)$, $\theta'(0)$ and $\phi'(0)$ are assumed.

5.6. Results and Discussion

The numerical values of the velocity, induced magnetic field, current density, temperature, the concentration skin friction and current density at the plate respectively for different values of the suction parameter (v_o), the magnetic parameter (M), the Prandtl number (P_r), the Soret number (S_o), the Schmidt number (S_c), the Grashof number (G_r), the magnetic diffusivity parameter (P_m), the Eckert number (E_c) and for the fixed values of modified Grashof number (G_m) are obtained and discussed. The values of M and G_r are taken to be large for cooling Newtonian fluid, since these large values correspond to a strong magnetic field and to a cooling problem that is generally encountered in nuclear engineering in connection with the cooling of reactors.

The most important fluids are atmospheric air and water and so the results are limited for Prandtl number $P_r=0.71$ and 7.00 (in particular, 0.71 represents air at 20°C and 7.0 corresponds to water at 20°C). The values 0.22 , 0.30 , 0.60 and 0.78 are also considered for S_c , which represents the specific condition of the flow (in particular 0.22 corresponds to hydrogen, while 0.30 corresponds to helium, 0.60 corresponds to water vapor that represents a diffusivity chemical species of most common interest in air and value 0.78 represents ammonia at a temperature at 25°C and 1 atmospheric pressure). The values of f_w , M , S_o , P_m , E_c and G_m are however chosen arbitrarily.

The obtained results are illustrated in Figs.(5.2)-(5.36) in case of air ($P_r=0.71$) and water ($P_r=7.0$). The velocity, the induced magnetic field, current density, temperature and concentration versus η -variable plots are shown in Figs.(5.2)-(5.8), (5.9)-(5.15), (5.16)-(5.22), (5.23)-(5.29) and (5.30)-(5.36) respectively for different value of $f_w, M, P_m, S_o, E_c, G_r$ and S_c .

The effect of the suction parameter f_w on the velocity is shown in Fig. (5.2). It is observed from this figure that an increase in f_w leads to a decrease in velocity in case of air ($P_r=0.71$) and water ($P_r=7.0$). The usual stabilizing effect of the suction parameter on the boundary layer growth is also evident from this figure. We also notice that for any value of f_w the velocity of air is greater than velocity of water. The velocity profiles are shown in Figs.(5.3)and(5.4) for different values of M and P_m . It is observed that an increase in the applied magnetic field parameter and magnetic diffusivity parameter leads to an increase in the velocity within the domain $0 < \eta < 0.7$ and $0 < \eta < 0.4$ respectively for both air and water. Further it is observed from these figures that the velocity distribution decreases gradually at the points where $\eta \geq 0.7$ and $\eta \geq 0.4$ respectively for both air and water. Figs.(5.5)-(5.7) show the velocity profiles for different values of S_o, E_c and G_r respectively. We notice that an increase in S_o, E_c and G_r (extremely cool plate) leads to a rise in the values of the velocity for both air and water. Fig. (5.8) shows the velocity profiles for different values of S_c . The velocity is greater for hydrogen ($S_c=0.22$ at temperature 25^0C and 1 atmospheric pressure) than ammonia ($S_c=0.78$ at temperature 25^0C and 1 atmospheric pressure) in case of both air and water. Further it is observed that the velocity distribution increases/decreases gradually near the plate and then decreases/increases slowly far from the plate. Here it is concluded that the maximum velocity occurs, in the vicinity of the plate and the rise and fall in values of the velocity are more dominant in the case of air ($P_r=0.71$) than of water ($P_r=7.0$). In all situations the velocity profiles always remain in phase.

Figs.(5.9)-(5.15) present the induced magnetic field for air ($P_r=0.71$) and water ($P_r=7.0$) respectively for different values of $f_w, M, P_m, S_o, E_c, G_r$ and S_c . It is observed from the Fig.(5.9) that the induced magnetic field decreases a little within the interval $0 \leq \eta \leq 0.4$ with an increase in suction parameter (f_w) for both air and water, but it increases within the interval $0.4 \leq \eta \leq 2.0$ with an increase in f_w for both air and water. It is further observed that in the case of air for the interval $0.4 < \eta < 2.0$, H remains negative. It is observed from Figs. (5.10) and (5.11) that the induced magnetic field decreases with the increase of M and P_m for both air and water. It is also found from these figures that the decrease effect is large. But it has a negative value approximately in the interval ($0.4 \leq \eta \leq 2.4$). We thus may conclude that the transverse magnetic field and magnetic field diffusivity have a strong role on the induced magnetic field. It

is observed from Figs. (5.12)-(5.14) that the induced magnetic field decreases with the increase of S_o , E_c and G_r in case of air and water. The decreasing effect is not so prominent near to the plate. In these figures, it appears that there is a back directional induced magnetic field in a considerable area of the boundary layer (approximately $0.4 \leq \eta \leq 2.4$). It is found that H has negligible effect for increase of G_r in case of water (Fig.5.14) and it is usual. In Fig. (5.15), the induced magnetic field is greater for ammonia ($S_c=0.78$ at temperature 25^0C and 1 atmospheric pressure) than hydrogen ($S_c =0.22$ at temperature 25^0C and 1 atmospheric pressure) for both air and water.

Figs.(5.16)-(5.22) present the current density profiles for air ($P_r=0.71$) and water ($P_r=7.0$) for different values of f_w , M , P_m , S_o , E_c , G_r and S_c . In Fig. (5.16), it is observed that the current density increases approximately in the domain $0 < \eta < 0.17$, and further decreases in the interval $0.17 < \eta < 1$ with the increase of f_w , for both air and water. From the point where $\eta \geq 1$, it is reduced to a certain value of η and becomes constant. Fig.(5.17) shows that the current density increases in the interval $0 < \eta < 0.6$ (approx.) and decreases when $\eta > 0.6$ for both air and water with increase in M . It is observed from Fig.(5.18) that the current density increases close to the plate within the interval $0 \leq \eta \leq 0.6$ (approx.). This increasing effect is very large. From the point where $\eta \geq 0.6$, current density decreases with the increase of P_m in the both air and water ($P_r=0.71$ & 7.0). Fig.(5.19) shows the minor increasing/decreasing effect of the current density for different values of S_o for air and water. The effect is reversed after $\eta \approx 0.72$. Fig.(5.20) shows the increase of the current density in the interval $0 < \eta < 0.7$ and decreases from $\eta > 0.7$ with increase of E_c for air and water. However the effects are minor for water. Figs.(5.21) shows that the current density has a minor increasing effect within the interval $0 \leq \eta \leq 0.6$ (approx.) and further it has a minor decreasing effect in case of air, but there is no effect in case of water for increasing values of G_r , while in Fig. (5.22), the current density has a minor decreasing effect within the interval $0 \leq \eta \leq 0.7$ (approx.) and further it has a minor increasing effect from $\eta \geq 0.7$ for increasing values of S_c for air, but in case of water the effect is negligible.

The temperature profiles are shown in Figs. (5.23)-(5.29) for different values of f_w , M , P_m , S_o , E_c , G_r and S_c for both air ($P_r=0.71$) and water ($P_r=7.0$). It is observed from Fig. (5.23) that the temperature has a decreasing effect as increase in suction parameter (f_w) for both air and water. From Fig. (5.24), it is observed that the temperature increases as M increase for both air and water. Fig.(5.25) shows that there is minor increasing effect of the temperature for increasing values of P_m in case of air; for water the temperature increases within the interval ($0 < \eta < 0.23$

approx.) and it decreases from $\eta > 0.23$ with increase in P_m . Also it is found from Figs. (5.26), (5.28) and (5.29) that the temperature distribution has a negligible effect with the increase of S_o , G_r and S_c respectively for both air and water. Fig. (5.27) shows that the temperature has a very large increasing effect close to the plate with the increase of E_c for both air and water. It is interesting to note that the temperature profiles are more sensitive for air ($P_r=0.71$) than of water ($P_r=7.00$).

The displayed Figs.(5.30)-(5.36) show the effect of the various parameters f_w , M , P_m , S_o , E_c , G_r and S_c on the concentration profiles for both air ($P_r=0.71$) and water ($P_r=7.0$). From Fig.(5.30), it is observed that the concentration decreases with increase of the suction parameter (f_w) for both air and water. It is observed from Fig.(5.31) that a minor decreasing effect of concentration occurs within the interval $0 < \eta < 0.22$ (approx.) and further it has a minor increasing effect from $\eta > 0.22$ in case of air whereas for water the minor decreasing effect of concentration occurs in the interval $0 < \eta < 0.55$ (approx.) with increase in M . From Fig.(5.32), it is seen that the concentration has a minor increasing effect with increase in magnetic diffusivity parameter (P_m), while from Fig.(5.33), it observed that the concentration increases close to the plate with the increase in Soret number (S_o). The decreasing effect of concentration is found in the interval $0 < \eta < 0.2$ for air and in $0 < \eta < 0.5$ for water approximately, after that interval the effect is reversed with increase in E_c [Fig(5.34)]. Fig.(5.35) focuses the minor decreasing effect of the concentration with increasing values of G_r for air but in case of water changes of G_r has practically no effect. In Fig.(5.36) leads to a decreasing effect of the concentration with increasing in S_c . It also show that the concentration is more for hydrogen ($S_c = 0.22$ at temperature 25°C and 1 atmospheric pressure) than ammonia ($S_c=0.78$ at temperature 25°C and 1 atmospheric pressure) for both air and water. It should be pointed that in all Figs.(5.29)-(5.36), the concentration profiles are more sensitive for water ($P_r=7.00$) than of air ($P_r=0.71$) near to the wall up to a certain point, thereafter they are reversed.

Finally the effects of various parameters on the skin friction (τ) and the current density at the plate (J_w) are tabulated in Tables 5.1-5.7. It is observed from Table 5.1 that the Skin friction (τ) decreases while the current density at the plate (J_w) increase with the increase of f_w for both air ($P_r=0.71$) and water ($P_r=7.00$). Whereas in Tables 5.2-5.6 show that the Skin friction and the current density at the plate increases with the increase of M , P_m , S_o , E_c and G_r respectively for both air and water. From the last Table 5.7, it is observed that the skin friction and the current density at the plate both decrease with the increase of S_c for both air ($P_r=0.71$) and water ($P_r=7.00$).

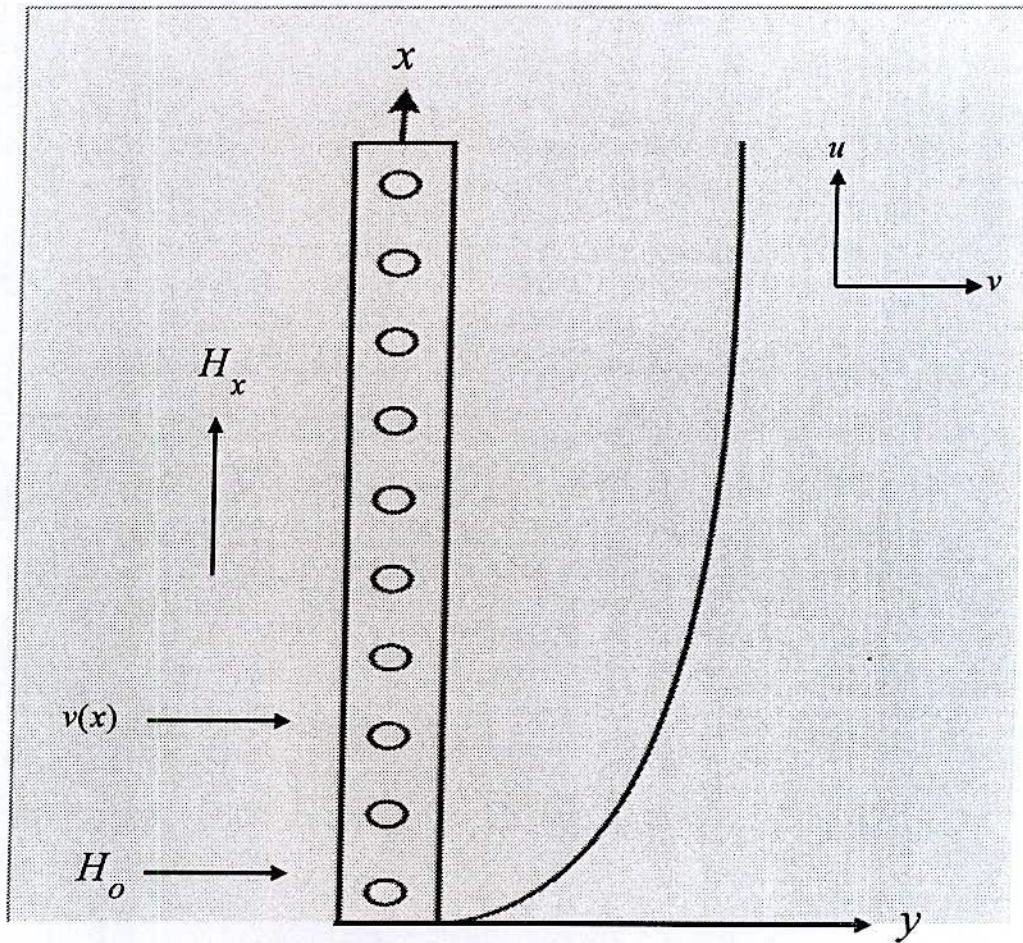


Fig. 5.1. Physical configuration and coordinate system.

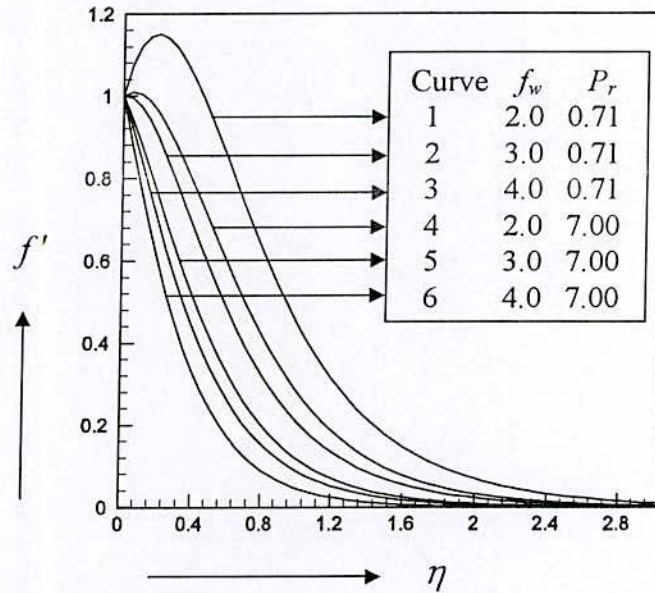


Fig.5.2. Velocity profiles (f') for different values of f_w , taking $G_r=5.0$, $G_m=2.0$, $M=1.0$, $P_m=1.0$, $S_o=2.0$, $S_c=0.6$ and $E_c=0.2$ as fixed.

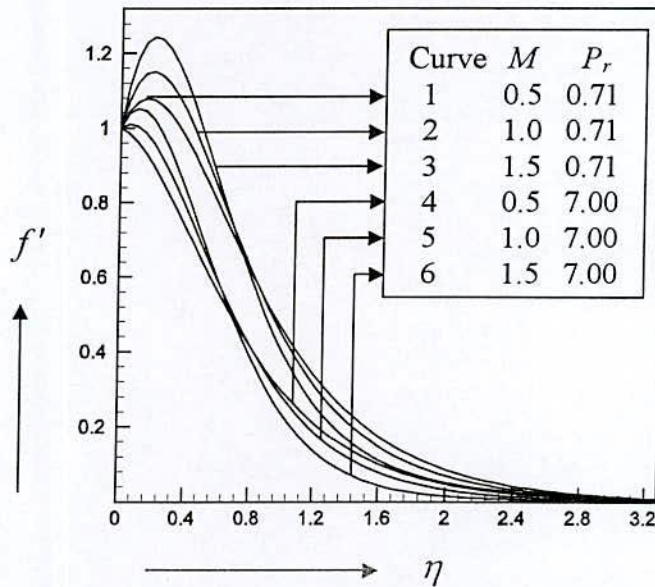


Fig.5.3. Velocity profiles (f') for different values of M , taking $f_w=2.0$, $G_r=5.0$, $G_m=2.0$, $P_m=1.0$, $S_o=2.0$, $S_c=0.6$ and $E_c=0.2$ as fixed.

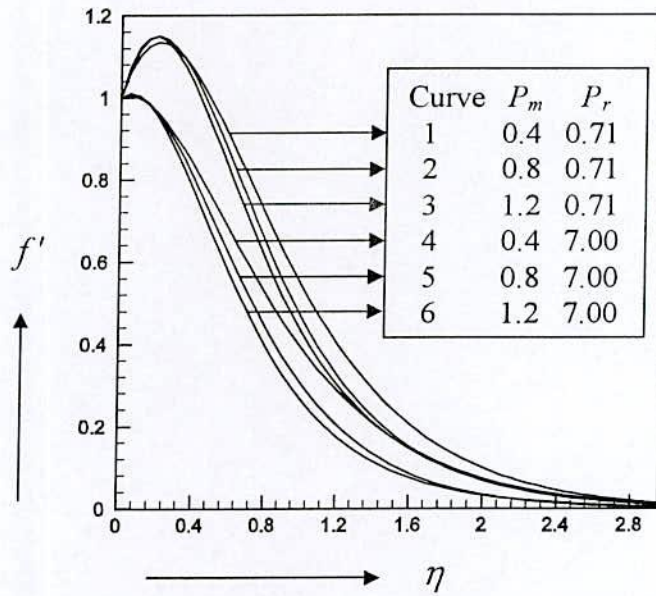


Fig.5.4. Velocity profiles (f') for different values of P_m , taking $f_w=2.0$, $G_r=5.0$, $G_m=2.0$, $M=1.0$, $S_o=2.0$, $S_c=0.6$ and $E_c=0.2$ as fixed.

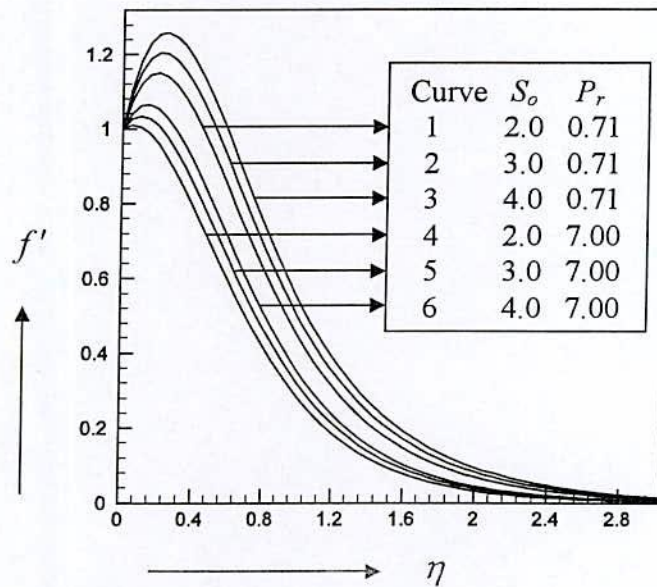


Fig.5.5. Velocity profiles (f') for different values of S_o taking $f_w=2.0$, $G_r=5.0$, $G_m=2.0$, $M=1.0$, $P_m=1.0$, $S_c=0.6$ and $E_c=0.2$ as fixed.

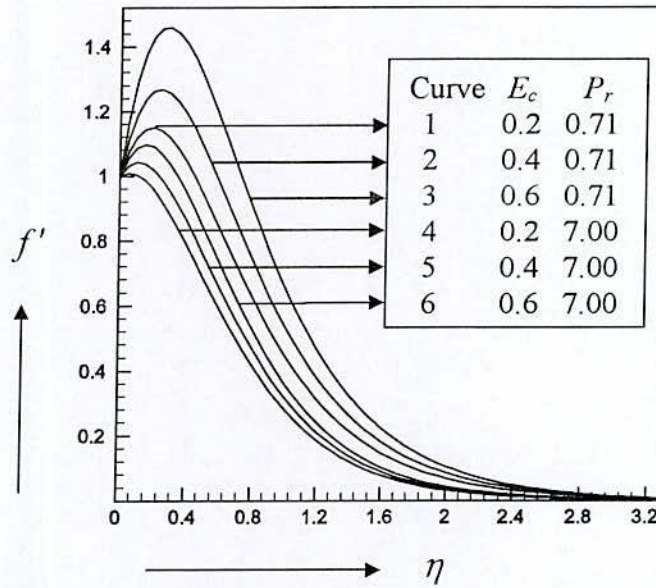


Fig.5.6. Velocity profiles (f') for different values of E_c , taking $f_w=2.0$, $G_r=5.0$, $G_m=2.0$, $M=1.0$, $P_m=1.0$, $S_o=2.0$ and $S_c=0.6$ as fixed.

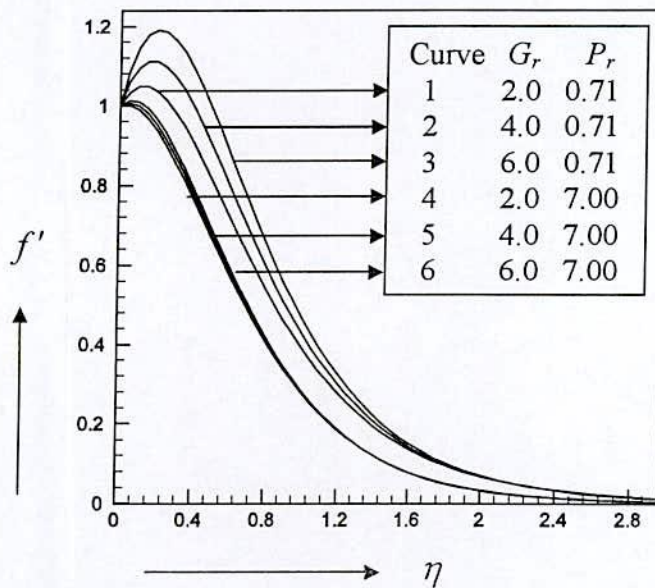


Fig.5.7. Velocity profiles (f') for different values of G_r , taking $f_w=2.0$, $G_m=2.0$, $M=1.0$, $P_m=1.0$, $S_o=2.0$, $S_c=0.6$ and $E_c=0.2$ as fixed.

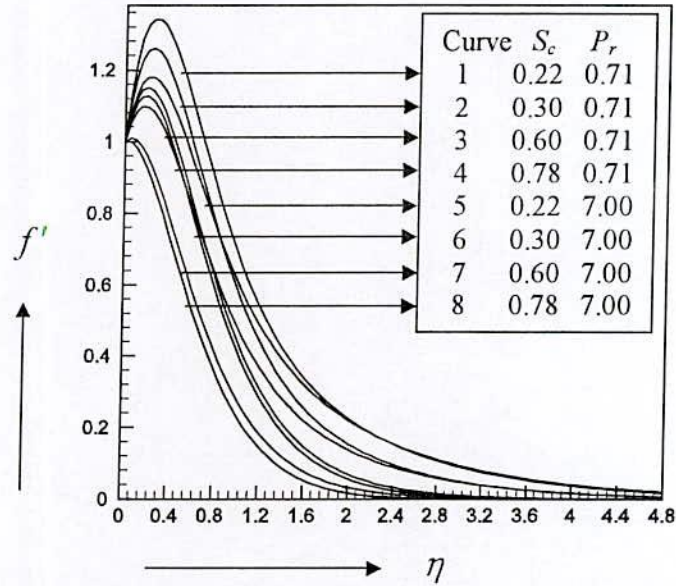


Fig.5.8. Velocity profiles (f') for different values of S_c taking $f_w=2.0$, $G_r=5.0$, $G_m=2.0$, $M=1.0$, $P_m=1.0$, $S_o=2.0$ and $E_c=0.2$ as fixed.

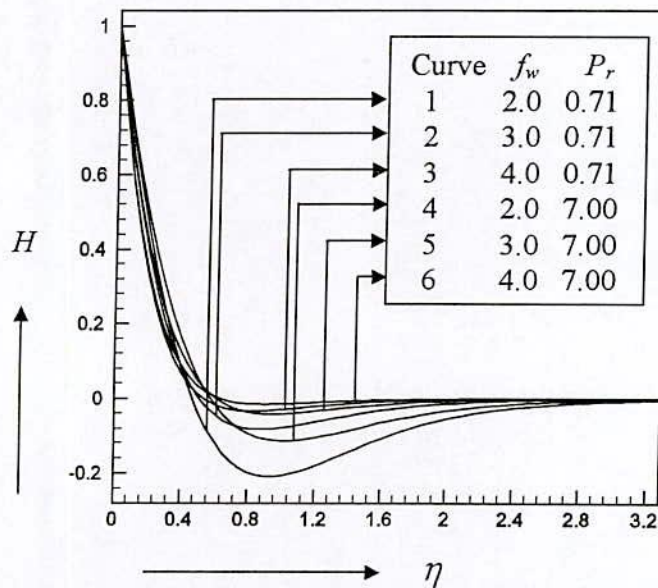


Fig.5.9. Induced magnetic field (H) for different values of f_w , taking $G_r=5.0$, $G_m=2.0$, $M=1.0$, $P_m=1.0$, $S_o=2.0$, $S_c=0.6$ and $E_c=0.2$ as fixed.

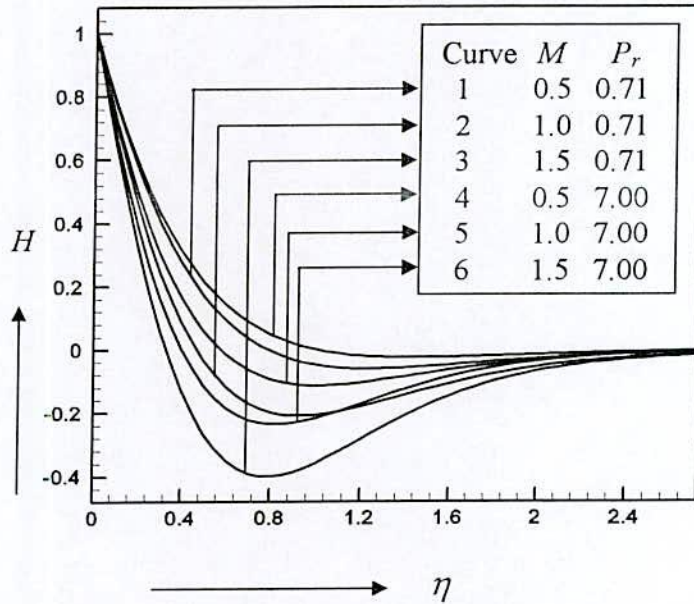


Fig.5.10. Induced magnetic field (H) for different values of M , taking $f_w=2.0$, $G_r=5.0$, $G_m=2.0$, $P_m=1.0$, $S_o=2.0$, $S_c=0.6$ and $E_c=0.2$ as fixed.

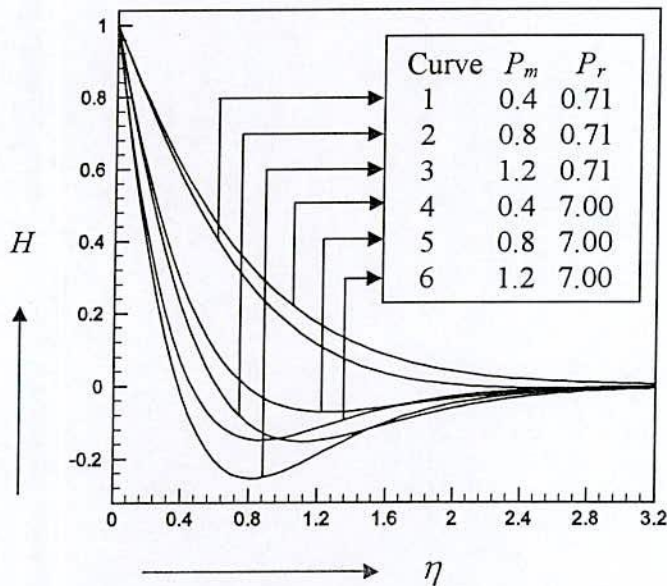


Fig.5.11. Induced magnetic field (H) for different values of P_m , taking $f_w=2.0$, $G_r=5.0$, $G_m=2.0$, $M=1.0$, $S_o=2.0$, $S_c=0.6$ and $E_c=0.2$ as fixed.

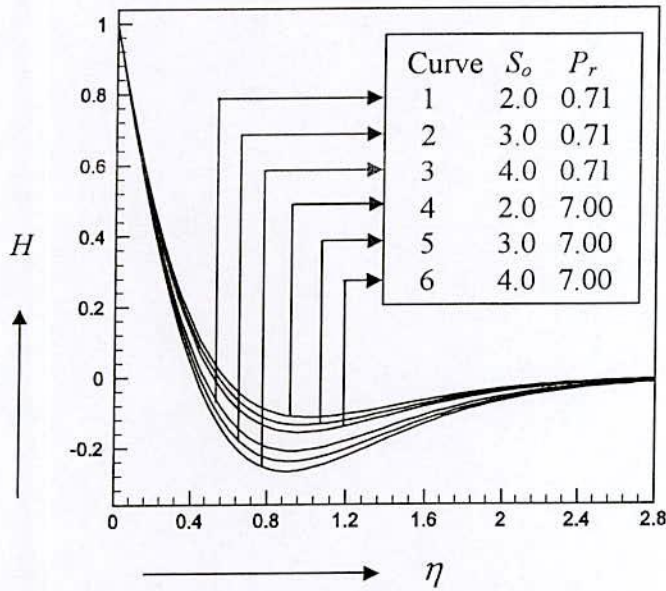


Fig.5.12. Induced magnetic field (H) for different values of S_o taking $f_w=2.0$, $G_r=5.0$, $G_m=2.0$, $M=1.0$, $P_m=1.0$, $S_c=0.6$ and $E_c=0.2$ as fixed.

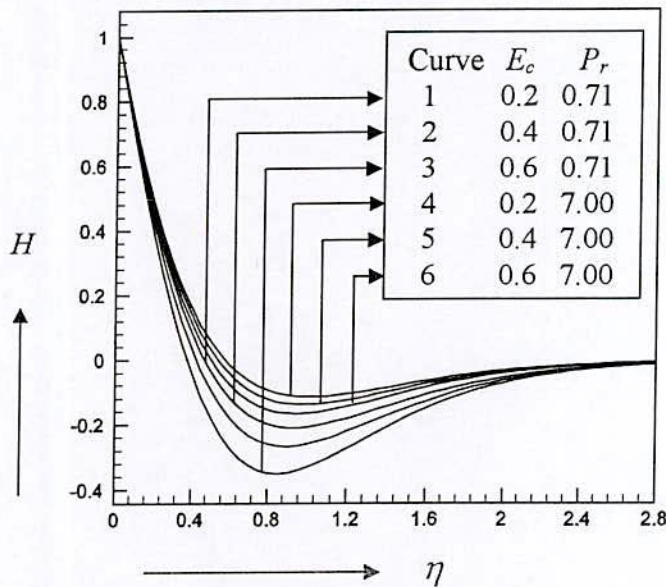


Fig.5.13. Induced magnetic field (H) for different values of E_c , taking $f_w=2.0$, $G_r=5.0$, $G_m=2.0$, $M=1.0$, $P_m=1.0$, $S_o=2.0$ and $S_c=0.6$ as fixed.

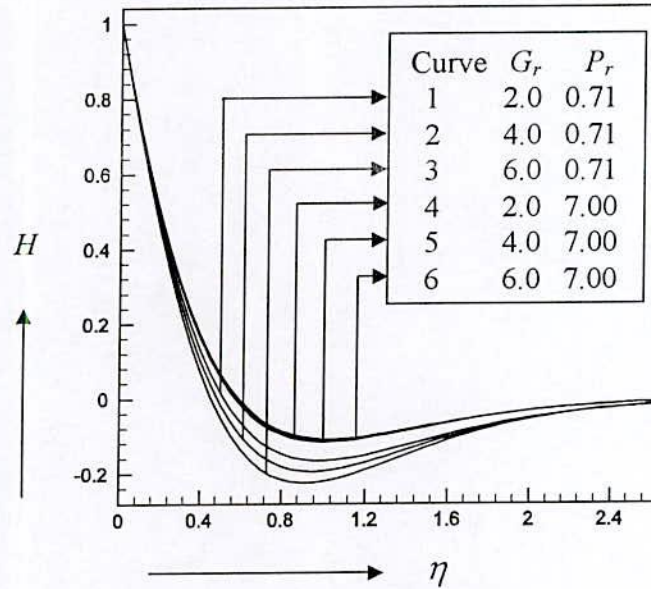


Fig.5.14. Induced magnetic field (H) for different values of G_r , taking $f_w=2.0$, $G_m=2.0$, $M=1.0$, $P_m=1.0$, $S_o=2.0$, $S_c=0.6$ and $E_c=0.2$ as fixed.

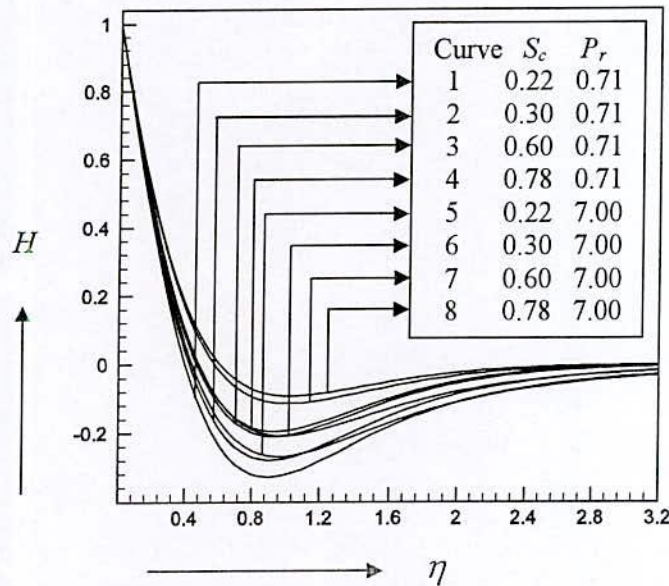


Fig.5.15. Induced magnetic field (H) for different values of S_c taking $f_w=2.0$, $G_r=5.0$, $G_m=2.0$, $M=1.0$, $P_m=1.0$, $S_o=2.0$ and $E_c=0.2$ as fixed.

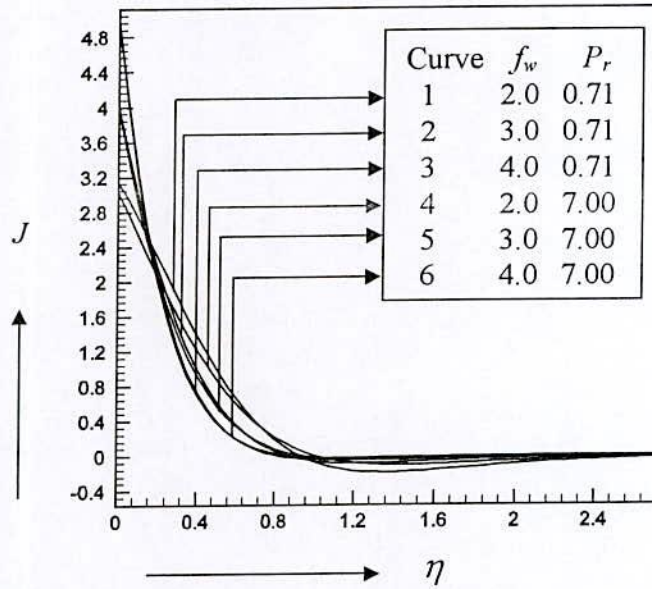


Fig.5.16. Current density profiles (J) for different values of f_w , taking $G_r=5.0$, $G_m=2.0$, $M=1.0$, $P_m=1.0$, $S_o=2.0$, $S_c=0.6$ and $E_c=0.2$ as fixed.

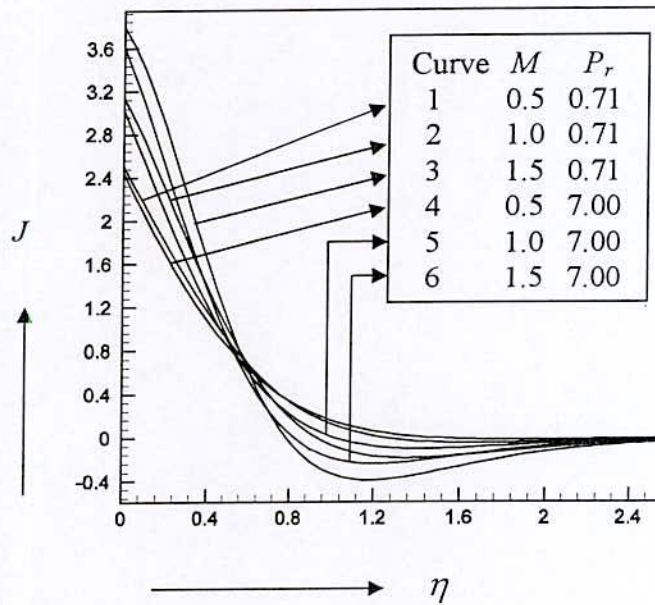


Fig.5.17. Current density profiles (J) for different values of M , taking $f_w=2.0$, $G_r=5.0$, $G_m=2.0$, $P_m=1.0$, $S_o=2.0$, $S_c=0.6$ and $E_c=0.2$ as fixed.

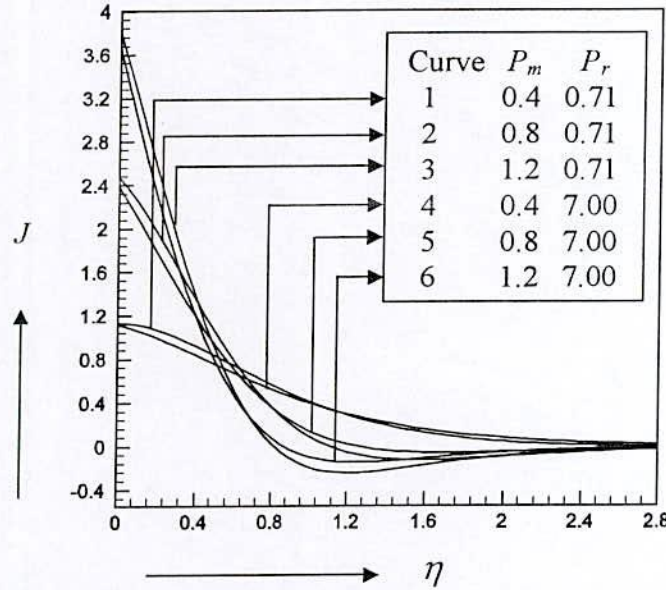


Fig.5.18. Current density profiles (J) for different values of P_m , taking $f_w=2.0$, $G_r=5.0$, $G_m=2.0$, $M=1.0$, $S_o=2.0$, $S_c=0.6$ and $E_c=0.2$ as fixed.

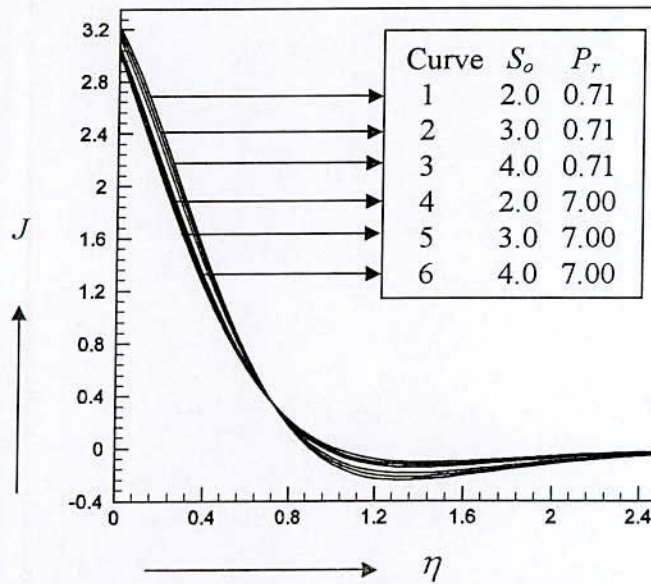


Fig.5.19. Current density profiles (J) for different values of S_o taking $f_w=2.0$, $G_r=5.0$, $G_m=2.0$, $M=1.0$, $P_m=1.0$, $S_c=0.6$ and $E_c=0.2$ as fixed.

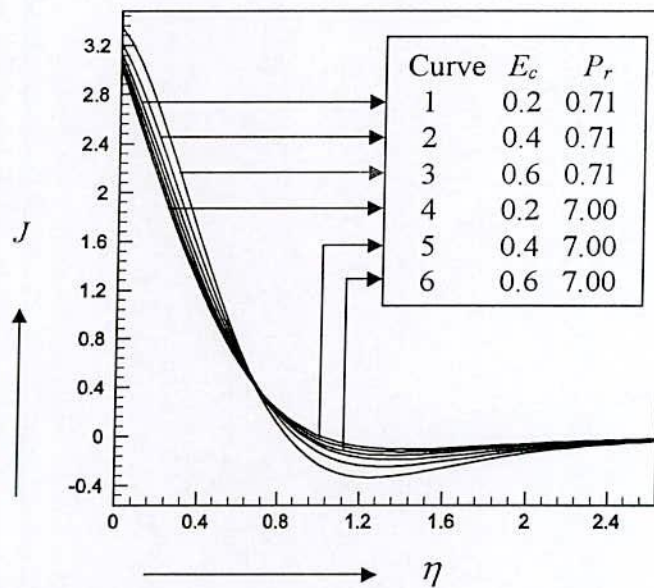


Fig.5.20. Current density profiles (J) for different values of E_c , taking $f_w=2.0$, $G_r=5.0$, $G_m=2.0$, $M=1.0$, $P_m=1.0$, $S_o=2.0$ and $S_c=0.6$ as fixed.

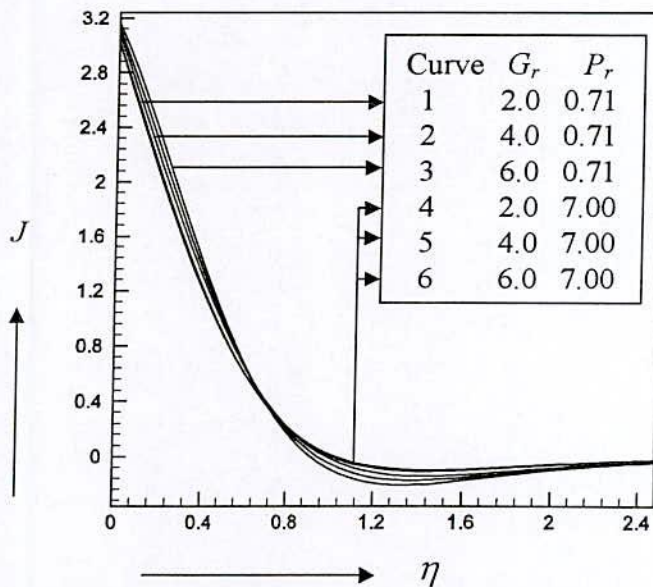


Fig.5.21. Current density profiles (J) for different values of G_r , taking $f_w=2.0$, $G_m=2.0$, $M=1.0$, $P_m=1.0$, $S_o=2.0$, $S_c=0.6$ and $E_c=0.2$ as fixed.

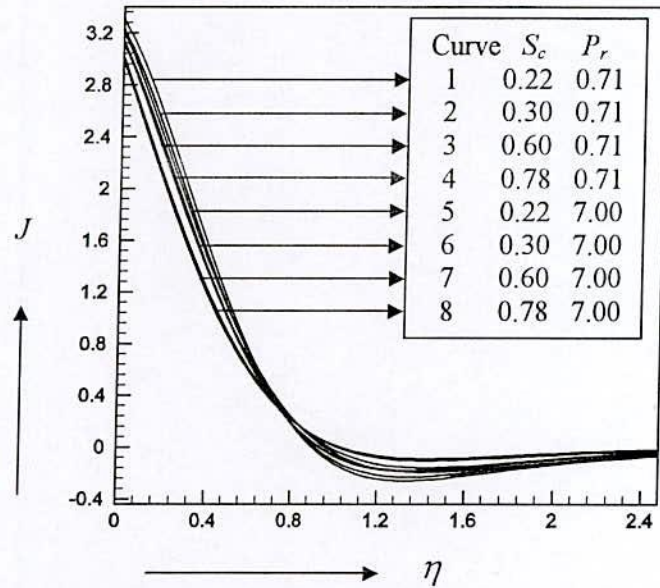


Fig.5.22. Current density profiles (J) for different values of S_c taking $f_w=2.0$, $G_r=5.0$, $G_m=2.0$, $M=1.0$, $P_m=1.0$, $S_o=2.0$ and $E_c=0.2$ as fixed.

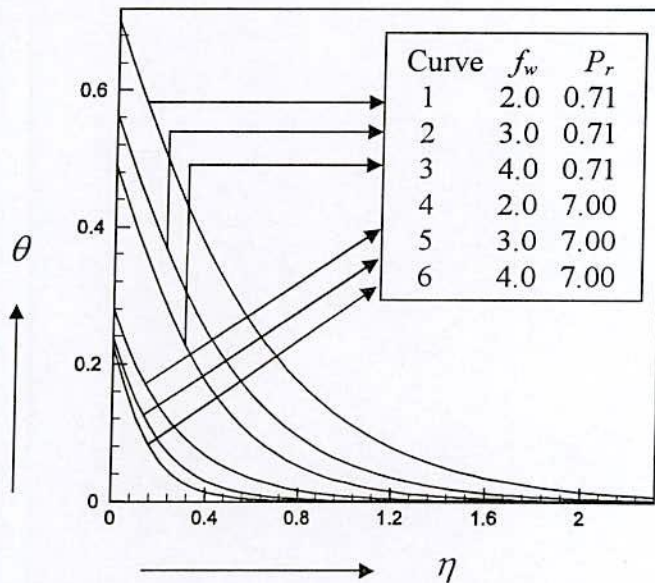


Fig.5.23. Temperature profiles (θ) for different values of f_w , taking $G_r=5.0$, $G_m=2.0$, $M=1.0$, $P_m=1.0$, $S_o=2.0$, $S_c=0.6$ and $E_c=0.2$ as fixed.

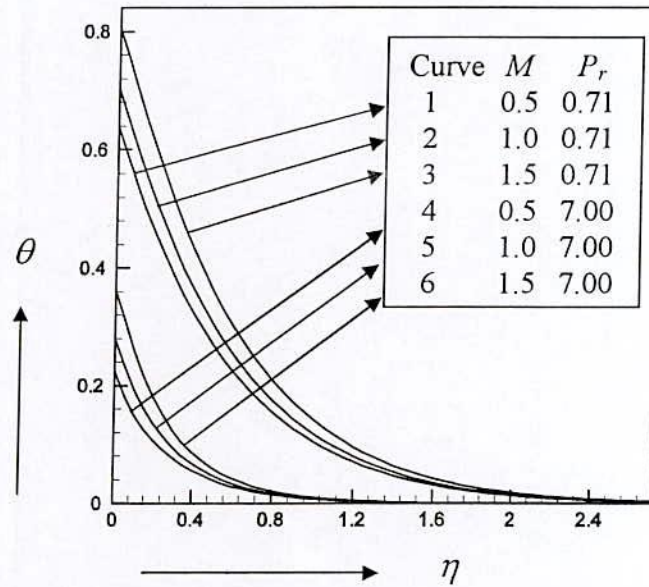


Fig.5.24. Temperature profiles (θ) for different values of M , taking, $f_w=2.0$, $G_r=5.0$, $G_m=2.0$, $P_m=1.0$, $S_o=2.0$, $S_c=0.6$ and $E_c=0.2$ as fixed.

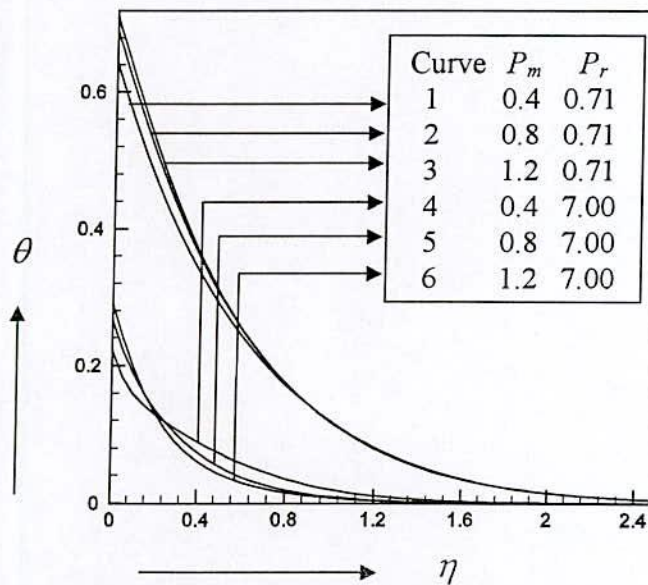


Fig.5.25. Temperature profiles (θ) for different values of P_m , taking $f_w=2.0$, $G_r=5.0$, $G_m=2.0$, $M=1.0$, $S_o=2.0$, $S_c=0.6$ and $E_c=0.2$ as fixed.

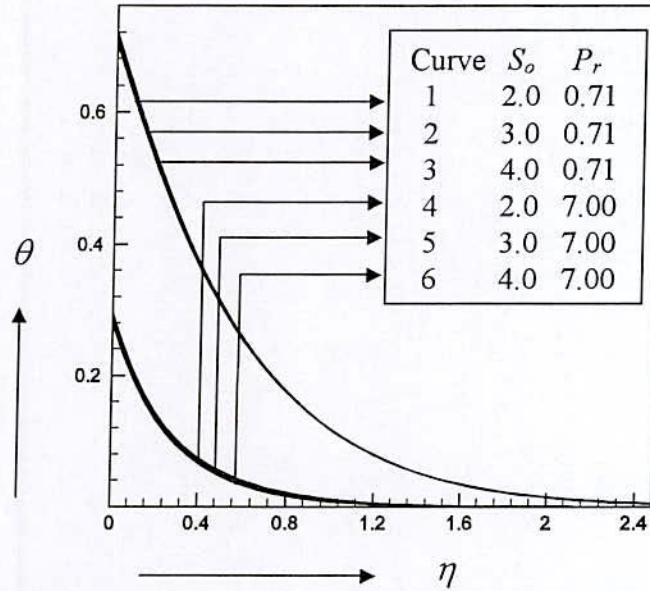


Fig.5.26. Temperature profiles (θ) for different values of S_o taking $f_w=2.0$, $G_r=5.0$, $G_m=2.0$, $M=1.0$, $P_m=1.0$, $S_c=0.6$ and $E_c=0.2$ as fixed.

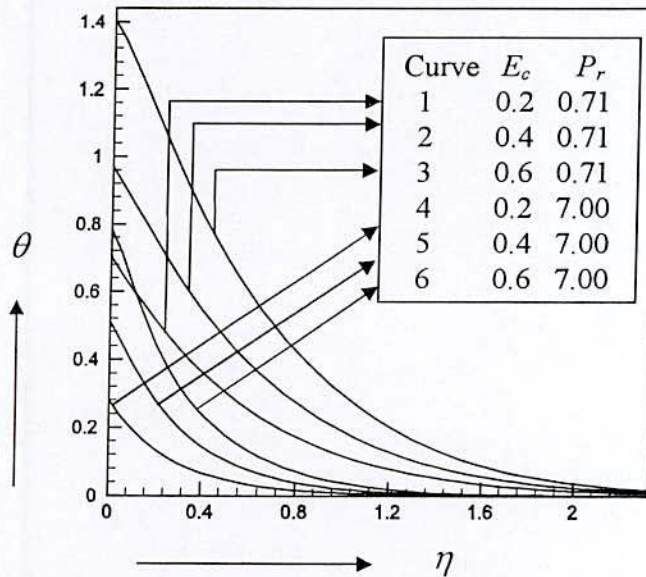


Fig.5.27. Temperature profiles (θ) for different values of E_c , taking $f_w=2.0$, $G_r=5.0$, $G_m=2.0$, $M=1.0$, $P_m=1.0$, $S_o=2.0$ and $S_c=0.6$ as fixed.

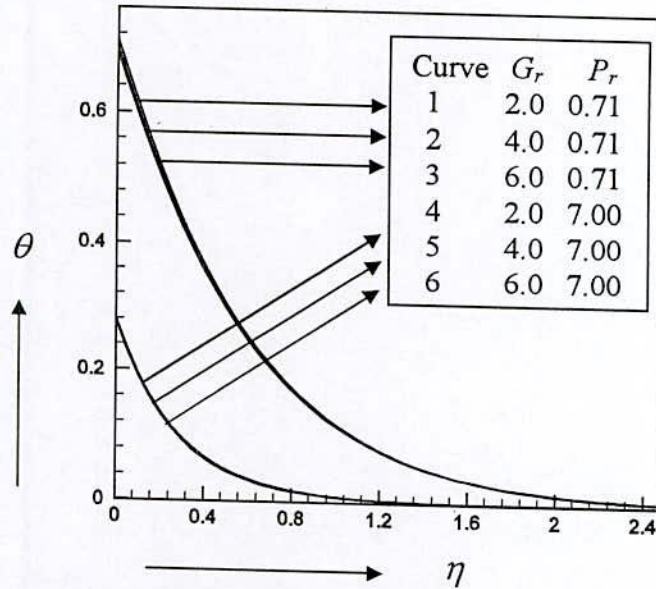


Fig.5.28. Temperature profiles (θ) for different values of G_r , taking $f_w=2.0$, $G_m=2.0$, $M=1.0$, $P_m=1.0$, $S_o=2.0$, $S_c=0.6$ and $E_c=0.2$ as fixed.

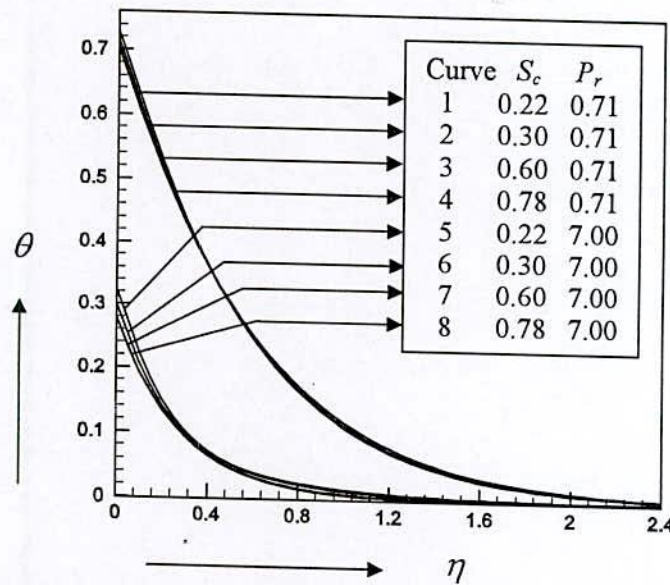


Fig.5.29. Temperature profiles (θ) for different values of S_c taking $f_w=2.0$, $G_r=5.0$, $G_m=2.0$, $M=1.0$, $P_m=1.0$, $S_o=2.0$ and $E_c=0.2$ as fixed.

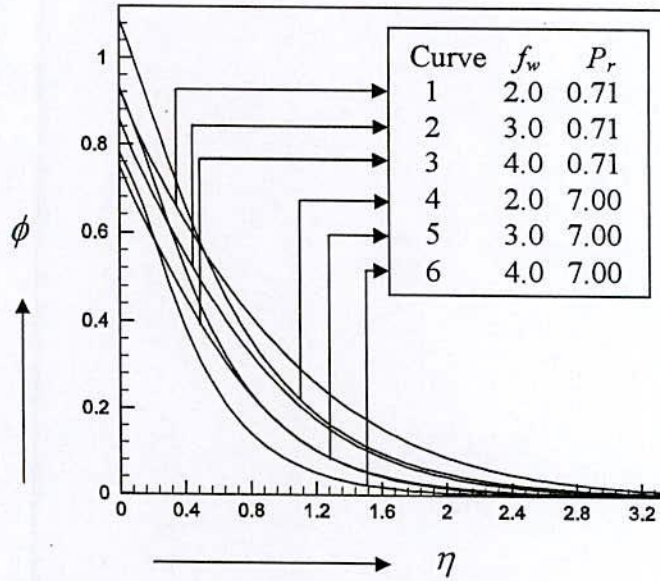


Fig.5.30. Concentration profiles (ϕ) for different values of f_w , taking $G_r=5.0$, $G_m=2.0$, $M=1.0$, $P_m=1.0$, $S_o=2.0$, $S_c=0.6$ and $E_c=0.2$ as fixed.

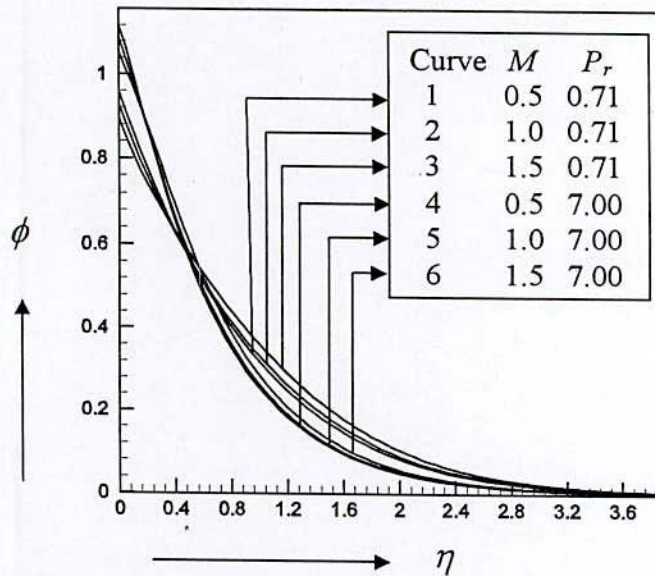


Fig.5.31. Concentration profiles (ϕ) for different values of M , taking $f_w=2.0$, $G_r=5.0$, $G_m=2.0$, $P_m=1.0$, $S_o=2.0$, $S_c=0.6$ and $E_c=0.2$ as fixed.

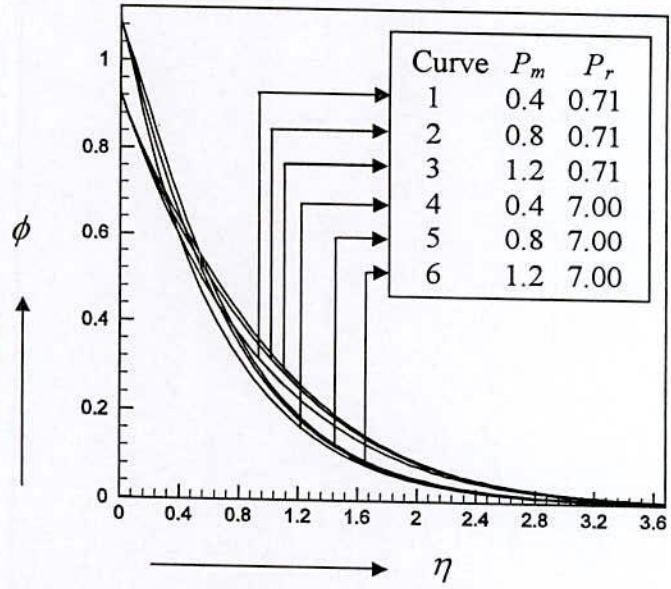


Fig.5.32. Concentration profiles (ϕ) for different values of P_m , taking $f_w=2.0$, $G_{r_s}=5.0$, $G_m=2.0$, $M=1.0$, $S_o=2.0$, $S_c=0.6$ and $E_c=0.2$ as fixed.

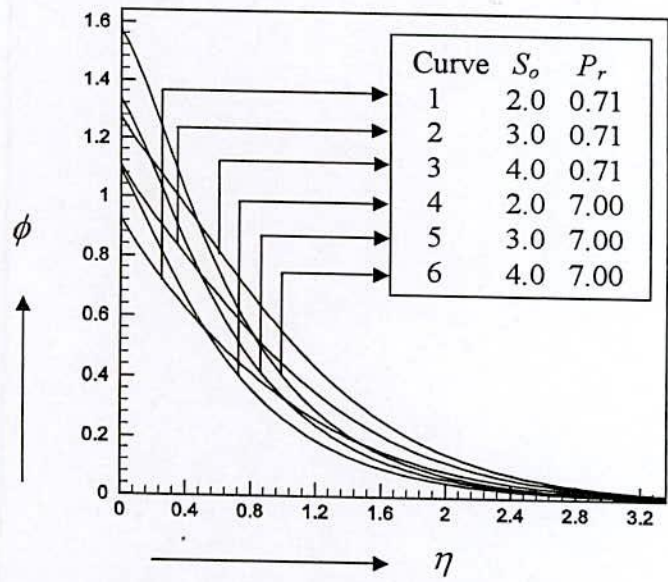


Fig.5.33. Concentration profiles (ϕ) for different values of S_o taking $f_w=2.0$, $G_{r_s}=5.0$, $G_m=2.0$, $M=1.0$, $P_m=1.0$, $S_c=0.6$ and $E_c=0.2$ as fixed.

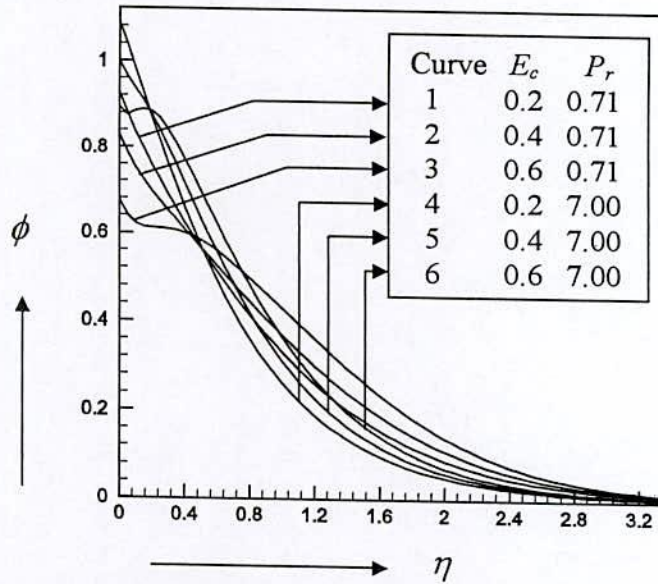


Fig.5.34. Concentration profiles (ϕ) for different values of E_c , taking $f_w=2.0$, $G_r=5.0$, $G_m=2.0$, $M=1.0$, $P_m=1.0$, $S_o=2.0$ and $S_c=0.6$ as fixed.

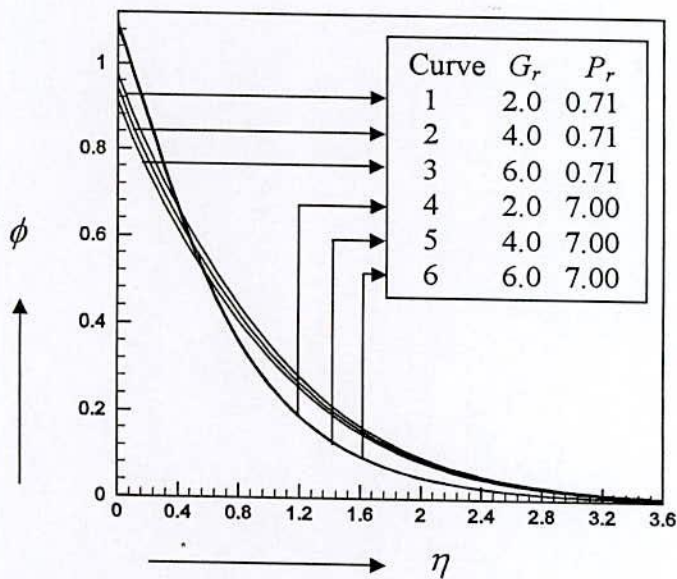


Fig.5.35. Concentration profiles (ϕ) for different values of G_r , taking $f_w=2.0$, $G_m=2.0$, $M=1.0$, $P_m=1.0$, $S_o=2.0$, $S_c=0.6$ and $E_c=0.2$ as fixed.

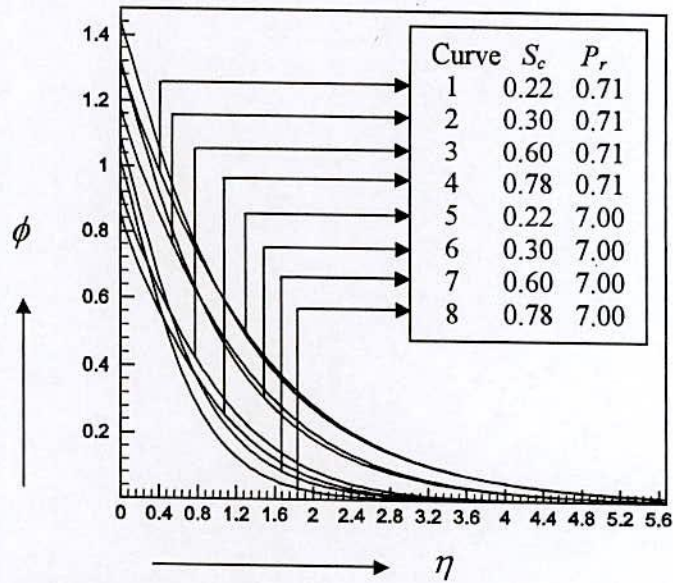


Fig.5.36. Concentration profiles (ϕ) for different values of S_c taking $f_w=2.0$, $G_r=5.0$, $G_m=2.0$, $M=1.0$, $P_m=1.0$, $S_o=2.0$ and $E_c=0.2$ as fixed.

Table 5.1. Numerical values proportional to τ and J_w for $G_r=5.0$, $G_m=2.0$, $M=1.0$, $P_m=1.0$, $S_0=2.0$, $S_c=0.6$ and $E_c=0.2$.

P_r	f_w	τ	J_w
0.71	2.00	1.7504487	3.1397836
0.71	3.00	0.1334494	4.0073649
0.71	4.00	-1.3793490	4.9760911
7.00	2.00	0.3756603	3.0252324
7.00	3.00	-0.9692224	3.9721669
7.00	4.00	-2.2420256	4.9636363

Table 5.2. Numerical values proportional to τ and J_w for $f_w=2.0$, $G_r=5.0$, $G_m=2.0$, $P_m=1.0$, $S_0=2.0$, $S_c=0.6$ and $E_c=0.2$.

P_r	M	τ	J_w
0.71	0.5	1.0777935	2.5055471
0.71	1.0	1.7504487	3.1397836
0.71	1.5	2.6215367	3.7948535
7.00	0.5	-0.1790336	2.4482994
7.00	1.0	0.3756603	3.0252324
7.00	1.5	1.0341457	3.6093244

Table 5.3. Numerical values proportional to τ and J_w for $f_w=2.0$, $G_r=5.0$, $G_m=2.0$, $M=1.0$, $S_0=2.0$, $S_c=0.6$ and $E_c=0.2$.

P_r	P_m	τ	J_w
0.71	0.4	1.4363195	1.1319077
0.71	0.8	1.6810228	2.4725643
0.71	1.2	1.7993199	3.8003870
7.00	0.4	0.2051305	1.1183955
7.00	0.8	0.3347863	2.3866975
7.00	1.2	0.4061518	3.6616874

Table 5.4. Numerical values proportional to τ and J_w for $f_w=2.0$, $G_r=5.0$, $G_m=2.0$, $M=1.0$, $P_m=1.0$, $S_c=0.6$ and $E_c=0.2$.

P_r	S_0	τ	J_w
0.71	2.0	1.7504487	3.1397836
0.71	3.0	2.1243856	3.1805336
0.71	4.0	2.4795386	3.2204364
7.00	2.0	0.3756603	3.0252324
7.00	3.0	0.7289248	3.0495142
7.00	4.0	1.0655068	3.0735690

Table 5.5. Numerical values proportional to τ and J_w for $f_w=2.0$, $G_r=5.0$, $G_m=2.0$, $M=1.0$, $P_m=1.0$, $S_0=2.0$ and $S_c=0.6$.

P_r	E_c	τ	J_w
0.71	0.2	1.7504487	3.1397836
0.71	0.4	2.5692719	3.2191873
0.71	0.6	3.8088607	3.3484654
7.00	0.2	0.3756603	3.0252324
7.00	0.4	0.8479453	3.0518631
7.00	0.6	1.3962218	3.0861721

Table 5.6. Numerical values proportional to τ and J_w for $f_w=2.0$, $G_m=2.0$, $M=1.0$, $P_m=1.0$, $S_0=2.0$ $S_c=0.6$ and $E_c=0.2$.

P_r	G_r	τ	J_w
0.71	2.0	0.8455845	3.0832078
0.71	4.0	1.4416931	3.1194953
0.71	6.0	2.0687643	3.1615646
7.00	2.0	0.1747779	3.0198196
7.00	4.0	0.3075216	3.0233496
7.00	6.0	0.4450613	3.0272044

Table 5.7. Numerical values proportional to τ and J_w for $f_w=2.0$, $G_r=5.0$, $G_m=2.0$, $M=1.0$, $P_m=1.0$, $S_0=2.0$ and $E_c=0.2$.

P_r	S_c	τ	J_w
0.71	0.22	2.9315276	3.3057810
0.71	0.30	2.4539569	3.2326812
0.71	0.60	1.7504487	3.1397836
0.71	0.78	1.5899836	3.1213931
7.00	0.22	1.8405574	3.2134430
7.00	0.30	1.2853197	3.1325942
7.00	0.60	0.3756603	3.0252324
7.00	0.78	0.1455284	3.0035110

References

- Adams, J. A. and McFadden, E.W. (1966), *Amer. Inst. Chem.Eng. J.*, 12, 842.
- Agrawal, H. L., Ram, P.C. and Singh, V.(1983), *Astrophys. Space Sci.*, 91, 445.
- Alfven, H. (1942). *Arkiv F. Mat. Astro. O. Fysik.*,295(2).
- Altan, T., Oh, S. and Gegel, H. (1979). *Metal Forming Fundamentals and Applications* (American Society of Metals, Metals Park).
- Baehr,H.D. and Stephan, K. (1998). *Heat and Mass transfer* (Springer, Berlin).
- Berezovsky, A.A., Martynenko, O.G. and Sokovishin, Yu. A.(1977). *J. Eng. Phy.* 33,32.
- Caldwell, D.R.(1974). *J. Fulid Mech.*, 64, 347.
- Chaudhary, R.C. and Sharma, B. K. (2006). *Journal of Applied Physics* 99, 034901.
- Chen, C.H.(2004). *Int. J. Eng. Sci.* 42,699.
- Faraday, M.(1832). *Experimental Researches in Electrically Phill*, Trans. 15, 175.
- Gebhart, B. and Pera, L. (1971). *Int.J. Heat Mass Transfer*, 14, 2025.
- Georgantopoulos, G. A. and Nanousis, N. D. (1980), *Astrophys. Space Sci.*, 67(1), 229.
- Groots, S.R.T. and Mozur, P.(1962). *Non-equilibrium thermodynamics*, North Holland, Amsterdam.
- Hurle, D.T.J. and Jakeman, E.(1971). *J. Fluid Mech.*, 47, 667.
- Kafoussis, N. G. (1992). *Astrophys. Space Sci.* 192, 11.
- Kawase, Y. and Ulbrecht, J.J.(1984). *Int.Commun. Heat Mass Transfer* 11, 143.
- Legros, J. C., Van Hook, W. K. and Thoms, G. (1968). *Chem. Phys. Lett.*, 2, 696.
- Levy, R. H. and Petschek, H. E. (1962). *Las Paper 62-100*, Los Angeles, California, June.
- Lin, H.T. and Wu, C.M.(1995). *Heat Mass Transfer* 30, 369.
- Lin, H.T. and Wu, C.M.(1997). *Heat Mass Transfer* 32, 293.
- Martynenko, O.G., Berezovsky, A.A. and Sokovishin, Yu. A.(1984). *Int. J.Heat Mass Transfer* 27, 869.
- Mollendrof, J.C. and Gebhart, B.(1974). *In Proceeding of the Fifth International heat transfer Conference, Tokyo, No. CT 1.3.*

- Nachtsheim, P.R. and Swigert, P. (1965), Numerical Solution of the System of Non-linear Equations of the Boundary layer type, NASA TND-3004.
- Nanousis, N.D. and Goudas, C. L. (1979). *Astrophys. Space Sci.*, 66(1), 13.
- Nanousis, N. (1992). *Astrophys. Space Sci.*, 191, 313.
- Ostrach, S.(1952). NACA TN, No. 2863.
- Ostrach, S.(1953). NACA TN, No. 1111.
- Ostrach, S.(1953). *Trans. Am Soc. Mech. Eng.* 75.
- Ostrach, S.(1954). NACA TN, No. 3141.
- Ostrach, S.(1955). NACA TN, No. 3458.
- Patankar, S. V. and Spalding, D. B. (1970). *Heat and Mass Transfer in Boundary Layer*. 2nd Edn., Intertext Books,London.
- Raptis, A. and Kafoussias, N. G. (1982). *Can. J. Phys.*, 60, 1275.
- Rosenberg, D. U. V. (1969). *Method of Numerical solutions of partial differential equations*. American Elsevier, New York.
- Rossow, V. J. (1957). NACATN 3971.
- Sami, A. and Al-Sanea (2004). *Int. J. Heat Mass Transfer* 47, 1445.
- Sattar and Alam (1994), *Indian J.Pure Applied Mathe.*, 25(6),679-688.
- Schlichting, H. (1968). *Boundary Layer Theory*, McGraw-Hill, New York.
- Singh ,A. K., Singh , Aj. K. and Singh, N.P.(2003). *Indian J, pure App.Math* 34, 429.
- Somers, F.V. (1956). *J. Appl. Mech.*, 23, 295.
- Soundalgeker, V.M., Ramana Murty, T.V. (1980). *Waerme-Staffuebertrag.* 14, 91
- Spalding, D. B.(1977). *GENMIX*, a general computer program for two dimensional Parabolic phenomena, Pergamon Press, Oxford, UK.
- Sutton, G. W. and Gloersen, P. (1961). *Phys. Today*, 14, 18.
- Weiss, Y. Ahoran, Y. and Shai, I.(1994). *Proceedings of the Tenth International Heat Conference* P.P. 7 and 179.